

# Geomorphic and Land Use Controls on Sediment Yield in Eastern USA

Author: Aakash Ahamed

Persistent link: <http://hdl.handle.net/2345/bc-ir:103788>

This work is posted on [eScholarship@BC](#),  
Boston College University Libraries.

---

Boston College Electronic Thesis or Dissertation, 2014

Copyright is held by the author. This work is licensed under a Creative Commons Attribution 4.0 International License. <http://creativecommons.org/licenses/by/4.0/>

Boston College  
The Graduate School of Arts and Sciences  
Department of Earth and Environmental Sciences

GEOMORPHIC AND LAND USE CONTROLS ON SEDIMENT YIELD IN  
EASTERN USA

a thesis

by

AAKASH AHAMED

submitted in partial fulfillment of the requirements

for the degree of

Master of Science

December, 2014

© copyright by AAKASH AHAMED  
2014

## ***Abstract***

The Reservoir Sedimentation Database (ResSed), a catalogue of reservoirs and depositional data that has recently become publicly available, allows for rapid calculation of sedimentation and capacity-loss rates over short (annual to decadal) timescales. This study is a statistical investigation of factors controlling average sediment yield ( $Y$ ) in eastern United States watersheds. I develop an ArcGIS-based model that delineates watersheds upstream of ResSed dams and calculate drainage areas to determine  $Y$  for 191 eastern US watersheds. Geomorphic, geologic, regional, climatic, and land use variables are quantified within study watersheds using GIS. Sediment yield exhibits a large amount of scatter, ranging from 4.7 to 3336 tonnes<sup>1</sup>km<sup>-2</sup>year<sup>-1</sup>. A weak inverse power law relationship between drainage area ( $A$ ) and  $Y$  ( $R^2 = 0.09$ ) is evident, similar to other studies (e.g., Koppes and Montgomery, 2009). Linear regressions reveal no relationship between mean watershed slope ( $S$ ) and  $Y$ , possibly due to the relatively low relief of the region (mean  $S$  for all watersheds is 6°). Analysis of variance shows that watersheds in formerly glaciated regions exhibit a statistically significant lower mean  $Y$  (159 tonnes<sup>1</sup>km<sup>-2</sup>year<sup>-1</sup>) than watersheds in unglaciated regions (318 tonnes<sup>1</sup>km<sup>-2</sup>year<sup>-1</sup>), while watersheds with different dam purposes show no significant differences in mean  $Y$ . Linear regressions reveal no relationships between land use parameters like percent agricultural, and percent impervious surfaces ( $I$ ) and  $Y$ , but classification and regression trees indicate a threshold in highly developed regions ( $I > 34\%$ ) above which the mean  $Y$  (965 tonnes<sup>1</sup>km<sup>-2</sup>year<sup>-1</sup>) is four times higher than watersheds in less developed ( $I < 34\%$ ) regions (237 tonnes<sup>1</sup>km<sup>-2</sup>year<sup>-1</sup>). Further, interactions between land use variables emerge in formerly glaciated regions, where increased agricultural land results in higher rates of annual capacity loss in reservoirs ( $R^2 = 0.56$ ). Plots of  $Y$  versus timescale of measurement (e.g., Sadler and Jerolmack, 2014) show that nearly the full range of observed  $Y$ , including the highest values, are seen over short survey intervals (< 20 years), suggesting that whether or not large sedimentation events (such as floods) occur between two surveys may explain the high degree of variability in measured rates.

## ***Acknowledgments***

This work was made possible by a research fellowship from Boston College Graduate school of Arts and Sciences and a fellowship from the James P. Skehan Graduate Research Fund. Thanks to Noah Snyder and Gabrielle David for mentorship and enthusiasm throughout. Thanks to Gail Kineke and Jeremy Shakun for serving on my committee. Thanks to John Ebel for support to attend and present at conferences. Thanks to G. Michael Barnett for serving as essentially another advisor. Thanks to Austin Hopkins, Shakib Ahmed, and Austin Nijuis for ArcGIS and Matlab collaboration on this project. Thanks to Vanessa Napoli, Ellen Kristiansen, Chris Soeller and all the other graduate students in the department. Thanks to Dorothy Merritts, Robert Walter, Roger Thomas, and Candace Grand Pre for previous mentorship and instruction on related topics. Thanks to Meera Rao, Julian Muster, Brian Knudsen, James Tracy, Andrew Metersky, Kelly Marchisio, family, and friends.

## **Table of Contents**

### **1. Introduction**

- 1.1 Study Goals and Objectives*
- 1.2 Background and Previous Work*
  - 1.2.1 Determining Y: Methods of Measurement*
  - 1.2.2 Geomorphic Controls on Y*
  - 1.2.3 Geologic and Regional Controls on Y*
  - 1.2.4 Climatic Controls on Y*
  - 1.2.5 Land Use Controls on Y*
- 1.3 Dams and Reservoirs in the United States*
  - 1.3.1 National Inventory of Dams (NID) and Reservoir Sedimentation Database (ResSed)*
  - 1.3.2 Importance and Sustainability of Reservoirs*
- 1.4 Hypotheses*

### **2. Methods**

- 2.1 Watershed Delineation and Independent Variable Calculations*
- 2.2 Sediment Yield (Y) and Erosion Rate (E) Calculations*
  - 2.2.1 Trap Efficiency, Upstream Dams and Effective Yield (Y')*
  - 2.2.2 Annual Percent Capacity Loss Calculations*
- 2.3 Correlation Analyses – Simple Linear Regressions*
- 2.4 Analysis of Variance, Boxplots, Categorical Linear Regressions*
- 2.5 Classification and Regression Tree Analyses (CART)*
- 2.6 Principal Component Analysis (PCA)*

### **3. Results**

- 3.1 Watershed Delineation and finalization of dataset*
- 3.2 Geomorphic Controls (S, A, MaxEI, MinEI)*
- 3.3 Geologic and Regional Controls (geologic age, glaciated vs. unglaciated, physiographic province)*
- 3.4 Climatic Controls (MAT, MAP)*
- 3.5 Land Use Controls (I, Ag, F)*
- 3.6 Capacity and Capacity Loss*
- 3.7 The Sadler Effect*

### **4. Discussion**

- 4.1 Watershed Delineation*
- 4.2 Geomorphic Controls*
- 4.3 Geologic and Regional Controls*
- 4.4 Climatic Controls*
- 4.5 Land Use Controls*
- 4.6 The Sadler Effect*
- 4.7 Incomplete Trapping and Upstream Reservoirs*
- 4.8 Capacity loss, Remaining Capacity, and Reservoir Sustainability*

### **5. Conclusions**

### **6. Figures and Tables**

### **7. References**

### **8. Appendices**

## 1. Introduction

Dams and reservoirs are critical economic resources for their role in providing hydroelectric power, drinking water, irrigation, flood control, and recreation. However, reservoirs cannot perform these functions unless they have capacity to accumulate additional sediment (Graf et al., 2010). Dams alter the natural flow regime of rivers by creating reservoirs that inhibit terrestrial sediment transport (Poff et al., 1997). There are thought to be between 2.6 million and 8 million dams and artificial water bodies in the United States today (Renwick et al., 2001; Smith et al., 2002). The National Inventory of Dams (NID) is currently the most comprehensive database of United States dams and reservoirs. However, it only covers 80,000 dams, a miniscule fraction of the total. Small dams not catalogued within the NID account for approximately 20% of the standing water area across the United States and have important ramifications for hydrology, sedimentology, geochemistry, and ecology (Smith et al., 2002). Small dams also intercept about as much sediment as larger, better-documented reservoirs (Smith et al., 2002). There is a particularly high density of dams in the eastern United States, where structures have been built since European settlement in the early 1600s (Smith et al., 2002; Walter and Merritts, 2008; Merritts et al., 2011).

The cumulative impact of dams has a significant effect on sediment transport at the continental scale. A number of noteworthy large-scale processes are affected by reservoir sedimentation. Dams limit sediment transport to the continental shelf, causing subsidence and increased coastal erosion (Fitzgerald et al., 2008). Dams alter habitats and ecosystems within their watersheds by impeding streamflow and nutrient cycling (Walter and Merritts, 2008; Merritts et al., 2011). These changes have implications for carbon storage and sequestration (Vorosmarty et al., 2003), as well as stream restoration and dam removal projects (Pearson et al., 2011; Conlon, 2013).

Humans have arguably become the most important agents affecting geomorphic processes on Earth's surface (e.g., Hooke, 1994; Wilkinson and McElroy, 2007). Anthropogenic changes to the landscape cause alterations to water flow and sediment transport, resulting in fundamental changes to the fluxes of water and sediment to the ocean. Specific anthropogenic activities relevant to sedimentary deposition in reservoirs include the deforestation of hillslopes, the conversion of forests and grasslands to cropland, and widespread development and urbanization resulting in the expansion of impervious surfaces (Arnold, 1996; Bierman et al., 2005; Walter and Merritts, 2008). Over the last 3-4 centuries, anthropogenic activities have contributed to extensive alteration of rivers and other water bodies, particularly in the United States. As such, the Environmental Protection Agency (EPA) has classified 44% of US rivers, lakes, and estuaries as "impaired" water bodies that do not meet water quality standards (EPA, 2004).

Understanding the processes driving sediment transport within watersheds is fundamental to quantifying river inputs to the ocean and predicting the evolution of low-gradient landscapes like the eastern US. Measuring sediment yield ( $Y$ ), defined as the total mass of sediment per unit area eroded from a drainage basin over time (Griffiths et al., 2006), can aid in assessing remaining reservoir capacity, rate of capacity loss ( $C$ ), and provide the temporal framework to determine when reservoirs must be dredged or dams must be modified (Minear and Kondolf, 2009). Additionally, sedimentation rate ( $R$ ), which describes how rapidly sediment is being deposited behind a dam, can be used as an

important tool to guide river restoration, habitat remediation, and dam removal projects; practices that are gaining momentum in impaired northeastern water bodies (e.g., Kasprak et al., 2008; Snyder et al., 2008, Merritts et al., 2011). This study uses depositional data from reservoirs in order to understand the importance of geomorphic, land use, geologic, regional and climatic controls on sediment yield ( $Y$ ) at the landscape level.

The primary controls on  $Y$  are drainage area (e.g. Milliman and Syvitski, 1992; Wilkinson and McElroy, 2007; Koppes and Montgomery, 2009), and slope (e.g. Montgomery and Brandon, 2002). Other factors like precipitation, runoff, climate, tectonic setting, regional geology, lithology, and vegetation have a less important impact on  $Y$  (Milliman and Syvitski, 1992; Hicks et al., 1996; Leeder et al., 1998; Burbank et al., 2003; Koppes and Montgomery, 2009). Basin wide erosion rate ( $E$ ) is a measure of how much soil and rock has been weathered and removed from a watershed, and can be estimated from  $Y$  simply by dividing by rock density. Henceforth in this analysis,  $Y$  and  $E$  will be considered interchangeable parameters.

### *1.1 Study goals and objectives*

Determining  $Y$  values across a suite of watersheds will provide valuable insight about larger scale controls driving erosion and deposition. This study is a statistical investigation of factors controlling watershed sediment yield ( $Y$ ) in the eastern United States. In this thesis, data from The Reservoir Sedimentation Database (ResSed), a subset of the NID, is used to quantify watershed-scale sediment yield ( $Y$ ) and erosion rate ( $E$ ) for eastern United States watersheds. I quantify independent variables from various geospatial sources within study watersheds to examine correlations between  $Y$  and geomorphic, geologic, regional, climatic, and land use variables. The relative importance of drainage area ( $A$ ), slope ( $S$ ), relief ( $K$ ) fraction impervious surface ( $I$ ), fraction agricultural ( $Ag$ ), fraction forested ( $F$ ), precipitation ( $MAP$ ), and temperature ( $MAT$ ) are evaluated. I further examine regional and spatial trends in  $Y$  and gauge how different dam purposes and water management strategies impact  $Y$ .

### *1.2 Background and Previous Work*

In order to understand how intrinsic and extrinsic geomorphic, land use, geologic, regional and climatic controls influence  $Y$ , it is important to first understand how  $Y$  is empirically measured. A plethora of quantitative research has been dedicated to measuring  $Y$ , a fundamental parameters in geomorphology, over different timescales (Section 1.2.1). There are a number of well-characterized relationships between geomorphic controls and  $Y$  (Section 1.2.2). Many researchers also emphasize the importance of geologic and regional controls (Section 1.2.3), climate (Section 1.2.4), as well as land use and anthropogenic modifications to the landscape (Section 1.2.5) as important factors regulating  $Y$ .

#### *1.2.1 Determining $Y$ : Methods of Measurement*

Though this study uses reservoir sedimentation exclusively to compute  $Y$ , a number of methods have been used to measure  $Y$  over different timescales. Thermochronometry is used to estimate exhumation rates on geologic (greater than  $10^5$  year) timescales (Montgomery and Brandon, 2002; Burbank et al., 2003).

Thermochronometry uses radiometric dating and the closure temperature of minerals to gain insight about the thermal history of a specific rock, mineral, or geologic unit (Reiners, 2005). Radiometric dating is first used to determine the age of the sample. Minerals have a specific closure temperature, and using an assumed geothermal gradient of the lithosphere, a cooling depth at which the rock or mineral was formed can be determined. An exhumation rate, or the rate at which overlying material has been removed to reveal the exposed surface, is obtained by dividing the radiometric age by the cooling depth (Reiners, 2005). This method describes a point measurement, meaning that cooling ages and exhumation rates are only calculated for a sample at a specific point on the land surface. Performing thermochronometry at multiple sites within a watershed allows for estimation of  $Y$ . Thermochronometry can be applied to apatites, zircons, sphene, and volcanic glasses (Reiners, 2005).

Cosmogenic radionuclide dating can be used to measure  $Y$  on millennial ( $10^3$ - $10^6$  year) timescales (Bierman and Steig, 1996; Bierman and Nichols, 2004; Koppes and Montgomery, 2009). Cosmic rays bombard materials at earth's surface, which dislodges protons or neutrons from elements and converts them to different elements or isotopes called cosmogenic nuclides in a process known as spallation (Bierman and Steig, 1996). These cosmogenic nuclides decay at known and constant rates. Cosmic ray absorption on earth takes place within the uppermost 60 cm – 100 cm of rock or soil (Gosse and Phillips, 2001), so absolute ages can be determined by measuring the concentration of cosmogenic nuclides while taking in to account their decay rates (Willenbring et al., 2013). Applying this method to a sample (e.g., sediment from a fluvial sandbar) assumes that all upstream parts of the watershed contribute to the sample, making it representative of the mean composition of a watershed (Bierman and Steig, 1996).

Reservoir sedimentation, the method used to measure  $Y$  in this study, has been used to measure basinwide erosion rates ( $E$ ) from annual ( $10^0$ ) to centennial ( $10^2$ ) timescales (e.g. Snyder et al., 2004; Minear and Kondolf, 2009). The volume of sediment trapped in a reservoir is typically quantified through repeat bathymetric measurements or sediment cores (Morris and Fan, 1998). Bathymetric measurements compute reservoir  $R$  by differencing two surveys of the reservoir bottom (e.g. Childs et al., 2003; Snyder et al., 2004). After dividing  $R$  by basin area ( $A$ ),  $Y$  is obtained. The total volume of sediment in the reservoir can be estimated if a pre-dam topographic map of the area is available (Snyder et al., 2004). Estimation of  $Y$  from sediment cores involves interpolating sedimentary surfaces based on layer characteristics or radiometric measurements taken between cores in discrete locations (Foster and Walling, 1994; Snyder et al., 2004). Total reservoir volume can be measured if cores extend to depths corresponding to the pre-dam river bottom (Snyder et al., 2004). Assuming that no sediment passes through the reservoir, these methods measure  $Y$ , as sediment deposited in reservoirs can be derived from all parts of the watershed except where trapped by upstream reservoirs or other depositional sites. In this study,  $Y$  is estimated exclusively from reservoir sedimentation data (Section 1.3.1).

Suspended sediment concentrations offer annual to decadal ( $10^0$  –  $10^1$  year) timescale measurements of  $Y$  (Milliman and Syvitski, 1992). These rates are measured in situ by using sediment samplers and sediment traps. An assumption embedded in this method is that samples collected during the time of measurement are representative of the long-term system average. Sediment rating curves, plots of suspended sediment

concentrations against water discharge, are developed in order to estimate suspended sediment concentrations when the sampling interval is insufficient to characterize the continuous record (Walling, 1977).

The aforementioned methods have all been used effectively to estimate  $Y$  and  $E$ . However, it is important to consider a phenomenon called the Sadler Effect when comparing measurements of  $Y$  over different timescales. The Sadler Effect refers to the decreasing apparent thickness of sedimentary strata when measured over increasing timescales (Sadler, 1981; Sadler 1999). The Sadler Effect arises because long averaging times are more likely to preserve hiatuses in sedimentary deposition (Schaller et al., 2001). Therefore, comparing rates measured over different timescales can be spurious. Further, certain dating techniques can be subject to inherent inaccuracies and biases due to the nature of measurement (Sadler, 1999).

Cosmogenic methods used to measure  $Y$  on millennial timescales produce low  $Y$  for long averaging times and high  $Y$  for short averaging times (Sadler and Jerolmack, 2014). Despite shorter timescales of measurement, some reservoir sedimentation studies measuring  $Y$  have been shown to produce spuriously low values because short-term ( $<10^2$  year) measurements may miss large, rare events (Kirchner et al., 2001). Further, dam management strategies can influence whether sediment is preserved in reservoirs. For instance, flood control dams withhold water when downstream flooding is likely, and may trap more sediment during floods than during typical conditions. These factors can create unconformities within the reservoir's depositional history and influence the thickness of reservoir deposits.

Suspended sediment concentrations are measured over short ( $10^0 - 10^1$  year) timescales, and can be skewed depending on conditions during the time of measurement. Deposition is an episodic process (Sadler and Jerolmack, 2014), and fast accumulation rates cannot be sustained for long periods. Short pulses of deposition alternate with long periods of inactivity (Sadler and Jerolmack, 2014). Concordantly, suspended sediment samples collected during times of inactivity may produce low  $Y$  measurements (e.g. Schaller et al., 2001) and samples collected during times of high transport (floods) may produce large  $Y$  measurements. Rating curves aid in the identification of irregular periods, but still exhibit considerable variability (280% for annual curves, 900% for monthly curves) in suspended sediment concentrations (Walling, 1977).

### 1.2.2 Geomorphic Controls on $Y$

Geomorphologists have long sought to characterize relationships between sediment yield ( $Y$ ), erosion rate ( $E$ ) and geomorphic parameters like mean watershed slope ( $S$ ), drainage area ( $A$ ), and watershed relief ( $K$ ) (e.g. Gilbert, 1877; Milliman and Meade, 1983). Interactions between these parameters are important to better understand controls driving sediment transport at the watershed scale. Determining the degree of influence of tectonic, geomorphic, and erosional factors on topography allows researchers to better predict how natural systems will evolve in response to climate change and anthropogenic influence.

Ahnert (1970) reported a linear relationship between  $E$  and local relief ( $K$ ), which is defined as the difference in minimum and maximum elevation within a watershed. Summerfield and Hulton (1994) reported that  $K$  and runoff were the dominant controls on  $E$  in major world drainage basins. Pinet and Souriau (1988) reported correlations between

$E$  and mean basin elevation, suggesting that tectonically active and inactive environments exhibit different scaling relationships. Working in the Olympic Mountains in northwest Washington State, Montgomery and Brandon (2002) found a linear relationship between mean watershed slope ( $S$ ) and  $E$  in areas of low relief ( $S < 25^\circ$ ) and a power-law relationship between  $S$  and  $E$  in areas of high relief ( $S > 25^\circ$ ). Tectonically active regions are typically characterized by much higher  $S$  and  $K$  and therefore are capable of having much higher  $E$  (Koppes and Montgomery, 2009).

Milliman and Syvitski (1992) suggest that topography and drainage area ( $A$ ) are the primary controls on  $Y$ , while other controls like precipitation and runoff have a lesser impact. In a study analyzing 280 of the world's rivers, Milliman and Syvitski (1992) report an inverse power law relationship between  $A$  and  $Y$ . They attribute this finding to larger watersheds having additional upstream areas to store sediment. They acknowledge that comparisons between  $Y$  and  $A$  can give questionable results because  $A$  is a factor on both axes (Waythomas and Williams, 1988). The inverse power law relationship between  $A$  and  $Y$  is also suggested by Renwick et al. (2001), who use data from United States reservoirs, Koppes and Montgomery (2009), who compile  $E$  data from glacial, fluvial and composite landscapes, and Larsen et al. (2014), who model  $Y$  from  $S$  in 265 United States watersheds.

An important aside to geomorphic controls is the concept of thresholds and the complex response of drainage systems in geomorphology (e.g. Schumm, 1979). Systems tend to exhibit a characteristic response above a certain threshold value and a different response below a certain threshold value. Thresholds account for large portions of the variability associated with erosion and sedimentation studies (Schumm, 1979). Though geomorphic variables are thought to be the most crucial processes influencing  $Y$ , geologic and regional factors play a significant role as well.

### *1.2.3 Geologic and Regional Controls on $Y$*

Syvitski and Milliman (2007) report that geologic factors like lithology account for 65 percent of the variability in  $Y$  across 488 rivers whose geographical range covers 63% of the earth's surface. Syvitski and Milliman (2007) also emphasize the importance of recent and major glaciations as factors controlling  $Y$ . The late Cenozoic era has seen a substantial increase in erosion rates measured in both terrestrial and oceanic regions (Molnar and England, 1990; Molnar, 2004). Though Willenbring and Von Blackenberg (2010) attribute this perceived increase to the Sadler Effect, other researchers have cited the importance of climate change, particularly glacial-interglacial cycling as an effective erosive agent in high latitude regions (Molnar, 2004). Molnar (2004) points to an increase in the amplitude and frequency of climate change in the late Cenozoic as a unifying mechanism to account for increased erosion during this time. He suggests that continual adjustment of the system to disequilibrium conditions explains increased rates of erosion and deposition.

One crucial factor associated with fluctuations in climate is the advance and retreat of continental glaciers. Glaciation has been shown to exert an important influence on topography (Brozovic et al., 1997), and fluvial processes cannot easily rework large-scale glacial landforms like eskers and moraines. Given the importance of continental glaciation in controlling the availability of sediment and the influence of glacial history in

shaping topography of the northern United States, regional and geologic history must be considered when evaluating  $Y$  within formerly glaciated areas.

Wilkinson and McElroy (2007) suggest a sediment discharge of 5 gigatons per year to the oceans during the early Phanerozoic eon. This value is measured from preserved volumes of sedimentary rock. During the Neogene period and Pliocene epoch, oceanic sediment discharge increased to 16 gigatons per year and 21 gigatons per year respectively. At present, measured and modeled rates reach 75 gigatons per year (Wilkinson and McElroy, 2007).

Further,  $Y$  has been shown to vary between different geomorphic regions in California (Mearns and Kondolf, 2009). Lithology is also a factor governing  $Y$ , and basins made up of younger, softer rocks may exhibit higher  $Y$  than those made of older, harder rocks. Physiographic provinces combine geomorphic and geologic factors in to one variable. As such, it is reasonable to expect physiographic provinces to exhibit different  $Y$  due to distinctive geomorphic characteristics, varying underlying rock and soil types, and characteristic of relief and biota that contribute to their uniqueness.

#### 1.2.4 Climatic Controls on $Y$

Geographically distinct climatic regions are also characterized by different  $Y$  estimates (Milliman and Syvitski, 1992; Wilkinson and McElroy, 2007; Koppes and Montgomery, 2009). One might expect higher  $Y$  in regions with higher mean annual precipitation ( $MAP$ ). However, Langbein and Schumm (1958) show that  $Y$  is large where  $MAP$  is low because vegetation is too sparse to resist the erosive capacity of heavy rain and runoff. They find that  $Y$  decreases past a certain precipitation threshold due to the presence of vegetation, but again increases in areas of high precipitation because erosive rainfall processes outweigh the stabilizing influence of vegetation on soil.

Furthermore, mean annual temperature ( $MAT$ ) regulates biomass production and distribution (Nearing et al., 2004), in turn impacting  $Y$  by influencing vegetation, soil cohesion, and runoff. Temperature also dictates whether precipitation falls as rain or snow, which changes its erosive power (Nearing et al., 2004). Given a warming climate, areas previously characterized by snowfall are likely to shift to rainfall, thereby causing a corresponding increase in runoff and  $Y$  (Nearing et al., 2004). Leeder et al. (1998) also emphasizes the importance of climate ( $MAP$  and  $MAT$ ) in regulating vegetation and the importance of vegetation in regulating  $Y$ .

Wilkinson and McElroy (2007) report that climate plays a significant role in the global distribution of continental erosion and state that the highest erosion rates generally occur in regions characterized by high precipitation and low latitude. Working in the Himalayas, Burbank et al. (2003) finds that intense local precipitation can amplify  $E$  in high relief catchments. Montgomery and Brandon (2002) also acknowledge the influence of climate, among other factors, in dictating the nature of a linear, exponential, or power law relationships between erosion and topographic indices.

On the other hand, some researchers find little correlation between climate and  $Y$ . Riebe et al. (2001) use cosmogenic nuclides to measure erosion rates in a region in the Sierra Nevada characterized by large variations in  $MAP$  and  $MAT$ . Despite climatically different regimes, they find little variation in erosion rates and no correlation between climate and erosion. Milliman and Syvitski (1992) emphasize that climate exerts only a secondary influence on  $Y$  compared to geomorphic parameters like drainage area ( $A$ ) and

runoff. Walling and Webb (1983) emphasize that there is no simple relationship concerning the relationship between climate and sediment yield.

### 1.2.5 Land Use Controls on $Y$

Human impacts affect  $Y$  in counterbalancing ways (Milliman and Syvitski, 1992). On one hand, dams limit terrestrial sediment discharge to the ocean (Milliman and Syvitski, 1992; Fitzgerald et al., 2008). On the other hand, deforestation, poor soil conservation, and urbanization have been shown to increase sedimentation on the Atlantic continental shelf (Meade, 1982).

Saunders and Young (1983) suggest that moderate land use can increase  $Y$  by a factor of 2-3, while intensive land use can increase  $Y$  by an order of magnitude. Montgomery (2007) shows that erosion rates from conventionally plowed agricultural areas are on average 1-2 orders of magnitude greater than background rates of soil production, erosion under native vegetation, and longterm geological erosion.

The eastern US has been a center of manufacturing and industry since the Industrial Revolution in the mid-1800s. Anthropogenic landscape modifications have fundamentally altered the water and sediment transport regime of the region (Steyaert and Knox, 2008). Hillslopes were deforested to fuel industry and infrastructure. The creation of roads, parking lots, and buildings has drastically increased the amount of impervious cover in the area. In order to provide power for textile and lumber mills, tens of thousands of dams were erected along rivers in the region (Walter and Merritts, 2008). These modifications may have significant ramifications for  $Y$ .

Deforestation is one anthropogenic activity which can act to significantly increase  $Y$ . Deforestation reduces leaf interception, evapotranspiration, and tree rooting strength (Beschta, 1978; Dubé, 1995). Concordantly, deforestation results in increased amounts of surface runoff (Jones and Grant, 1996), as well as decreased soil cohesion. In turn,  $E$  in clear-cut watersheds is much higher than in natively vegetated landscapes (Beschta, 1978; Bierman et al., 1997), and leads to soil loss and subsequent sedimentation in rivers (Noel et al., 1986). Logging in the 19<sup>th</sup> century led to a period in which 50-80% of the land in central New England was clear-cut (Foster, 1992). Bierman et al. (1997) find that alluvial fans have aggraded more quickly in the last 200 years than in the previous 8000 years, and argue that this is evidence that deforestation has substantially increased hillslope  $E$  in Vermont since European settlement.

Impervious surfaces limit infiltration, which increases the volume and velocity of stormwater runoff in urban regions (Arnold, 1996). Ninety-three percent of roads in America were unpaved in 1904 (Southworth and Ben-Joseph, 1995). Since then, urban and suburban development has dramatically increased the percent of impervious land within watersheds ( $I$ ). This results in lower infiltration rates, greater amounts of runoff, greater peak discharges during storm events, and increased streambank erosion (Arnold, 1996). However, impervious surfaces shield underlying sediment beneath them from hillslope transport processes like rainsplash and sheetwash. The interplay between these two competing processes must be considered when studying relationships between urbanization and  $Y$ .

Pimentel et al. (1995) indicate that agricultural practices are easily the most significant contributor to global anthropogenic erosion, while compilations of global studies show that  $E$  in agricultural areas is nearly forty times greater than  $E$  estimated

from sediment volumes preserved in the geologic rock record (Montgomery, 2007). Koppes and Montgomery (2009) report that some of the world's highest  $E$  results from transient response of systems to modern agriculture. Wilkinson and McElroy (2007) use the universal soil loss equation to estimate agriculture induced  $E$  and use data from GTOPO30, a global digital elevation model (DEM), to estimate background  $E$  rates. They suggest that agriculture amplifies  $E$  by almost 30 times the natural rate, as present measured and modeled fluxes due to cropland erosion are about 75 gigatons per year (Wilkinson and McElroy, 2007). Further, they indicate that the accumulation of postsettlement alluvium in high order tributaries and in reservoirs due to agriculture is now the most significant geomorphic process shaping the face of the earth, even greater than fluvial erosion and Pleistocene glaciation.

The eastern United States has been subjected to prolific dam construction, widespread deforestation, unprecedented urbanization, and intense agricultural activity since European settlement. These factors may be delivering excessive amounts of sediment to eastern US reservoirs.

### *1.3 Dams and Reservoirs in the United States*

Milliman and Syvitski (1992) hypothesize an annual sediment discharge of 20 gigatons to the ocean prior to the widespread proliferation of dams in the second half of the 20<sup>th</sup> century. They postulate that this amount represents a doubling since farming and deforestation began to occur 2000-2500 years ago, but indicate that dam construction has partially offset anthropogenic amplification of sediment discharge to the oceans. Fitzgerald et al. (2008) indicate that since sediment supply for most barrier coasts is waning or exhausted due to dam construction, coastal erosion and subsidence will increase due to sea level rise.

Renwick et al. (2001) and Smith et al. (2002) use satellite imagery from the National Landcover Database (NLCD) to show that there are between 2.6 million and 8 million small, artificial water bodies across the continental US. Most of these are reservoirs located in the eastern half of the country (Smith et al., 2002). These small dams have enormous ramifications for continental hydrology, sedimentology, geochemistry, and ecology, as they account for approximately 20% of the standing water area in the United States (Smith et al., 2002). Further, small dams intercept about as much sediment as larger, better-documented reservoirs (Smith et al., 2002).

Walter and Merritts (2008) show that widespread damming in the mid-Atlantic region of the eastern US caused rapid deposition in valley bottoms, resulting in blankets of "legacy sediment" that persist today, sometimes meters thick. Merritts et al. (2011) demonstrate that dams and their subsequent removal or breach leads to stream incision, bank erosion, and increased suspended sediment load in rural, urban, and agricultural areas.

#### *1.3.1 National Inventory of Dams (NID) and the Reservoir Sedimentation Database (ResSed)*

The National Inventory of Dams (NID) is a catalogue of over 84,000 operational dams in the United States (USACE, 2002). Each of these dams is either 25 feet (7.2 m) or higher, holds more than 50 acre feet (61,674 m<sup>3</sup>) of water, or is considered a significant hazard if it fails. ResSed, a subset of the NID, is a catalogue of reservoirs and relevant

data maintained by the USGS and the Subcommittee on Sedimentation (SOS). It contains detailed data from 6,616 surveys from 1,823 reservoirs in the United States (Gray et al., 2010; Figure 1). ResSed represents a compilation of the most detailed measurements of reservoir sedimentation in the United States to date. Reservoir surveys were primarily conducted by the Army Corps of Engineers and are typically either bathymetric or sediment cores (Ackerman, 2009). Data span from 1755 to 1997, with 95 percent of surveys occurring between 1930 and 1990, during the “golden age” of dam construction (Gray et al., 2010). The database contains a wide array of reservoirs that range in size from small farm ponds to the 658 km<sup>2</sup> Lake Powell (Gray et al., 2010). However, ResSed primarily contains data for smaller-scale reservoirs (Graf et al., 2010).

This is the first study that uses ResSed data to quantify  $Y$  and  $E$ . The database can be used for a multitude of purposes, including calculating changes in reservoir storage (e.g. Graf et al., 2010), and quantifying sediment budgets. Previous studies have used the Reservoir Sedimentation Survey Information System (RESIS), the predecessor to ResSed in order to estimate total amount of sedimentation in small impoundments (e.g. Renwick et al., 2001) and annual rates of reservoir capacity loss (e.g. Graf et al., 2010). Graf et al. (2010) caution using RESIS for higher order analyses due to three principal reasons: the episodic nature of surveys and the failure of the surveys to capture the long term system average, the focus of the database on small reservoirs, and the uneven distribution of survey sites across the United States.

Despite these limitations, ResSed adds 317 new reservoirs to RESIS, while improving georeferencing, linking the database to the National Inventory of Dams, and creating a more navigable, relational database in a Microsoft Access environment. The recent digitization of ResSed permits rapid calculation of  $E$  and  $Y$  and allows for previously unconsidered spatial analyses using GIS software that can be used to better understand and predict the major factors influencing  $Y$ .

Dams and their corresponding reservoirs are ideal places to measure  $Y$  on intermediate timescales. These anthropogenic modifications to the environment have drastically altered the hydrologic regime in many parts of the world, and studies of this kind are crucial to better comprehend the complex response of the hydrologic system to recent anthropogenic forcings.

### *1.3.2 Importance and Sustainability of Reservoirs*

Dams and their reservoirs are ubiquitous anthropogenic features across the United States. Dams and reservoirs perform many integral functions (Section 1), but are only able to do so as long as they have the necessary capacity to accumulate additional sediment (Graf et al., 2010). Reservoir sedimentation poses a problem, particularly in regions with high  $Y$  (Minear and Kondolf, 2009). Dredging and other remediation strategies can be prohibitively expensive as maintenance techniques (Minear and Kondolf, 2009). Even in reservoirs that are not totally filled with sediment, excessive  $Y$  can interfere with outlet works, damage turbines, and cause upstream backwater flooding (Minear and Kondolf, 2009). Little work has been done concerning the sustainability of eastern US reservoirs, as scientists have paid more attention to the tectonically active and rapidly eroding western US (Minear and Kondolf, 2009; Graf et al., 2010).

### *1.4 Hypotheses*

Building from the extensive body of work carried out by previous researchers, I postulate relationships between a suite of independent variables and  $Y$  in eastern US watersheds.

(1) Slope

(a) Watersheds with higher relief and higher mean slope ( $S$ ) will have higher  $Y$ . (b) Watersheds with  $S$  less than  $25^\circ$  will exhibit a linear relationship with  $Y$  and watersheds with  $S$  greater than  $25^\circ$  will exhibit an exponential relationship with  $Y$  (Montgomery and Brandon, 2002).

(2) Drainage Area

(a) Watersheds with smaller drainage area ( $A$ ) will exhibit higher  $Y$  (Milliman and Syvitski, 1992). (b) The relationship between  $A$  and  $Y$  will be an inverse power law (Koppes and Montgomery, 2009; Larsen et al., 2014).

(3) Geologic and Regional Controls

(a) Watersheds in formerly glaciated regions will have lower  $Y$  than watersheds in unglaciated regions. (b) Watersheds with younger rocks will exhibit higher  $Y$  than watersheds with older rocks. (c) Sediment yield will vary between physiographic provinces.

(4) Climate

(a) Watersheds characterized by higher mean annual precipitation ( $MAP$ ) will have higher  $Y$  (Langbein and Schumm, 1958). (b) There will be no correlation between mean annual temperature ( $MAT$ ) and  $Y$ .

(5) Land Use

(a) Watershed impervious surface area ( $I$ ; percent of watershed) will exhibit a positive relationship with  $Y$  (Arnold, 1996). (b) Watershed agricultural area ( $Agr$ ; percent of watershed) will show a positive exponential relationship with  $Y$  (Koppes and Montgomery, 2009). (c) Watersheds with large percentages of forested area ( $F$ ) will have a negative relationship with  $Y$  (Bierman et al., 1997).

(6) Dam Function

The purpose of the dam and management strategy associated with the dam and reservoir will influence the measurements of  $Y$ , particularly in flood control dams.

## 2. Methods

The goal of this study is to determine  $Y$ , the dependent variable, across a suite of watersheds and gauge which independent variables correlate with  $Y$ . Independent variables are selected in order to explore the influence of geomorphic factors, geology and regional setting, climate, and land use. Sediment yield ( $Y$ ) is calculated from ResSed data as described in Section 2.2. Independent variables are obtained from National Land Cover Database (NLCD), PRISM precipitation and temperature data (<http://www.prism.oregonstate.edu/>), and fields in ResSed. Independent variables are quantified within watersheds to facilitate comparisons.

### 2.1 Watershed Delineation and Independent Variable Calculations

In this study, I use reservoir sedimentation data to calculate watershed sediment yield ( $Y$ ) and test hypotheses related to independent variables within study watersheds. This necessitates delineation of watershed boundaries associated with each dam in the ResSed database, so corresponding independent variables can be evaluated.

To accomplish this, I created a digital elevation model (DEM) spanning most of the eastern United States by mosaicking ~120 tiles of 1 arc-second ( $0.0003^\circ$  latitude or about 30 meter) elevation data from the National Map (<http://nationalmap.gov/viewer.html>). All of the DEM data were reprojected in the Universal Transverse Mercator (UTM) Zone 19 North coordinate system under the North American Datum of 1983 (NAD83) and resampled to 30 m pixel resolution. The ellipsoidal UTM coordinate system accounts for the curvature of the earth and is appropriate for the regional scale study area.

Using latitude and longitude coordinates for the location of each Eastern US dam in the ResSed database, I developed a model in ArcGIS 10.1 (Figure 2) that delineates watersheds using a DEM. First, void points are filled using the Fill function. Next, Flow Direction is computed to characterize the direction of flow for every cell in the grid. The Flow Accumulation function is used to define a stream network of point draining in to one another. Finally, the Watershed tool is applied to trace watershed boundaries. Inaccuracies in delineations arose because of the nature of the Flow Accumulation function within ArcMap software. Flow Accumulation falters in lakes and reservoirs (Wobus et al., 2006) because these standing bodies of water have similar elevations throughout their surface areas. Therefore, Flow Accumulation lines do not pass directly through the exact locations of ResSed dams. As such, dam locations were manually adjusted in order to fall along flow accumulation paths so watersheds could be traced with the best possible accuracy.

Drainage area ( $A$ ) values listed in ResSed are determined from 1:24,000 topographic maps and the NID (Stallard et al., 2001), and were used as a quality control metric to ensure that watersheds delineated in ArcGIS were accurate. Watershed area values that matched those in ResSed to within 10% (Section 3.1) were used in this study; the remaining watersheds were excluded from the analyses presented here (Figure 1).

Slope was calculated at each pixel in the DEM using the Slope function in ArcGIS. Slope is the first derivative of the DEM and represents the spatial change in elevation. Using the Summary Statistics tool in ArcGIS, I calculated mean slope within each study watershed ( $S$ ), as well as minimum and maximum slope and relief ( $K$ , the difference between minimum and maximum elevation). Data concerning minimum basin elevation ( $MinEl$ ) and maximum basin elevation ( $MaxEl$ ) are included in the ResSed database and are also considered as geomorphic variables.

Regional and geologic parameters were obtained from the USGS Geologic Map of North America dataset (<http://ngmdb.usgs.gov/gmna/>). Minimum and maximum geologic age of rocks were classified within each study watershed. The dataset also contains a line demarcating the southern extent of the Laurentide ice sheet at the last glacial maximum. Study watersheds were classified as being in formerly glaciated regions or unglaciated regions. Watersheds were classified based on their physiographic provinces, using the corresponding USGS data layer

(<http://water.usgs.gov/GIS/metadata/usgswrd/XML/physio.xml>). Watersheds were further categorized based on dam functions listed in ResSed.

Climate data were obtained from the PRISM Climate Group (<http://www.prism.oregonstate.edu/>). Mean annual precipitation (*MAP*) and mean annual temperature (*MAT*) data were calculated for the 30-year span between 1961 and 1990. These years are used because they are the oldest available datasets and most ResSed surveys occurred during this time. *MAT* and *MAP* are quantified within study watersheds using the Summary Statistics tool.

Land use data were obtained from the National Land Cover Database (NLCD) managed by Multi Resolution Land Characteristics Consortium (MRLC) ([http://www.mrlc.gov/nlcd06\\_data.php](http://www.mrlc.gov/nlcd06_data.php)). These data were compiled during airborne mapping missions in 1992. The USGS and EPA used computational algorithms to classify imagery in to one of 16 landcover classes (Table 1).

Table 1: Classification scheme for NLCD data. Numbers are values associated with colored pixels in GIS software.

#### Land Cover Class Value and Description

 (11) Open Water	 (42) Evergreen Forest
 (12) Perennial Ice/Snow	 (43) Mixed Forest
 (21) Developed, Open Space	 (52) Shrub/Scrub
 (22) Developed, Low Intensity	 (71) Grassland/Herbaceous
 (23) Developed, Medium Intensity	 (81) Hay/Pasture
 (24) Developed, High Intensity	 (82) Cultivated Crops
 (31) Barren Land	 (90) Woody Wetlands
 (41) Deciduous Forest	 (95) Emergent Herbaceous Wetlands

To simplify the analysis, related classes were combined. Developed areas (Table 1; number 21-24) were characterized as impervious surfaces (*I*), regardless of the intensity of development. Forested areas (Table 1; number 41-43) were classified as forest (*F*) whether they were deciduous, evergreen or mixed. Hay, pasture, and cultivated crops (Table 1; number 81-82) were classified as agricultural area (*Ag*). Woody wetlands and emergent herbaceous wetlands (Table 1; number 90, 95) were classified as wetlands (*W*). The Tabulate Area function in ArcGIS was used in order to determine the percentage of each landcover class within study watersheds.

#### 2.2 Sediment Yield (*Y*) and Erosion Rate (*E*) Calculations

Volumetric reservoir sedimentation rate ( $R$ ) for each watershed was calculated from ResSed data by dividing the “tot\_per\_seddep” ( $D$ , acre ft.) field in the RSED06 spreadsheet by “period\_yrs” ( $T$ , years) field:

$$R = \frac{D}{T} . \quad (1)$$

Acre-feet were converted to metric units ( $m^3$ ). Sedimentation rate ( $R$ ) was then divided by watershed area ( $A$ ) in order to obtain reservoir volumetric sediment yield ( $Y_v$ ;  $m^3 km^{-2} yr^{-1}$ ):

$$Y_v = \frac{R}{A} . \quad (2)$$

This normalizes the data and allows for intra-watershed comparison. Volumetric sediment yield ( $Y_v$ ) values were converted to mass yield ( $Y$ ; metric tonnes  $km^{-2} yr^{-1}$ ) using the density of reservoir sediment ( $\rho_{sed}$ ):

$$Y = Y_v \rho_{sed} . \quad (3)$$

Dendy and Champion (1973, 1978) estimated  $\rho_{sed}$  to be  $960 \text{ kg/m}^3$ , based on averaging bulk densities of grab samples at the top layer of reservoir sediment collected from over 1200 reservoirs across the continental US. However, actual densities may vary spatially and with depth. Snyder et al. (2004) obtained an average value of  $1,160 \text{ kg/m}^3$  for the entire sedimentary deposit of a California reservoir, Englebright Lake. The values obtained from Dendy and Champion (1973, 1978) are used in this thesis to facilitate comparison across the study area. This is an important simplification because  $\rho_{sed}$  exhibits local variability, even within individual reservoirs, due to factors such as compaction, organic content and grain size (e.g. Snyder et al., 2004).

Sediment mass yield ( $Y$ ) was divided by rock density ( $\rho_{rock}$ ;  $2650 \text{ kg}^1 \text{m}^{-3}$ , standard density of quartz) to obtain watershed erosion rate ( $E$ ;  $\text{mm/yr}$ ) in order to facilitate comparison to other studies:

$$E = Y / \rho_{rock} . \quad (4)$$

### 2.2.1 Trap Efficiency, Upstream Dams, and Effective Sediment Yield

Two principal limitations with  $Y$  values calculated in this analysis are evident. First, the reported  $Y$  values are minima because reservoirs do not trap all of the sediment delivered from upstream; some remains in suspension and travels through the dam outlet. Second, the reported  $Y$  values are minima because they do not account for trapping of sediments by upstream reservoirs within a given watershed. We can correct for this if the locations of upstream dams are known, but, as explained above, ResSed contains a small fraction of the total number of dams in the U.S. The second issue can be addressed by recalculating  $Y$  using the “net sed contributing area” field in ResSed, which considers only the area of a watershed that contributes sediment to a given reservoir. These

“effective yield” ( $Y$ ; tonnes/km<sup>2</sup>/year) values are higher than  $Y$  values because net sediment contributing areas are smaller than the entire watershed areas.

### 2.2.2 Annual Percent Capacity Loss Calculations

Annual percent capacity loss ( $C$ ; %) was calculated by dividing the original reservoir capacity ( $OC$ ), listed in ResSed as the “org\_cap\_acft\_13” field, by the sedimentation rate ( $R$ ) and multiplying by 100 to obtain a percent:

$$C = \left[ \frac{OC}{R} \right] * 100 . \quad (5)$$

Capacity data in ResSed are sparse, and  $C$  was only calculated where available.

### 2.3 Correlation Analyses – Simple Linear Regression

Simple linear regressions are an effective tool to judge the relationship between two independent quantities. In this thesis, simple linear regressions are used to test hypotheses that relate sediment yield to geomorphic, geologic, regional, climate, and land use independent variables. In order to characterize the relationships between various independent variables and watershed sediment yield ( $Y$ ), simple linear regressions depicting  $Y$  as a function of geomorphic, geologic, regional, climate, and land use variables were constructed. These models sought to test the relationship between a  $Y$  and a single independent variable and determine if an obvious trend was evident. To account for order of magnitude or greater ranges in the data,  $Y$ , the dependent variable was always log-transformed when regressions were performed. Independent variables were also log-transformed if there were large ranges in the data. When both variables are transformed, the plot is referred to as a logarithmic scatterplot. When only the dependent variable is transformed, the plot is referred to as a log-linear scatterplot.

Coefficient of determination ( $R^2$ ) and probability ( $p$ ) values were computed for each regression to judge the strength of correlation and the statistical significance of the relationship. A widely used technique in statistics,  $R^2$  measures how well observations are replicated by the model as the proportion of total variance explained by that independent variable (Barlow, 1989).  $P$  values describe the statistical probability that the null hypothesis ( $\alpha = 0.05$ , no correlation between variables exists) is true; low  $p$  values ( $<0.01$ ) support correlation between the variables because it indicates that there is a low probability that the null hypothesis is true. Each regression was tested to meet regression assumptions of homoscedasticity: that the data are independent of one another and that the residuals are normally distributed (Barlow, 1989).

### 2.4 Analysis of Variance, Boxplots, Categorical Linear Regressions

Analysis of Variance (ANOVA) was used to test for significant differences in mean  $Y$  within categorical variables (e.g., dam function, glacial history, physiographic province, watershed size, and geologic age of rocks in basin). Boxplots were constructed to help visualize the data. The Tukey Honest Significant Difference (Tukey HSD) method was used to determine which differences in mean  $Y$  are statistically significant.

Linear regressions between  $Y$  and the independent variables listed in Table 2 were also considered while holding individual categorical variables constant (Appendix 3; Table A3.1). Watersheds were classified based on size, glacial history, dam function, and

physiographic province, and linear regressions were performed for all independent variables within each subcategory. Strength of correlation was evaluated using the techniques presented in Section 2.3.

### 2.5 Classification and Regression Tree Analyses

Classification And Regression Trees (CART) are a recursive partitioning, non-parametric, decision tree learning technique that splits data based on thresholds in dependent and independent variables (De'ath and Fabricus, 2000). Features that make regression trees attractive for this type of analysis include efficacy in identifying interactions between independent variables, handling missing data, and straightforward description of nonlinear relationships (Anderson et al., 2004). CART analyses perform well in identifying thresholds, interactions, and nonlinear relationships between independent variables (Flores et al., 2006).

The statistical package RPART was used in conjunction with RStudio software to complete CART analyses. In order to construct a tree, RPART determines the single variable that best splits the data into two groups using a method that measures impurity. In this case, the method applied is the Gini Index (Therneau and Atkinson, 1997), which determines the difference in the sum of squares between the initial group and the two subgroups as the basis for splitting. After the initial split is performed, the process is repeated separately within each subgroup until no improvements can be made. The result is a “decision tree” that can then be pruned in order to highlight the most important variables in the dataset. Pruning involves reducing the size of a decision tree by removing sections of the tree that have little classification power. The goal of pruning is to reduce complexity and increase predictive accuracy.

Classification and regression trees have a number of beneficial characteristics. Residuals do not have to be normally distributed and missing data do not require exclusion of records (Breiman et al., 1984). CART analyses were applied in this study in order to determine which variables exert the most influence on  $Y$  as well as to determine threshold in the data (e.g. classify watersheds as small, medium, or large) and look for trends within those classes.

CART analyses found significant thresholds in  $A$  at values of  $8.3 \text{ km}^2$  and  $88.3 \text{ km}^2$  (Figure A2.4). This led me to categorize study watersheds as small ( $0-8.3 \text{ km}^2$ ), medium ( $8.3 \text{ km}^2 - 88.3 \text{ km}^2$ ) and large ( $> 88.3 \text{ km}^2$ ) to examine relationships among these categorical classifications within linear regressions (e.g., Figure A3.2). Watersheds were also classified based on dam function (Figure A3.3), glacial history (Figure A3.4), and physiographic province (Figure A3.5). Appendix 3 gives examples of these classification schemes applied to  $S$  data plotted against  $Y$ . All of the aforementioned analyses were performed within this categorical framework, and relationships between independent variables and  $Y$  within categorical variables were examined (Appendix 3; Table A3.1).

### 2.6 Principal Components Analysis (PCA)

Principal components analysis (PCA) looks for factors that account for the most variance in a dataset (Jolliffe, 2005). Principal components are linear combinations of independent variables that make up the underlying structure in the data (Hothorn and Evritt, 2009). The dataset is first deconstructed into a series of eigenvectors, each with a

specific eigenvalue. Eigenvectors demarcate the splits where there is the most variance within the dataset, and the eigenvalues are numbers that describe the amount of variation related to the corresponding eigenvector (Joliffe, 2005). The number of eigenvectors and eigenvalues is the same as the number of variables contained within the dataset (Hothorn and Evritt, 2009). The two eigenvectors with the highest eigenvalues are the principal components (Hothorn and Evritt, 2009).

Once principal components have been identified, the dataset is transformed so that PC1 and PC2 are plotted orthogonally. Eigenvectors and eigenvalues for each variable are plotted on the axes and provide insight about which variables account for the most variance and which are the most similar to one another. The variables exhibiting the highest loadings account for most of the variance and contain the most information (Sanborn and Bledsoe, 2006). The covariance matrix is examined in order to gain insight about the strength of positive or negative relationships between variables. PCA was used in this study to determine which independent variables have the most significant influence on  $Y$ , and which independent variables are strongly related to one another (Appendix 2).

Table 2: Summary of variables, symbols, units, and data sources used in this study.

<b>Dependent Variables</b>	<b>Symbol</b>	<b>Description</b>	<b>Units</b>	<b>Source</b>
Basin Wide Sediment Yield	$Y$	Calculated from ResSed sedimentation data and watershed delineations (eqs. 1 – 3)	Mass/area/time (Tonnes/km <sup>2</sup> /year)	ResSed
Basin Wide Erosion Rate	$E$	Calculated by dividing $Y$ by assumed rock density ( $\rho_{rock}$ ; eq. 4)	Length/time (mm/year)	ResSed
Annual Percent Capacity Loss	$C$	Calculated by dividing original capacity by $R$ (eq. 5)	Percent per time (% / year)	ResSed
<b>Independent Variables</b>	<b>Symbol</b>	<b>Description</b>	<b>Units</b>	<b>Source</b>
<b>Geomorphologic</b>				
Watershed Area	$A$	Calculated from watershed delineation in ArcGIS (Section 2.1)	Area (km <sup>2</sup> )	Delineations based on Latitudes and Longitudes listed in Res Sed. DEM data is from The National Map. See Section 2.1 for URL of data source.
Mean Watershed Slope	$S$	Calculated using functions in ArcGIS (Section 2.1) and averaged within delineated watersheds	Degrees (°)	DEM data is from The National Map. See Section 2.1 for URL of data source.
Relief	$K$	Calculated by differencing the maximum watershed elevation and minimum watershed elevation	Meters (m)	DEM data is from The National Map. See Section 2.1 for URL of data source.
Minimum Basin Elevation	$MinEl$	The minimum elevation within a study	Meters (m) above sea level	ResSed

		watershed		
Maximum Basin Elevation	<i>MaxEl</i>	The maximum elevation within a study watershed	Meters (m) above sea level	ResSed
<b>Climatic</b>				
Mean Annual Precipitation	<i>MAP</i>	Yearly average of precipitation recorded between 1961-1990	Millimeters/year (mm/year)	PRISM Rasters
Mean Annual Temperature	<i>MAT</i>	Yearly average of temperature recorded between 1961-1990	Degrees Celsius (°C)	PRISM Rasters
<b>Geologic</b>				
Maximum Geologic Age	Various	Oldest rock within watershed determined from USGS Geologic map of North America	Time (Geologic Period)	USGS Geologic map of North America
Minimum Geologic Age	Various	Youngest rock within watershed determined from USGS Geologic map of North America	Time (Geologic Period)	USGS Geologic map of North America
Glacial History	Yes/No	Whether watershed falls within extent of Laurentide Ice Sheet during last glaciations	Categorical	USGS Geologic map of North America
Physiographic Province	Various	Subdivisions of the US based on physiographic maps constructed by the USGS	Categorical	USGS Map of Physiographic Regions
<b>Land Use</b>				
Impervious Surface Area	<i>I</i>	Percent of watershed containing roads, houses, or other impermeable surfaces.	Percent (%) of watershed	NLCD 2001 Mission Rasters
Forested Area	<i>F</i>	Percent of watershed containing forested land.	Percent (%) of watershed	NLCD 2001 Mission Rasters
Agricultural Area	<i>Agr</i>	Percent of watershed containing agricultural land, cultivated land, or pasture.	Percent (%) of watershed	NLCD 2001 Mission Rasters
Grassland/Shrub Area	<i>Sh</i>	Percent of watershed containing grassland or shrubs.	Percent (%) of watershed	NLCD 2001 Mission Rasters
Wetland Area	<i>W</i>	Percent of watershed containing wetlands.	Percent (%) of watershed	NLCD 2001 Mission Rasters
Barren Land	<i>B</i>	Percent of watershed containing barren land.	Percent (%) of watershed	NLCD 2001 Mission Rasters
Dam Type or Function	Various	Function of the dam at the outlet of the study watershed	Categorical	ResSed

### 3. Results

#### 3.1 Watershed Delineation and Finalization of Dataset

Four hundred and sixty-nine reservoirs contained in the eastern United States were analyzed (Figure 1). Two hundred and seventy out of these watersheds delineated in ArcGIS matched area values listed in the ResSed database to within 10% (Appendix 1). Of the 270 sites, 54 were missing depositional data. Further, 8 watersheds were eliminated from the dataset due to spuriously large  $E$  values, ranging from 25 mm/yr to 3264 mm/yr. Lastly, various independent variables were missing or could not be quantified within 17 study watersheds. These were also excluded from the master dataset, yielding a total of 191 study watersheds (Figure 1; Appendix 1).

The mean and standard deviation  $Y$  of the study watersheds analyzed is  $260 \pm 370$  tonnes<sup>1</sup>km<sup>-2</sup>yr<sup>-1</sup> (Figures 3-4). This value is in reasonable agreement with the median  $Y$  of 172.8 tonnes<sup>1</sup>km<sup>-2</sup>yr<sup>-1</sup> calculated for 66 California reservoirs in Minear and Kondolf (2009). Watershed sediment yield in the study area spans from 4.7 tonnes<sup>1</sup>km<sup>-2</sup>yr<sup>-1</sup> to 3300 tonnes<sup>1</sup>km<sup>-2</sup>yr<sup>-1</sup>, and exhibits a log-normal distribution (Figure 3; Appendix 1).

The mean and standard deviation  $E$  in the study area is  $0.108 \pm 0.147$  mm/yr (Figure 5). Erosion rates range from 0.0024 mm/yr to 1.26 mm/yr (Figure 5; Appendix 1). These rates span similar orders of magnitude compared to  $E$  presented in Milliman and Syvitski (1992), which range from 0.0007 mm/yr to 37.7 mm/yr.

Effective sediment yield ( $Y'$ ) was calculated for each reservoir using the “net sed contributing area” field in ResSed, as described in Section 2.2.1. The mean and standard deviation  $Y'$  is  $280.4 \pm 384$  tonnes<sup>1</sup>km<sup>-2</sup>yr<sup>-1</sup> (Figure 3B). Though mean  $Y'$  values are incrementally higher, there is little difference between  $Y$  and  $Y'$  (Figure 3). As such,  $Y'$  values were not used in correlation analyses.

#### 3.2 Geomorphic Controls ( $S$ , $A$ , $MaxEl$ , $MinEl$ )

Surprisingly, the data do not show a positive relationship between mean slope ( $S$ ) and  $Y$  (Figures 6-7). Hypothesis 1a, which predicts that watersheds with higher mean slope ( $S$ ) and higher relief ( $K$ ) would have higher  $Y$ , is not supported by the results. No simple relationship exists between  $S$  and  $Y$  (Figures 6-7). A weak but statistically significant negative relationship between  $K$  and  $Y$  emerges (Figures 8-9). Following the findings of Montgomery and Brandon (2002), I hypothesized (Hypothesis 1b) that watersheds with  $S$  less than 25° will exhibit a linear relationship with  $Y$  and watersheds with  $S$  greater than 25° will exhibit an exponential relationship with  $Y$ . Watersheds with  $S$  less than 25° exhibit no relationship with  $Y$  (Figure 7), and no watersheds in this study had  $S$  greater than 25° (Figure 6), so the second part of this hypothesis could not be tested.

As predicted in Hypothesis 2 and described by other researchers (e.g., Milliman and Syvitski, 1992; Renwick et al., 2001; Koppes and Montgomery, 2009; and Larsen et al., 2014)  $Y$  increases as watershed area ( $A$ ) decreases. Figure 10 shows a weak inverse power law relationship between  $Y$  and  $A$ , supporting Hypothesis 2c. Additionally, correlations depicting  $Y$  as a function of minimum basin elevation ( $MinEl$ ) and maximum basin elevation ( $MaxEl$ ) could not be tested because the regression assumption of homoscedasticity was violated (Appendix 3; Figure A3.1). CART analyses show that

small watersheds ( $A < 5 \text{ km}^2$ ) at lower elevations ( $MaxEl < 825 \text{ m}$  above MSL) have high  $Y$  ( $846 \text{ tonnes}^1\text{km}^{-2}\text{yr}^{-1}$ ;  $n=15$ ; Figure 11) relative to other watersheds.

### 3.3 Geologic and Regional Controls (geologic age, glaciation, physiographic province)

The ANOVA models support Hypothesis 3a, that study watersheds in formerly glaciated regions have lower  $Y$  than watersheds in unglaciated regions. Study watersheds in formerly glaciated regions ( $n=57$ ) have a mean  $Y$  of  $159 \text{ tonnes}^1\text{km}^{-2}\text{yr}^{-1}$  as opposed to study watersheds in unglaciated regions ( $n=134$ ) that have a mean  $Y$  of  $308 \text{ tonnes}^1\text{km}^{-2}\text{yr}^{-1}$  (Figure 12). ANOVA models and boxplots of  $Y$  by minimum and maximum geologic age (Figure 13) do not support hypothesis 4b, which predicts that study watersheds with younger rocks would have higher  $Y$  than watersheds with older rocks. This hypothesis could not be confirmed or denied because these results do not meet standards for statistical significance determined by the ANOVA model ( $p > 0.07$  for all ages).

ANOVAs indicate that the Valley and Ridge and New England physiographic provinces have lower mean  $Y$  (Valley and Ridge:  $60 \text{ tonnes}^1\text{km}^{-2}\text{yr}^{-1}$ ,  $n=12$  and New England:  $73 \text{ tonnes}^1\text{km}^{-2}\text{yr}^{-1}$ ,  $n=5$ ) than all other physiographic provinces (Figure 14). ANOVAs and the Tukey HSD test reveal that the Valley and Ridge mean  $Y$  is not statistically significant from mean  $Y$  ( $p \text{ value} = 0.3$ ), while the New England mean  $Y$  is a significant deviation from mean  $Y$ , and explains to a 95% confidence interval ( $p = 0.05$ ). The New England result supports hypothesis 4c, that different physiographic regions of the US would exhibit different  $Y$ .

### 3.4 Climatic Controls (MAT, MAP)

Simple linear regressions show that there is a very weak positive relationship between mean annual precipitation (MAP; Figure 15) and  $Y$  (Figure 16). This does not support Hypothesis 4a, which predicts a positive relationship. However, there is a moderately strong positive relationship ( $R^2=0.48$ ,  $p<0.001$ ) between MAP and  $Y$  within the Central Lowland physiographic province (Figure 17). Unexpectedly, there is a stronger positive relationship between mean annual temperature (MAT; Figure 18) and  $Y$  (Figure 19). As reported previously, study watersheds falling within the spatial extent of the Laurentide ice sheet at the last glacial maximum have characteristically lower  $Y$  than other study watersheds (Figure 12); this may reflect the same correlation.

### 3.5 Land Use Controls (I, Ag, F, dam purpose)

Simple linear regressions show a weak positive correlation between percent watershed impervious surface cover ( $I$ ; Figure 20) and  $Y$  (Figure 21), suggesting that hypothesis 5a (watershed impervious surface area will exhibit a positive relationship with  $Y$ ) may be valid. CART analyses show a threshold  $I$  value of 34%; and  $Y$  values for watersheds with  $I > 34\%$  ( $n=7$ ) exhibit a significantly higher mean  $Y$  ( $965 \text{ tonnes}^1\text{km}^{-2}\text{yr}^{-1}$ ) compared to watersheds with  $I < 34\%$  ( $n=184$ ), which exhibit a significantly lower mean  $Y$  ( $237 \text{ tonnes}^1\text{km}^{-2}\text{yr}^{-1}$ ; Figure 22).

Percent watershed agricultural land ( $Ag$ ; Figure 23) was hypothesized (5b) to exhibit a positive exponential relationship with  $Y$ . This hypothesis is not supported by the data, as regressions suggest that  $Ag$  is not correlated with  $Y$  (Figure 24).

I expected that watersheds with a high percentage of forested area ( $F$ ; Figure 25) would have low  $Y$  and watersheds with low  $F$  would have high  $Y$  (Hypothesis 5c). There is no evidence supporting this hypothesis, and there appears to be no relationship between  $F$  and  $Y$  (Figure 26).

Grassland and shrubs ( $Sh$ ), wetlands ( $W$ ) and barren land ( $B$ ) exerted little influence on  $Y$  (Appendix 1). These parameters were sparse throughout most study watersheds (Appendix 1). CART Analyses excluded these independent variables from all constructed regression trees (e.g. Figure 13, Figure 23).

Hypothesis 6 suggested that dam purpose and management strategy play a role in regulating measured  $Y$  values. There is no evidence for significant differences between dam type and mean  $Y$  (Figure 27). However, hydroelectric dams are characterized by a positive power law relationship between  $Y$  and  $S$  (Figure 28). Principal components analysis (Figure 29; Appendix 2) shows that  $S$  and  $F$  are the most closely related variables in the dataset. Unexpectedly, a similar positive power law relationship is evident between  $Y$  and  $F$  (Figure 30).

### 3.6 Capacity and Capacity Loss

Figure 31 shows annual percent capacity loss ( $C$ ) for eastern US ResSed Watersheds where data are available ( $n=76$ ). Only 76 watersheds were analyzed because capacity data in ResSed are sparse. Annual percent capacity loss among study watersheds ranges from 0.01% to 6.09% with a mean of 0.64%. When it became clear that simple linear regressions produced little correlation between independent variables and  $Y$ , I began to suspect that independent variables might be more closely related to  $C$ . I constructed the same plots as described above, except substituting  $C$  as the dependent variable instead of  $Y$ . Within glaciated regions, I found power law relationships between  $A$  and  $C$  (Figure 32), as well as  $A_g$  and  $C$  (Figure 33).

### 3.7 The Sadler Effect

After simple linear regressions yielded little correlation among most independent variables and  $Y$ , I began to postulate alternate mechanisms controlling  $Y$ . Timescale of measurement has been cited as an important factor controlling  $Y$  in recent geomorphic literature (e.g., Sadler, 1981; Sadler, 1999 Schumer et al., 2001; Jerolmack and Sadler, 2007; Jerolmack and Paola, 2010; Willenbring and Von Blackenburg, 2010; Finnegan et al., 2014; Sadler and Jerolmack, 2014). Plots of survey interval against  $Y$  (Figure 34) show that the highest  $Y$  values are measured over short timescales while long timescales of measurement produce low  $Y$  values, although the correlation is weak. Short timescales (< 20 yr) appear to contain the full range of observed  $Y$  values (Figure 34).

## 4. Discussion

### 4.1 Watershed Delineation

Watersheds whose ArcGIS-calculated  $A$  values fell within 10% of the ResSed values were considered in this analysis (Figure 1). Forty-one percent of watersheds analyzed fit  $A$  to within 10 percent and contained the sedimentation data necessary to estimate  $Y$ . The discrepancy between some GIS areas and ResSed  $A$  values is partially due to inaccuracies in dam locations listed within the ResSed database (Stallard et al.,

2001). The coordinates of some ResSed dams are the coordinates for the nearest post office (Ackerman, 2009), which always yield incorrect watershed delineations when fed into a DEM based model (Figure 2).

Additionally, as stated in Section 2.1, standing bodies of water cause errors in the Flow Accumulation function in ArcMap software (Wobus et al., 2006) due to uniform water surface elevation. This problem was prevalent in my analyses, and required manual correction of dam locations in ArcMap software to match flow accumulation lines and properly delineate watersheds. To maximize usefulness of the database, latitude and longitude locations of dams should be corrected to fall along flow accumulation paths. This would allow for swift and accurate digital calculation of watershed areas in GIS software, which ResSed is currently lacking. Correcting dam locations in ResSed would allow for this study to be extended to a national scale.

#### 4.2 Geomorphic Controls

No correlations existed between  $S$  and  $Y$  (Figure 7). It is reasonable to expect a positive and causal relationship between  $S$  and  $Y$  because areas with higher slopes have higher potential energy, making it easier to initiate sediment transport. Larson et al. (2014) show that more than 50 percent of total denudation and 40% of chemical denudation occur at the steepest 10 percent of earth's surface. Montgomery and Brandon (2002) show a positive linear relationship between  $S$  and  $Y$  until about  $25^\circ$ , and a power law relationship at  $S > 25^\circ$ . It is curious, therefore, that these relationships are absent in this study.

The low relief of the landscape and the resolution of the DEMs are two possibilities for the lack of an observed relationship between  $S$  and  $Y$ . Firstly, this study does not cover any watersheds with  $S > 25^\circ$  (Figure 6), which eliminates any chance of observing the power law relationship suggested by Montgomery and Brandon (2002). Low slopes ( $<20^\circ$ ) may not have as important an effect on  $Y$  as those  $> 20^\circ$ . The analyses presented here suggest that other factors besides  $S$  play a more critical role in regulating  $Y$  in the eastern United States. Further, Montgomery and Brandon (2002) studied the Olympic Mountains in Washington in the western US in an effort to limit variability among other factors that may influence  $E$ . This study covers a far broader geographic and geomorphic area (Figure 1), which opens the possibility for other local factors (e.g., vegetation, soil type, management strategies, etc.) to exert considerable influence on  $Y$ .

Larsen et al. (2014) show that  $S$  calculated from DEMs decrease as an inverse power law function with increasing DEM grid scale. In turn,  $S$  values in these analyses may be skewed to underrepresent true watershed slopes as a result of the coarse 30-m grid scale. According to Larsen et al. (2014), using a higher resolution DEM data produces higher  $S$  values, though significant discrepancies only begin to arise at less than 30-m resolution. Changing the grid scale would not draw out correlations between  $S$  and  $Y$  since  $S$  will simply increase by a constant factor as resolution increases, resulting in no change in the relationship between  $S$  and  $Y$ .

This study also examined relationships between  $S$  and  $Y$  while holding various categorical variables constant. There was no correlation between  $S$  and  $Y$  even when the data is controlled for glacial history (glaciated or unglaciated), watershed size (small, medium, large), and physiographic province, (Figures A3.2, Figure A3.4, Figure A3.5), indicating that a relationship between  $S$  and  $Y$  does not emerge when accounting for other

sources of variability. However, when the data is controlled for dam function (Figure A3.3), a fairly robust positive power law relationship ( $R^2 = 0.55$ ,  $p < 0.001$ ) arises between  $S$  and  $Y$  in watersheds dammed for hydroelectric power generation (Figure 28). However, this could simply be an artifact of small sample size ( $n=13$ ).

Many compilations of studies detail a weak inverse power law relationship between  $A$  and  $Y$  (e.g., Milliman and Syvitski, 1992; Renwick et al., 2001; Koppes and Montgomery, 2009; Larsen et al., 2014). The same relationship is evident in this study (Figure 10), though the study watersheds examined here are in smaller catchments than the aforementioned studies. Renwick et al. (2001) obtained comparable  $R^2$  values (0.02 – 0.2) when plotting  $Y$  as a function of  $A$  for reservoirs within RESIS database, meaning that  $A$  explained a similar amount of variability within  $Y$ . This suggests that the improved data continuously being added to ResSed follows to the same relationships present between  $A$  and  $Y$  in the RESIS database.

The characteristic inverse power law relationship arises because larger watersheds are able to store sediment in many additional locations (e.g., point bars, terraces, floodplains, other reservoirs, natural lakes) besides the reservoir (Milliman and Syvitski, 1992; Larsen et al., 2014). The cumulative area of these sediment sinks increase with  $A$ .

The regressions between minimum basin elevation (*MinEl*) and maximum basin elevation (*MaxEl*; Figure A3.1) do not meet regression assumptions because the residuals are not normally distributed, so no statement can be made about the relationship between elevation and  $Y$ . As stated in the previous section,  $Y$  should increase as a function of elevation, because higher watersheds are more likely to have small  $A$ , high  $S$  and high  $K$ . This does not appear to be the case in this study. CART analyses that considered all numerical variables (Figure 11) surprisingly show that study watersheds below 825 m *MaxEl* exhibit higher  $Y$  than those above 825 m *MaxEl*. This result represents another important threshold in this study, specifically characterizing the complex relationship between elevation and  $Y$ . This result reflects a complex relationship and an overall change in the magnitude of  $Y$  at the threshold *MaxEl* of 825 m. Contrary to the findings of Milliman and Syvitski (1992), who emphasize the importance of small, mountainous rivers in controlling global continental erosion, the threshold  $Y$  value suggests that  $Y$  is actually higher at lower elevations. This may be due to increases in human settlements beneath this threshold elevation, and the accompanying practices of agriculture and urbanization that result in higher  $Y$ .

#### 4.3 Geologic and Regional Controls

Sites south of the extent of the Laurentide Ice Sheet during the last glaciation have characteristic and statistically significant ( $p < 0.01$ ) higher  $Y$  than glaciated watersheds (Figure 12). The phenomenon is likely owed to the substantial glacial overprint on the sediment transport regime in the region, and supports hypothesis 3a. Glaciers are effective at moving large amounts of sediment, and can limit the availability of sediment within watersheds by localizing deposits in features like moraines, eskers, and kames. Due to this, rivers, dams, and reservoirs that currently occupy valley bottoms carved by glaciers may have access to substantially less sediment than rivers in previously unglaciated regions. Additionally, glacially transported gravel can armor streambeds and inhibit fine sediment transport to reservoirs.

Geologic age does not appear to be an important factor in controlling  $Y$ . Hypothesis 3b postulated that watersheds with younger rocks will have higher  $Y$  because younger rocks are typically less metamorphosed, composed of soft sedimentary rocks, and therefore easier to erode. However, there appears to be no relationship between geologic age and  $Y$  (Figure 13). The lowest  $Y$  occurs in watersheds with Jurassic rocks, but does not constitute a statistically significant deviation from other geologic ages ( $p = 0.35$ ; Figure 13).

When no telling relationships arose between  $Y$  and fundamental geomorphic, geologic, and regional variables, I began to look for additional ways to categorize watersheds to look for differences in  $Y$ . I found that  $Y$  varies within distinct physiographic regions of the eastern US (Figure 14), supporting hypothesis 3c. Physiographic provinces combine geomorphic and geologic factors into one variable. Two physiographic provinces, Valley and Ridge ( $n=12$ ) and New England ( $n=5$ ), exhibit characteristically lower  $Y$  than all others in the region, but only New England has a mean  $Y$  that is significant. Similarly, Minear and Kondolf (2009) found considerable variability in  $Y$  in distinct geomorphic provinces in California. This finding suggests that distinct physiographic and geomorphic regions can exhibit markedly different morphological character. Lower mean  $Y$  in the New England physiographic province could be due to regional glaciation and the tendency of formerly glaciated watersheds to exhibit lower  $Y$ .

#### 4.4 Climatic Controls

Though I hypothesized there would be linkages between  $MAP$  and  $Y$  (Hypothesis 4a), I was aware that most studies found climate to play a secondary role in affecting  $Y$  compared to geomorphic and land use watershed characteristics (e.g. Milliman and Syvitski, 1992; Montgomery and Brandon, 2002; Wilkinson and McElroy, 2007). Indeed, there is little correlation between mean annual precipitation measured between 1961 and 1990 ( $MAP$ ), and  $Y$  (Figures 15-16), except in the Central Lowland physiographic province (Figure 17).

It is not surprising that there is no correlation between  $MAP$  and  $Y$ . Studies exploring linkages between  $MAP$  and  $E$  present interesting and complex feedbacks and thresholds. In arid regions with low  $MAP$ ,  $E$  is typically low, as the bulk of sediment transport occurs during episodic events (Langbein and Schumm, 1958). I do not observe lower  $Y$  in areas of lower  $MAP$  in this study, except in the Central Lowland, which may exhibit this relationship because it is on the lower end of overall  $MAP$  (Figure 17). Langbein and Schumm (1958) report that as  $MAP$  increases,  $E$  also increases. However, this relationship is dissolved when a threshold  $MAP$  is reached due to the development of vegetation (Leeder, 1998). Vegetation acts to diminish  $E$  in a number of ways. Leaf interception reduces rainsplash erosion. Plant roots consolidate sediment and increase the shear stresses required for initiation of motion. Plants use water to perform photosynthesis. In the context of this study,  $MAP$  is probably not variable enough to exert a tractable influence on  $Y$ , because every watershed is vegetated and all study watersheds are located in temperate climate regions.

Mean annual temperature ( $MAT$ ) correlates more strongly with  $Y$  than any other independent variable. This is a surprising result, since I hypothesized (Hypothesis 4b) that there would be no relationship between these parameters. Figures 18 and 19 suggest a moderate correlation between  $MAT$  and  $Y$ . In colder regions, more water precipitates as

snow instead of rain, and watersheds are covered by snow or ice for parts of the year. These factors may act to decrease  $Y$ . It is possible that this relationship could emphasize the finding that formerly glaciated areas have lower mean  $Y$  than unglaciated areas (Figure 12), or that this relationship arises due purely to chance and scatter among the data.

#### 4.5 Land Use Controls

The NLCD 2001 dataset categorizes land into one of sixteen classes (Table 2). CART analysis (Figure 11, Figure 22) and principal components analysis (Figure 29; Appendix 2) reveal that the most significant land use factors affecting  $Y$  are percentages of impervious surface area ( $I$ ; Figure 20), agricultural area ( $Ag$ ; Figure 23), and forested area ( $F$ ; Figure 25) in each watershed. These land use variables were given the most attention in this study.

Watersheds are affected by  $I$  in counterbalancing ways. On one hand, impervious surfaces inhibit infiltration and increase the volume and velocity of stormwater runoff, thereby causing higher peak discharges and increased bank erosion during storms. On the other hand, impervious surfaces shield sediment beneath them from erosive processes like rainsplash and aeolian transport. Though a weak positive relationship between  $I$  and  $Y$  is evident in simple linear regressions (Figure 21), CART analyses show that watersheds with the highest  $I$  are characterized by a much higher mean  $Y$  than watersheds with low  $I$  (Figure 22). This finding suggests a threshold in  $I$  of 34% above which there is a significant change in the processes driving sedimentary deposition in reservoirs. Watersheds having greater than 34%  $I$  have a mean  $Y$  of  $965 \text{ tonnes}^1\text{km}^{-2}\text{yr}^{-1}$  ( $n=7$ ), whereas watershed that have less than 34%  $I$  have a mean  $Y$  of  $237 \text{ tonnes}^1\text{km}^{-2}\text{yr}^{-1}$  ( $n=184$ ). While this may be an artifact of small sample size of high  $I$  watersheds, other studies have drawn positive relationships between  $Y$  and  $I$  (Knox, 1972, Steyart and Knox, 2008), and this finding may indicate a critical threshold where stream bank erosion associated with  $I$  begins to outweigh the influence of  $I$  in shielding sediment from rainsplash and hillslope erosion in eastern US watersheds.

Agriculture has been shown to substantially amplify erosion rates (Montgomery, 2007; Wilkinson and McElroy, 2007). The analyses presented here do not reveal any correlations between watershed percent agricultural land ( $Ag$ ) and  $Y$  (Figure 24). There are a number of potential explanations for this lack of correlation. NLCD coverage was flown in 1992, whereas 95% of ResSed surveys were performed between 1930 and 1990 (Gray, 2010). Land that was classified as “agricultural” when Landsat collected data in 1992 may not have been agricultural land in the past, or may have been reforested since the data was collected. Agricultural areas are most prevalent on flat, low lying floodplains, where water is abundant and irrigation is easiest. As such, agricultural land has low  $S$ , which inhibits sediment transport.

Further, different crops require different methodologies in order to maximize production. Indeed, studies have shown that soils occupied by different crops have variable erosion rates (e.g. Matson et. al., 1997). Lumping all crop cultivation in to an “agricultural” category may literally and figuratively produce an “apples to oranges” comparison.

A fairly strong positive relationship exists between  $Ag$  and annual capacity loss ( $C$ ) in formerly glaciated areas (Figure 32). This finding suggests what many researchers

(e.g. Montgomery, 2007; Wilkinson and McElroy, 2007) have found; that agricultural practices increase the rate of delivery of sediment in to streams. Though this may be an artifact of small sample size ( $n=16$ ), this finding implies that agricultural activities may play a noteworthy role in controlling the distribution of sediment in formerly glaciated regions than in unglaciated regions.

I predicted that watersheds with a low percentage of forested area ( $F$ ; Figure 25) would have high  $Y$  (Hypothesis 5c). This claim was not supported by the data (Figure 26). Watersheds with lower  $F$  would typically have higher  $I$  and  $Ag$ , which have both been shown to increase  $Y$ . The absence of the relationship between  $F$  and  $Y$  suggests that while  $F$  acts to increase rooting strength and soil cohesion, the relationship between  $F$  and  $Y$  is complex. Areas with high  $F$  may be extremely different because of differences in climate, tree height, rooting depth, transpiration rate, and other factors. The results suggest that these differences influence variability in  $Y$  more than  $F$ .

Further, I discussed a positive relationship between  $S$  and  $Y$  within the power dams category (Figure 28) in Section 4.2. Principal components analysis shows that  $S$  and  $F$  are similar and related variables (Figure 29). This may be because there is less development at higher slopes, resulting in low  $I$  and high  $F$ . Bearing this in mind, I plotted  $Y$  as a function of  $F$  for power dams and observed a positive relationship (Figure 30). This correlation between  $F$  and  $Y$  among power dams was contrary to my hypothesis that watersheds with more forested land would exhibit lower  $Y$ , but may be an artifact of a relatively small subsample size.

I hypothesized that dam purpose may influence measurements of  $Y$  (Hypothesis 6). ResSed lists dams with the following purposes: flood control, power, water supply, irrigation, conservation, inactive, and multiple use (Figure 27). Some dams (i.e., flood control, irrigation) deliberately release pulses of water during certain environmental conditions (e.g., after floods) or certain times of the year (i.e., to provide irrigation for agriculture at the start of the growing season). These pulses of water have the potential to resuspend sediment deposited in reservoirs, creating unconformities within the depositional record and reducing apparent  $Y$ . Despite this, there are no significant differences between mean  $Y$  categorized by dam purpose (Figure 27).

#### *4.6 The Sadler Effect*

There are a number of limitations and assumptions associated with this study that may account for the lack of correlation between most independent variables with  $Y$ . The main reason is likely that the data are inherently noisy, ranging many orders of magnitude (Figure 3). Graf et al. (2010) state that RESIS, the predecessor to ResSed is of limited usefulness for higher order analyses for a number of reasons. ResSed is subject to the same limitations. First, the database focuses on small dams because they grew out of earlier work by the Soil Conservation Service (now the Natural Resource Conservation Service). Due to this, the data are mostly from upland dams rather than main stem rivers. Second, the distribution of reservoirs across the US (Figure 1) is very uneven because more attention was given to regions where federal and state agencies were particularly interested in reservoir sedimentation due to soil erosion (e.g. Great Plains) or in management of wetlands (e.g. Ohio). Lastly and most importantly, reservoir sedimentation surveys were conducted unevenly and episodically from 1755 to 1993. There was a dramatic decline of surveys after 1980. Graf et al. (2010) argue that the data

outside the window from 1950 to 1980 do not reflect the long-term average given known hydroclimatic variation during this time.

One particular finding points to the importance of hydrology in controlling  $Y$ . Figure 34 suggests that  $Y$  diminishes with increasing timescale of measurement. This phenomenon is known as “The Sadler Effect” and has been a hotly debated subject in recent geomorphic literature (e.g., Jerolmack and Sadler, 2007; Jerolmack and Paola, 2010; Willenbring and Von Blakenburg, 2010; Schumer et al., 2011; Finnegan et al., 2014).

In my analyses,  $Y$  is measured on timescales of  $<1$  year to  $\sim 200$  years (Appendix 1). Sadler (1981), Sadler (1999), Korup (2012) and Sadler and Jerolmack (2014), all report an apparent decrease in sediment accumulation rates with increasing measurement interval on timescales of  $10^3$  to  $10^6$  years, far greater than timescales of measurement in this study. The proposed mechanism for this phenomenon is the inclusion of an increasing number of erosional hiatuses in the sedimentary record for longer timescales over which deposition is measured. The analyses presented here suggest that  $Y$  decreases with increasing measurement interval, even over short timescales (Figure 34).

Contrary to the analyses presented in Sadler (1981), Sadler (1999), Korup (2012), and Sadler and Jerolmack (2014), in this study, diminishing  $Y$  values with increasing timescale of measurement probably do not reflect the inclusion of hiatuses preserved in the depositional record of ResSed reservoirs. Rather, variability in  $Y$  is a result of high hydrologic variability over short timescales ( $<20$  years). On these short timescales, watersheds with high  $Y$  values are likely to have experienced major flooding while watersheds with low  $Y$  values are not likely to have undergone significant flooding. Major flood events lead to anomalously high  $Y$  values when measured over shorter timescales.

Measurements of  $Y$  on short timescales may also be within a depositional hiatus at the time of measurement, thereby not capturing any significant floods and deposition between surveys and producing low  $Y$ . This point is also suggested by Kirchner et al., (2001), who indicate that  $Y$  determined from reservoir sedimentation is often low. However, it is just as plausible that  $Y$  measured on short timescales does include a period of rapid deposition (e.g., a significant flood), which causes high  $Y$  values. Lastly,  $Y$  measured on longer timescales can be subjected to resuspension and compaction, thereby creating an erosional hiatus and decreasing the apparent  $Y$ .

This study would benefit from a coupled analysis of hydrologic history during survey intervals within study watersheds. Flood frequency analysis could be employed to better understand the importance of individual flood events in influencing  $Y$ . The results (Figure 34) suggest that hydrology is an important control on deposition because short survey intervals contain the full spectrum of  $Y$  values. This indicates that short surveys contain both periods of little deposition and periods of anomalously high deposition (e.g., floods). As survey length increases, the episodic events become less important and have less of a signature in the depositional record, decreasing apparent  $Y$  values.

Preliminary hydrologic analyses offer potential limitations associated with this kind of study. Since most study watersheds are smaller, upland catchments, discharge data cannot typically be attained for the specific rivers or streams that ResSed dams occupy. Nevertheless, nearby gaging stations are likely to show a similar record that is a usable proxy for this analysis.

#### 4.7 Incomplete Trapping and Upstream Reservoirs

Two principal limitations in this analysis cause  $Y$  values to be minima. (1) Reservoirs do not trap all of the sediment delivered from upstream; some remains in suspension and travels through the dam outlet. (2) Reported  $Y$  values do not account for trapping of sediments by upstream reservoirs.

These limitations were addressed in Minear and Kondolf (2009) by constructing a spreadsheet-based model that takes in to account these factors. They correct measured  $Y$  values based on reservoir trap efficiency and the trap efficiencies of known upstream reservoirs. However, trap efficiency is a function of reservoir capacity and  $A$  (Brune, 1953). Capacity data are sparse in ResSed, which makes the calculation of reservoir trap efficiency challenging. Further, there are countless undocumented upstream reservoirs in these small catchments, because rivers in the eastern US have been dammed since the 1700s. Correcting  $Y$  values for known upstream reservoirs accounts for only a small proportion of the cumulative sediment being trapped by upstream reservoirs (Figure 3B).

#### 4.8 Capacity loss, Remaining Capacity, and Reservoir Sustainability

Figure 32 depicts mean annual percent capacity loss ( $C$ ) for ResSed watersheds in the eastern US where capacity data are available ( $n=75$ ). Annual rates of capacity loss in this study range from 0.01% to 6%. Concordantly, the expected reservoir lifetimes for the 75 sites in this study range from 10,000 years to 16.4 years. Reservoir sustainability is emerging as a significant problem, especially in areas with high sediment yield (Graf et al., 2010). Graf et al. (2010) indicate that mean annual rates of capacity loss are greater for reservoirs contained in the western US compared to the east. Determining rates of capacity loss has important implications for reservoir sustainability and remediation projects like dam removals.

When independent variables showed little correlation with  $Y$ , I used  $C$  as the dependent variable in an attempt to determine which independent variables were related to it. The same analyses that were conducted with  $Y$  were performed substituting  $C$  as the dependent variable, and categorical relationships within the context of independent variables (e.g. Figures A3.2-A3.5) were also considered. There was no relation between most independent variables and  $C$ . However, I found that formerly glaciated watersheds exhibit power law relationships between  $A$  and  $C$  (Figure 32) as well as  $A_g$  and  $C$  (Figure 33). The relationship between  $A_g$  and  $C$  is similar to the relationship that many researchers have described (e.g. Montgomery, 2007; Wilkinson and McElroy, 2007) have described, and I had expected, between  $A_g$  and  $Y$ . The relationship between  $A$  and  $C$  is perplexing because larger watersheds have more sediment sinks than small watersheds. Therefore, I would expect  $C$  to decrease as  $A$  increases, similar to the relationship between  $A$  and  $Y$  shown in Figure 11.

### 5. Conclusions

This study uses statistical techniques to investigate factors controlling watershed sediment yield ( $Y$ ) in eastern United States watersheds. Depositional data from ResSed, a USGS database, are used to calculate  $Y$ . ArcGIS software is used to quantify independent geomorphic, geologic, regional, climatic, and land use variables within study watersheds. The data show a large amount of scatter, spanning four orders of magnitude (Figure 3).

The well documented inverse power law relationship between drainage area ( $A$ ) and  $Y$  is evident among study watersheds (Figure 10). The data show no relationship between mean watershed slope ( $S$ ) and  $Y$  (Figure 7) except in the small subcategory of hydroelectric power dams (Figure 29).

Contrary to hypotheses and the findings of other researchers, little to no correlation between  $Y$  and watershed relief ( $K$ ; Figure 8), mean annual precipitation ( $MAP$ ; Figure 18), percent forested land ( $F$ ; Figure 27), percent agricultural area ( $Ag$ ; Figure 25), geologic age (Figure 15), or dam type (Figure 28) arises, except among small sample sizes when certain categorical variables are held constant (e.g. Figures 17, Figure 28, Figure 30). In terms of linear relationships, the most important variables influencing  $Y$  appear to be glacial history (Figure 12), mean annual temperature ( $MAT$ ; Figure 19), watershed impervious surface area ( $I$ ; Figure 21-22), and timescale of measurement ( $T$ ; Figure 34).

Thresholds exist above which there are significantly higher or lower  $Y$ , depending on the independent variable in question. Watersheds in formerly glaciated regions exhibit statistically significant ( $p < 0.01$ ) higher mean  $Y$  than watersheds in unglaciated regions (Figures 4-5; Figure 12). Climate appears to play a role, as  $Y$  increases as a function of  $MAT$  (Figure 19). Impervious surfaces ( $I$ ) appear to show a threshold value ( $I > 34\%$ ) in which urbanization and development causes increased runoff and streambank erosion, resulting in significantly higher  $Y$  for watersheds in more developed regions (Figure 22). Lastly, hydrology and timescale of measurement also appears to be an influential factor, as  $Y$  is highest at short survey intervals ( $< 20$  years) and decreases over greater measurement intervals ( $> 50$  years; Figure 34).

## 6. Figures

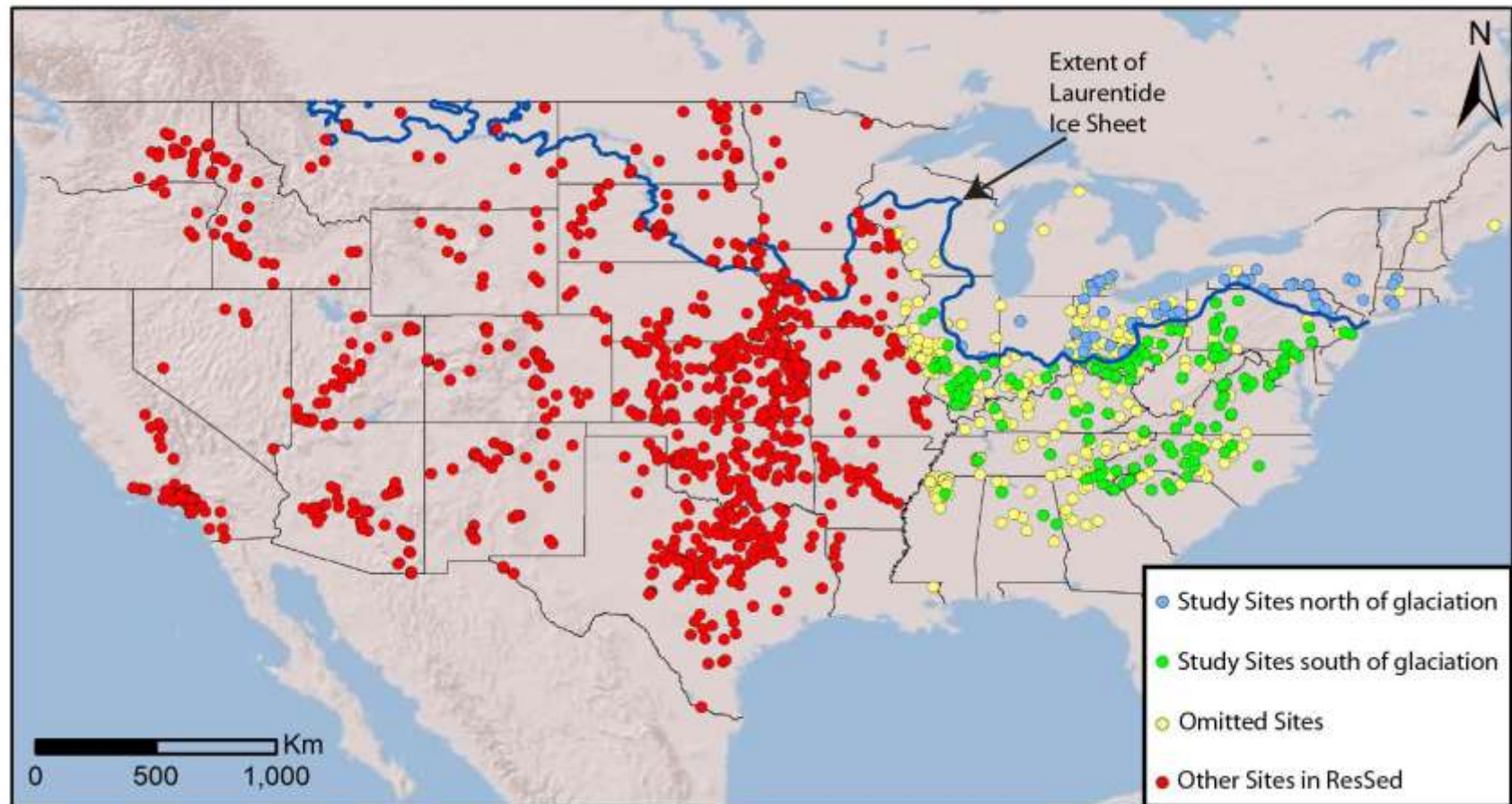


Figure 1: Sites contained within the ResSed Database. Green and blue markers indicate sites where data has been used in this study. Green markers show sites south of the Laurentide Ice Sheet. Blue Markers show sites north of the Laurentide Ice Sheet. Yellow markers indicate sites that have been omitted because watershed delineation was unsuccessful, depositional data were missing, or anomalously high  $Y$  values were calculated. Red markers indicate sites that were not included in this study.

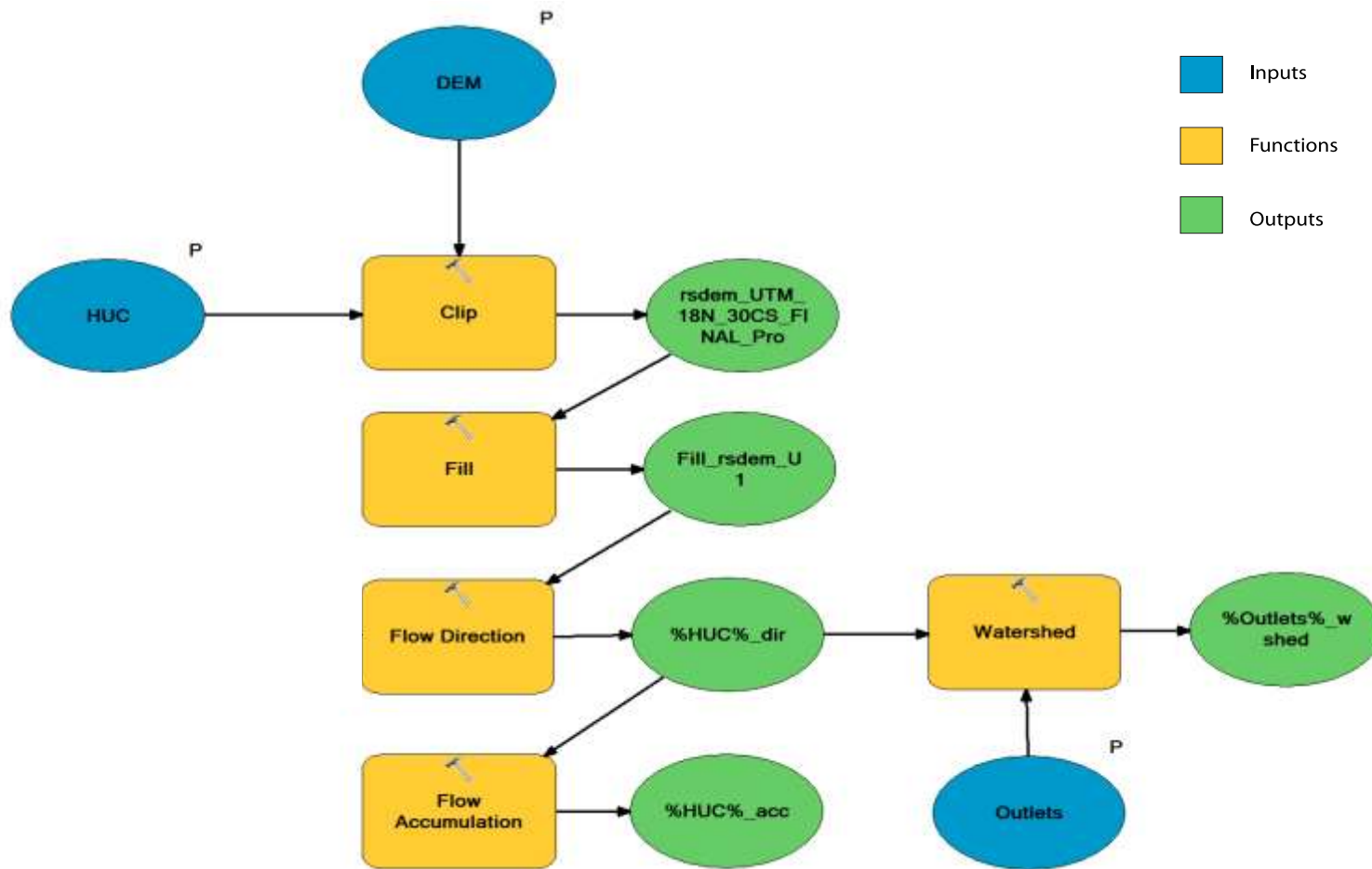


Figure 2: Pictographic depiction of the GIS model framework used to delineate watershed areas from DEMs using latitude and longitude data. Blue circles indicate inputs. Yellow rectangles indicate functions. Green circles indicate outputs.

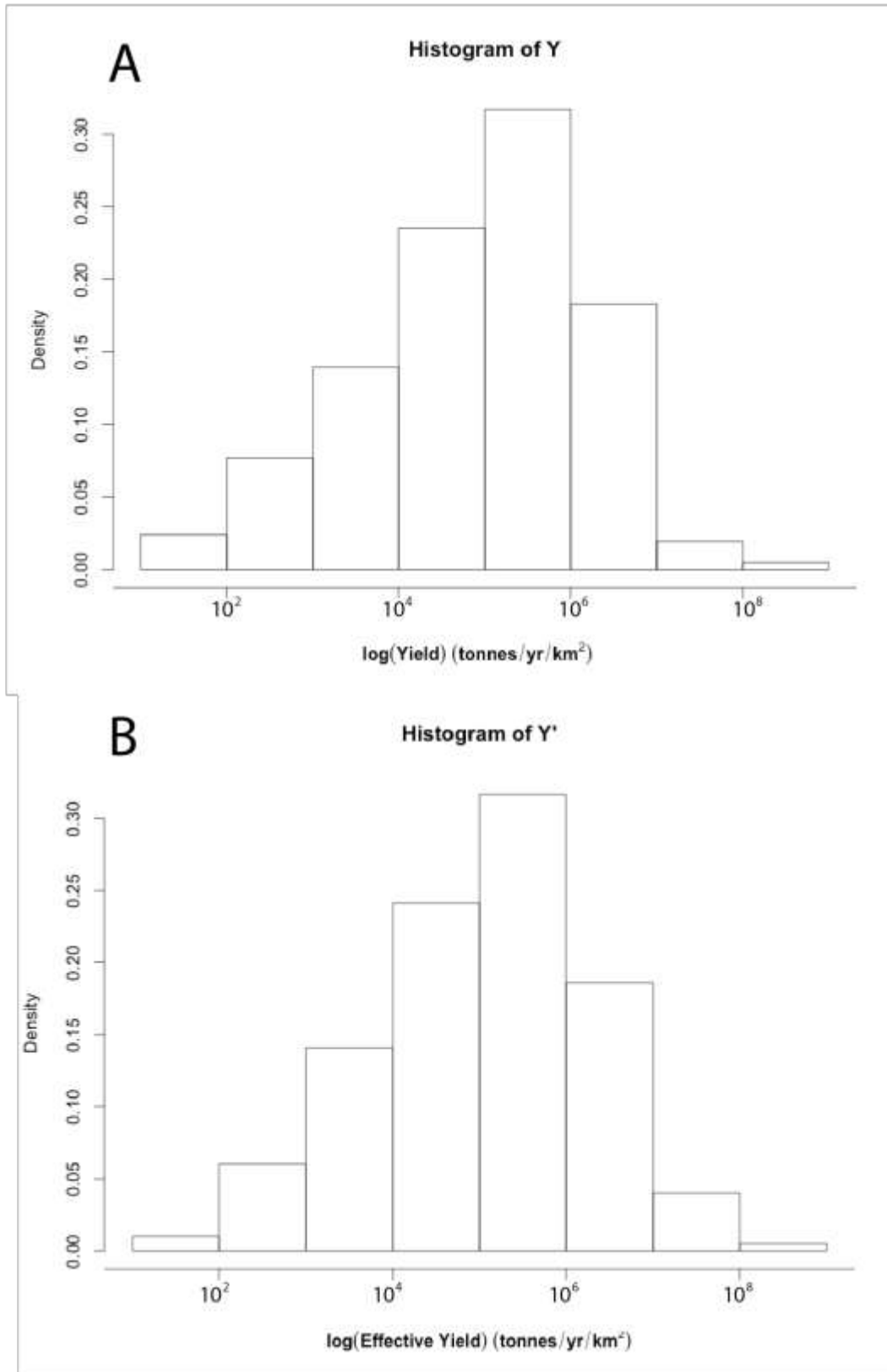


Figure 3: (A) Histogram of sediment yield ( $Y$ ; tonnes<sup>1</sup>km<sup>-2</sup>yr<sup>-1</sup>) in eastern US (n=191). (B) Histogram of effective sediment yield ( $Y'$ ; tonnes<sup>1</sup>km<sup>-2</sup>yr<sup>-1</sup>) in eastern US (n=191).

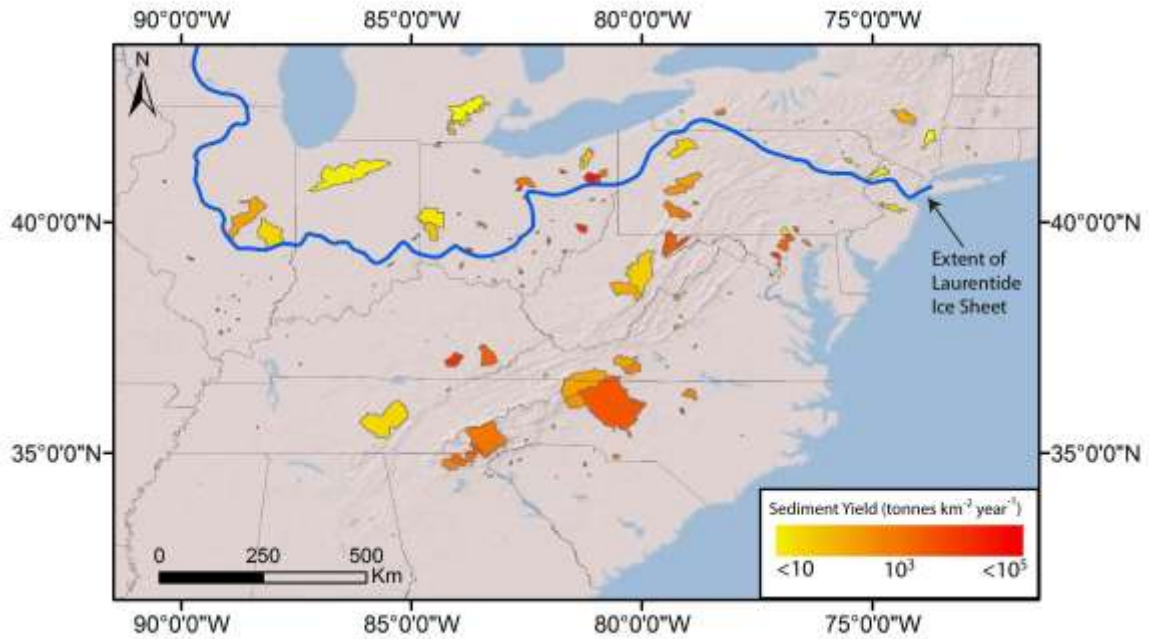


Figure 4: Map showing the spatial distribution of watershed average sediment yield ( $Y$ ,  $\text{tonnes km}^{-2} \text{ yr}^{-1}$ ) in the eastern US.

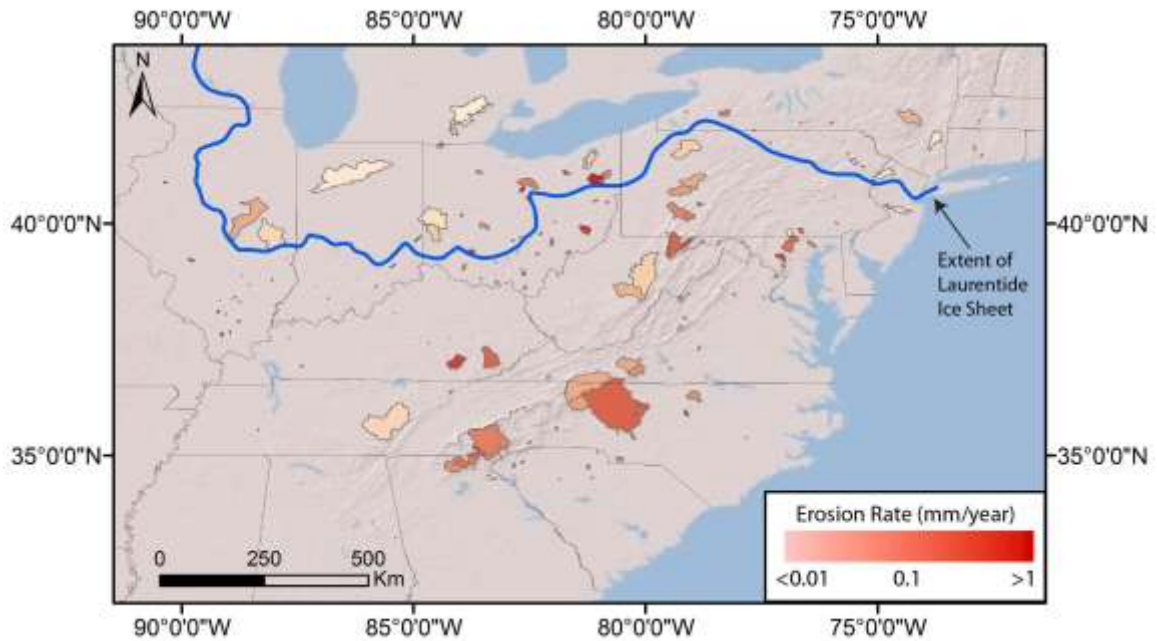


Figure 5: Map showing the spatial distribution of watershed average erosion rate ( $E$ ,  $\text{mmyr}^{-1}$ ) in the eastern US.

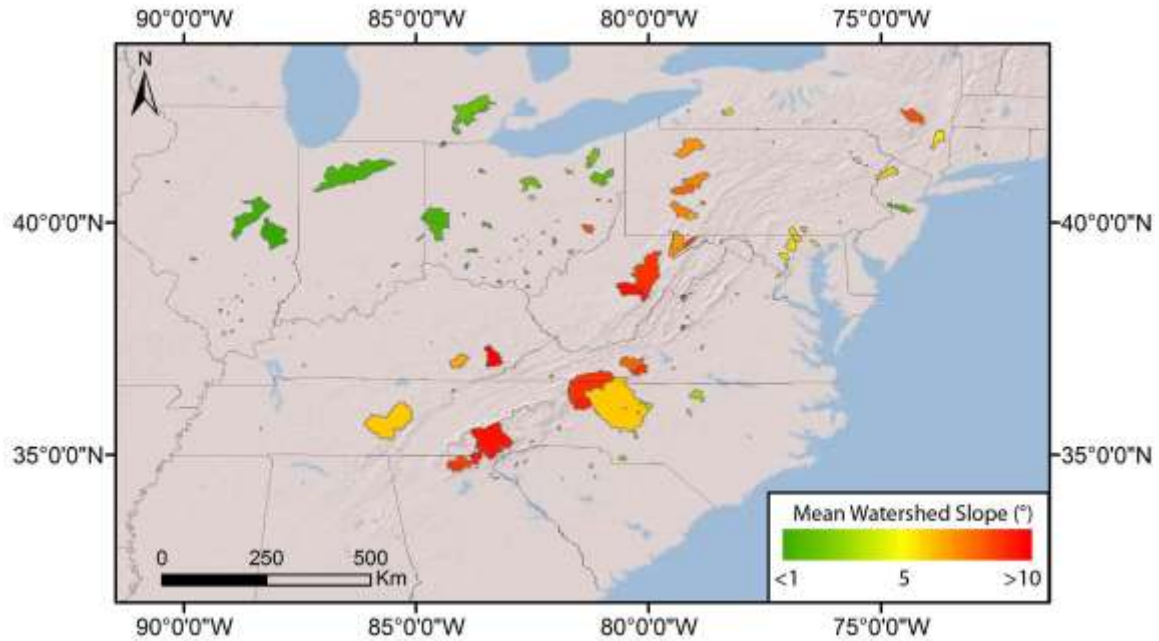


Figure 6: Map showing the spatial distribution of mean watershed slope ( $S$ , degrees) in ResSed watersheds of the northeastern US. Most of the higher  $S$  watersheds are in the Appalachian Mountains Region.

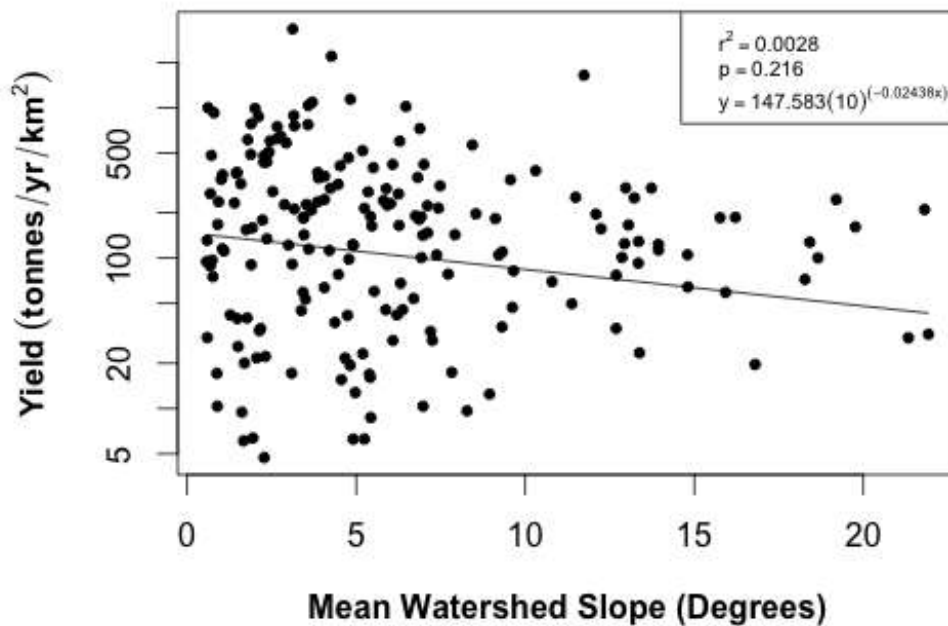


Figure 7: Log-linear scatterplot displaying  $Y$  as a function of mean watershed slope ( $S$ , degrees) for study watersheds in the eastern US. No obvious relationship between  $S$  and  $Y$  is evident.

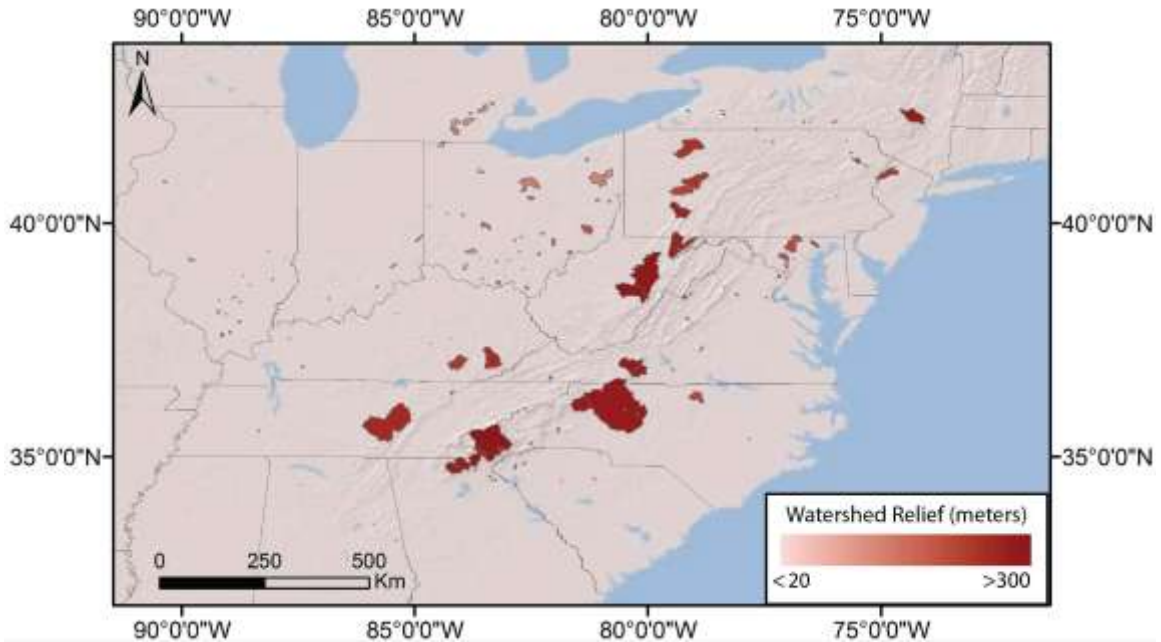


Figure 8: Map showing the spatial distribution of watershed relief ( $K$ , meters) in ResSed watersheds of the northeastern US.

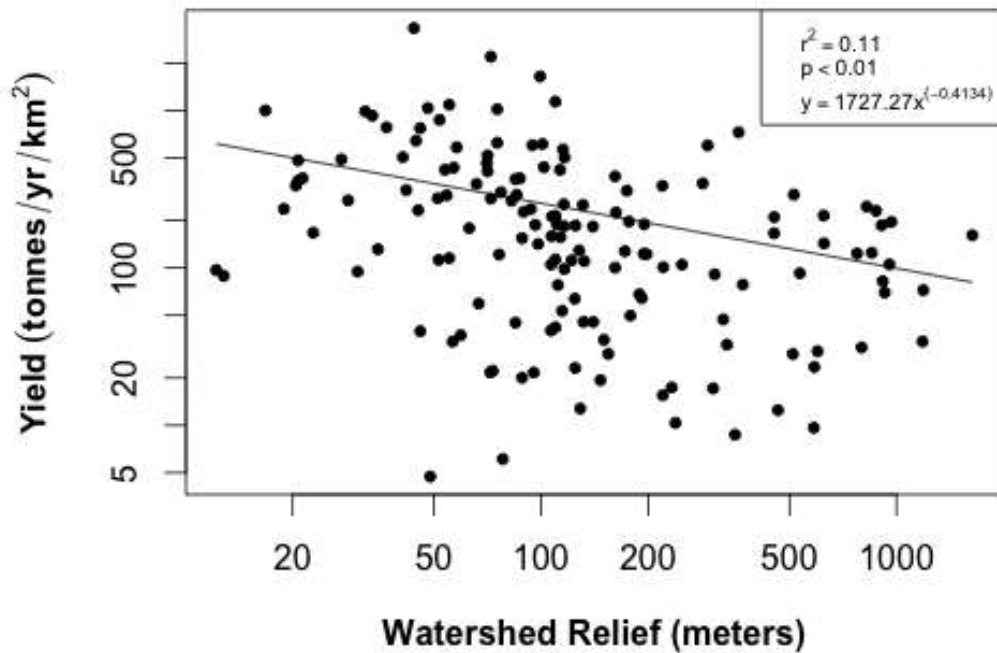


Figure 9: Logarithmic scatterplot depicting sediment yield ( $Y$ ; tonnes  $\text{km}^{-2}\text{yr}^{-1}$ ) as a function of relief ( $K$ , m). Surprisingly, there appears to be a negative relationship between  $Y$  and  $K$ .

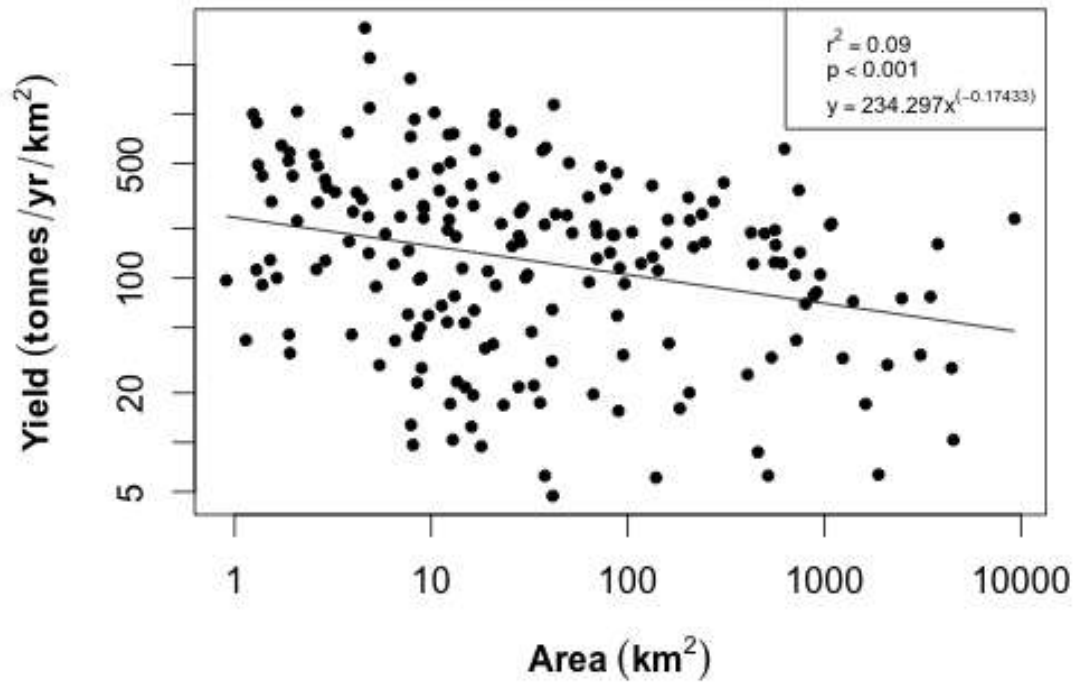


Figure 10: Logarithmic scatterplot displaying  $Y$  as a function of drainage area ( $A$ , km<sup>2</sup>). The inverse power-law relationship between  $A$  and  $Y$  found by Milliman and Syvitski (1992), Renwick et al. (2001), Koppes and Montgomery (2009), and Larsen et al. (2014) is evident.

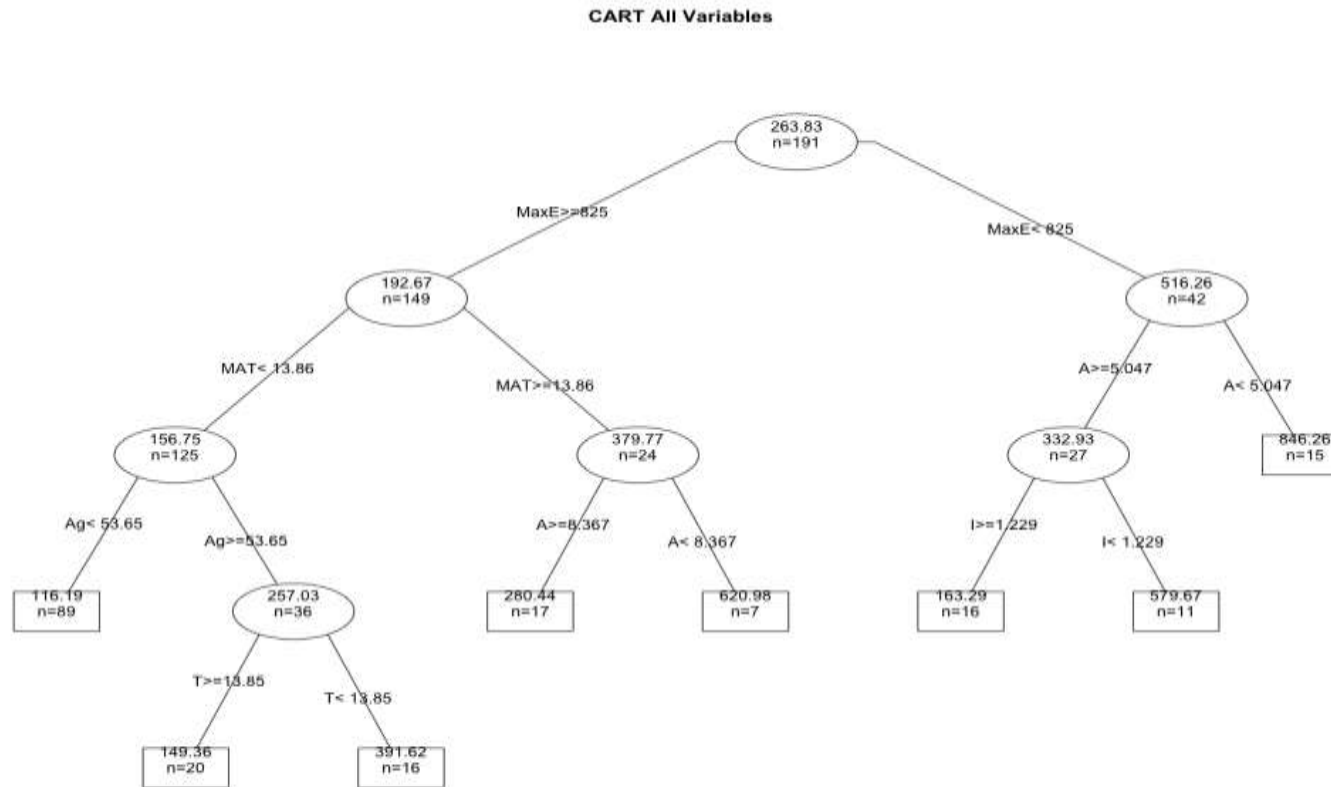


Figure 11: CART analysis performed with all numerical variables. Numbers in circles are the mean  $Y$  values for that particular split. Threshold values are shown on the lines, or “branches” of the tree. The number of study watersheds contained within the split are shown by “ $n=xxx$ ” within circles. Squares represent a terminal node of the tree. The right most terminal node shows that small watersheds ( $<5 \text{ km}^2$ ) lying below 825 m elevation exhibit the highest  $Y$  in the dataset. The tree has been pruned (complexity parameter = 0.05) in order to highlight the most important splits.

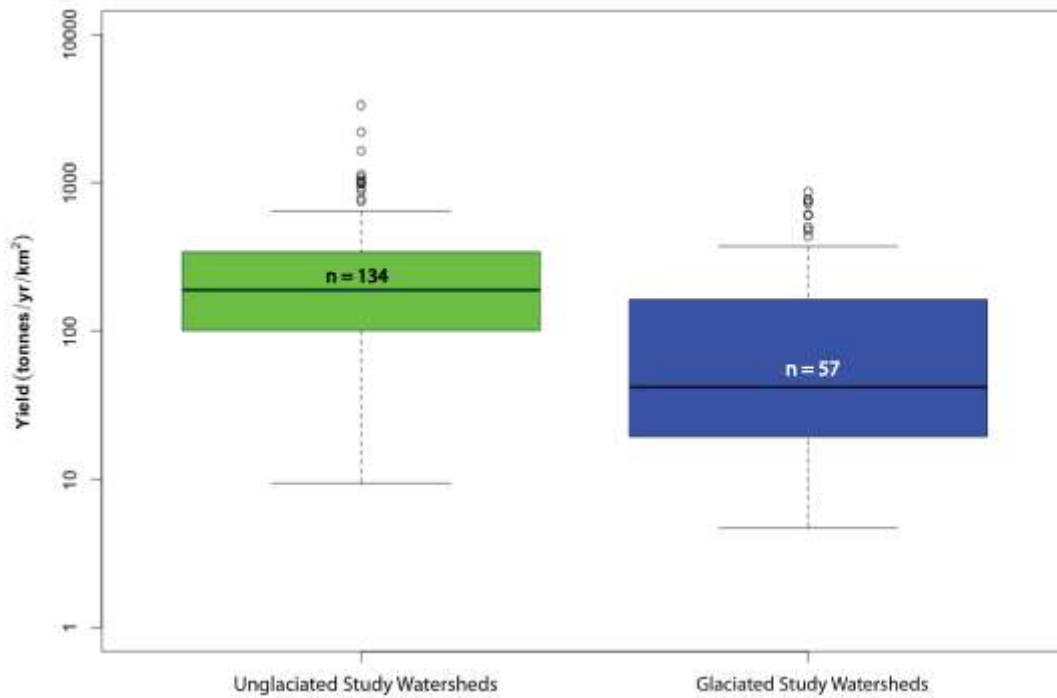


Figure 12: Boxplot showing mean and variability of  $Y$  values for watersheds falling within the extent of the Laurentide ice sheet (blue) and watersheds out of the extent of the Laurentide ice sheet (green). An ANOVA using the Tukey HSD method showed that the means are significantly different from each other.

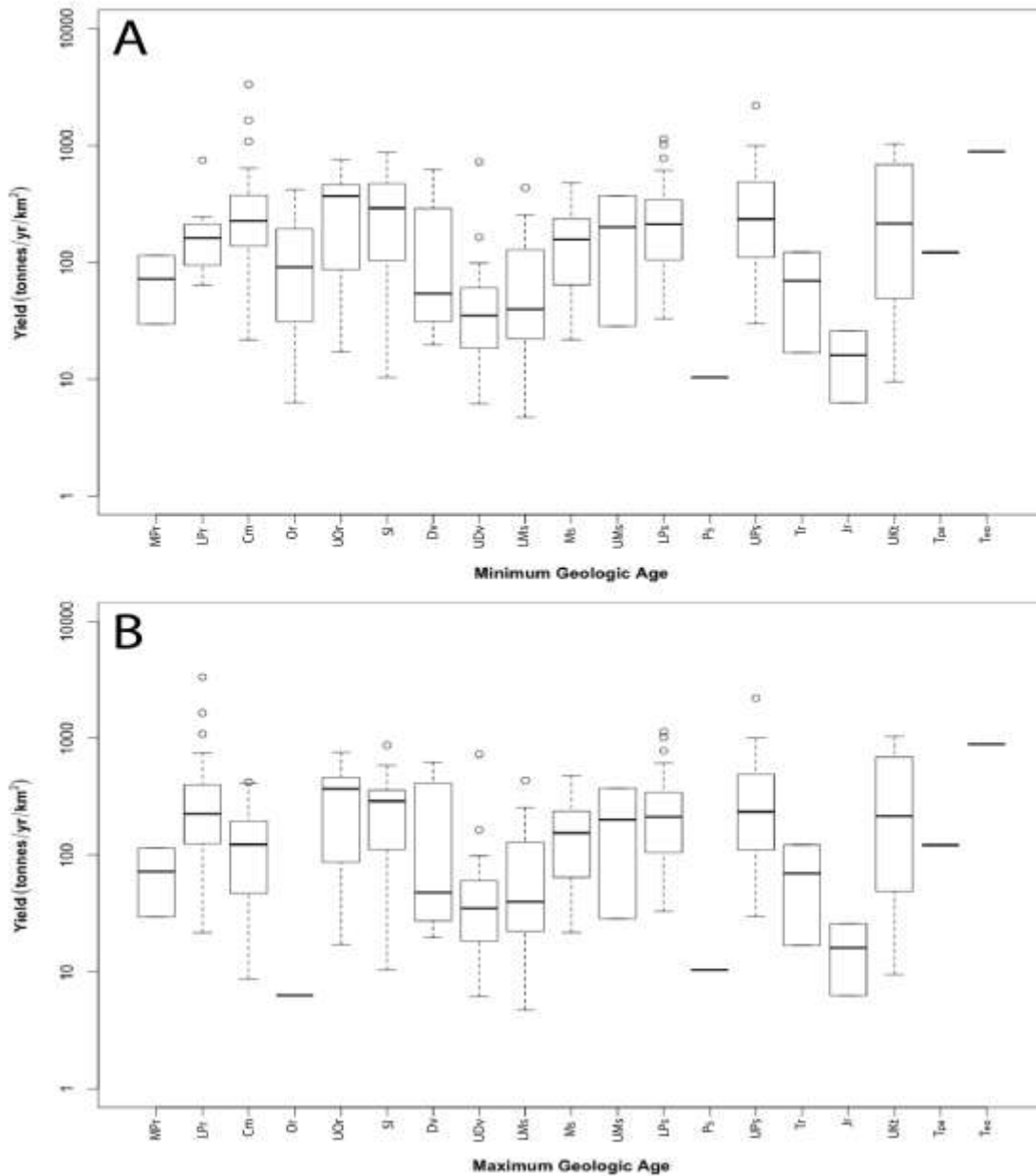


Figure 13: Boxplot depicting  $Y$  arranged chronologically by (A) minimum geologic age of rocks in the study watershed and (B) maximum geologic age of rocks in the study watershed. Geologic age symbols are those used in Wilkinson and McElroy (2007). Watersheds with Jurassic aged rocks appear to have lower  $Y$  than other all other ages, but this result is not statistically significant ( $p=0.35$ ). Symbols, in chronologic order are MPr: Middle Proterozoic, LPr: Late Proterozoic, Cm: Cambrian, Or: Ordovician, UOr: Upper Ordovician, Sl: Silurian, Dv: Devonian, UDv: Upper Devonian, LMs: Lower Mississippian, Ms: Mississippian, UMs: Upper Mississippian, LPs: Lower Pennsylvanian, Ps: Pennsylvanian, Ups: Upper Pennsylvanian, Tr: Triassic, Jr: Jurassic, UKt: Upper Cretaceous, Tpa: Paleocene, Teo: Eocene.

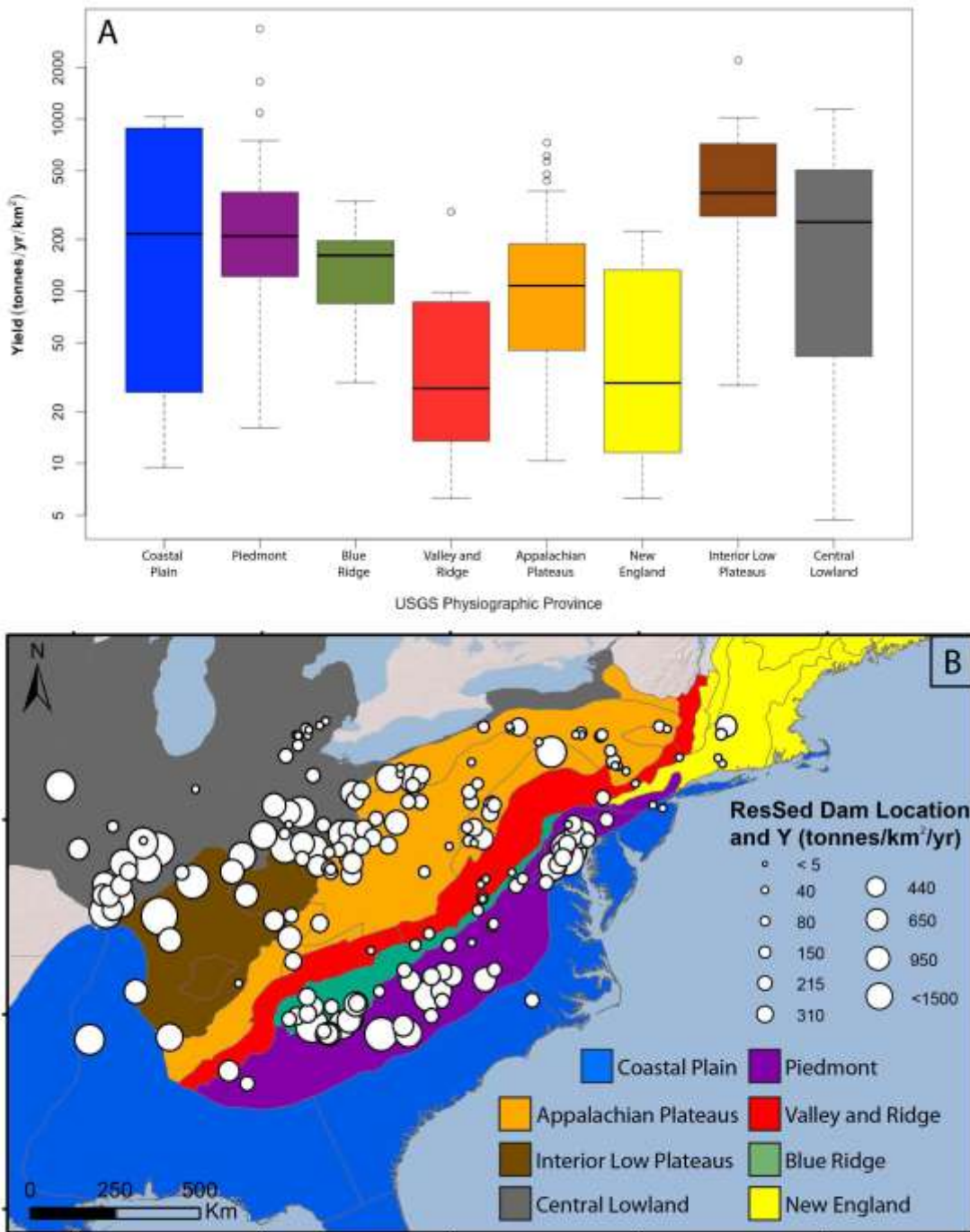


Figure 14: (A) Boxplot showing range of  $Y$  values categorized by USGS physiographic province. The New England (yellow,  $p=0.05$ ) physiographic provinces has statistically significant lower mean  $Y$  values. The Tukey HSD post-hoc test was used to determine significant differences between populations. (B) Map showing study dam locations,  $Y$ , and USGS physiographic provinces in the eastern US.

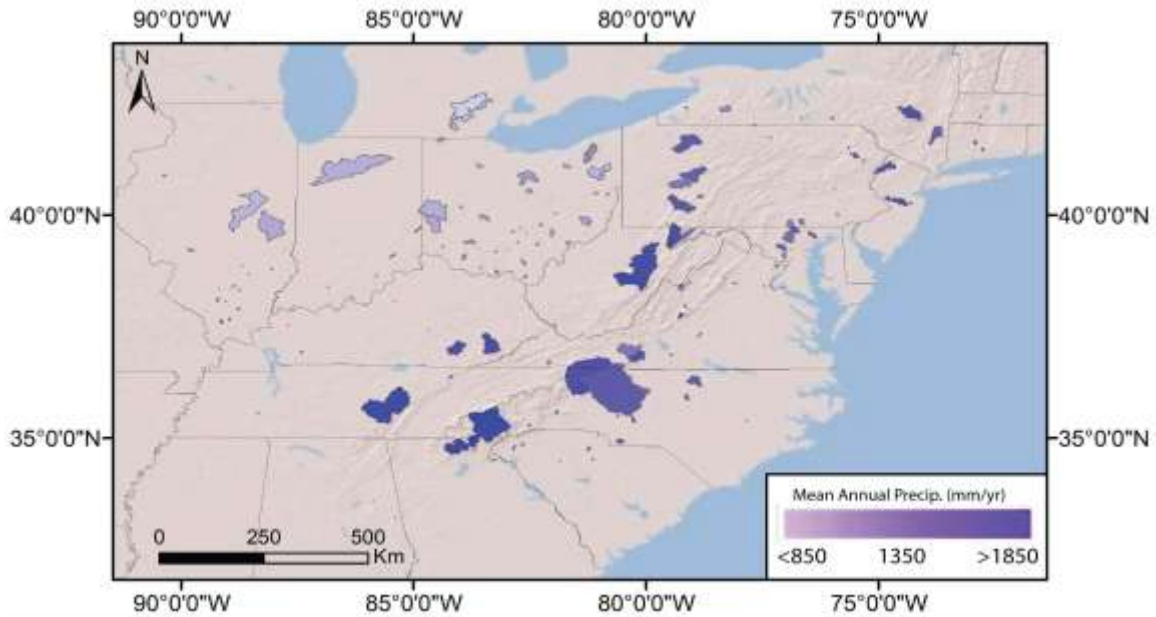


Figure 15: Map depicting the spatial distribution of mean annual precipitation (*MAP*; mm/year; measured between 1961 and 1990) within ResSed watersheds in the eastern US.

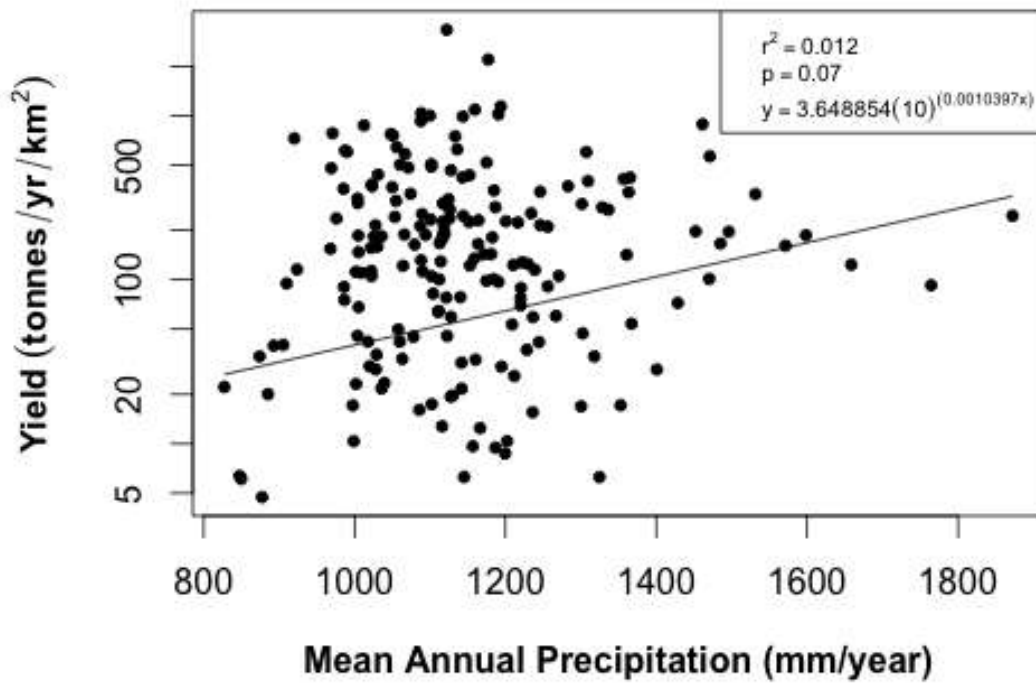


Figure 16: Log-linear scatterplot depicting *Y* as a function of mean annual precipitation (*MAP*; mm/year) within ResSed watersheds in the eastern US.

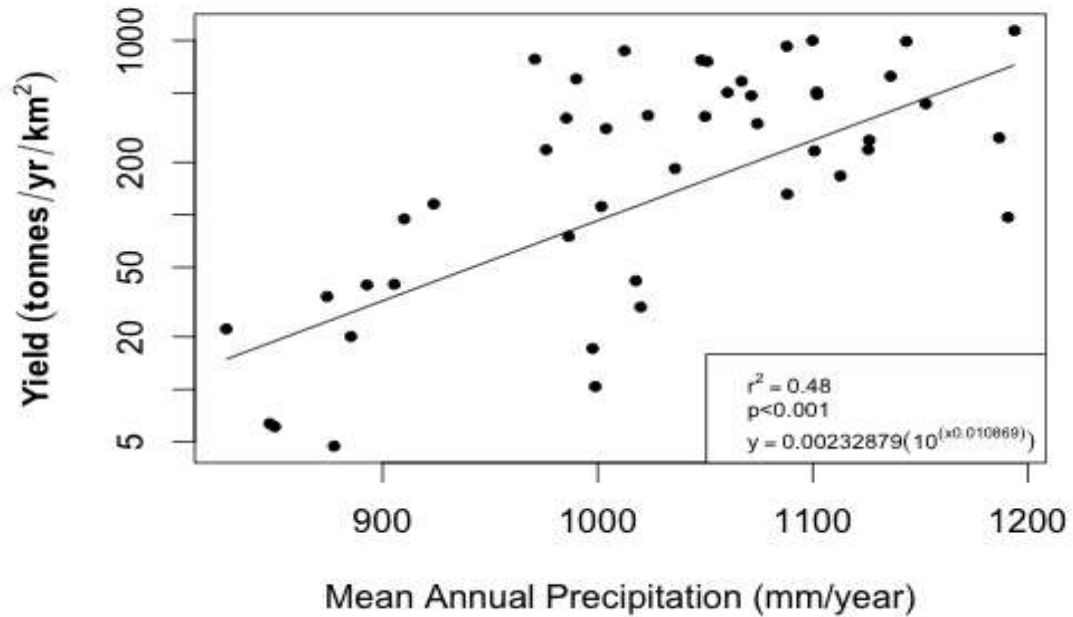


Figure 17: Log-linear scatterplot depicting a significant positive relationship between *Y* and mean annual precipitation (*MAP*; mm/year) within ResSed watersheds located in the Central Lowland physiographic province.

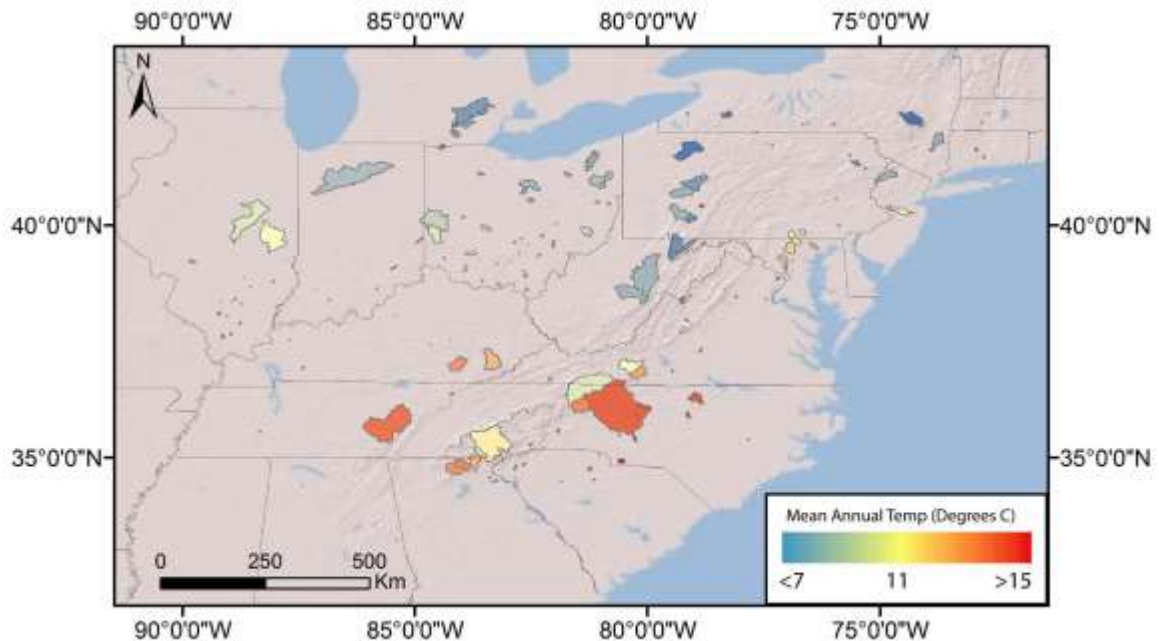


Figure 18: Map showing the spatial distribution mean annual temperature (*MAT*; Degrees Celsius) between 1961 and 1990 within ResSed watersheds in the eastern US.

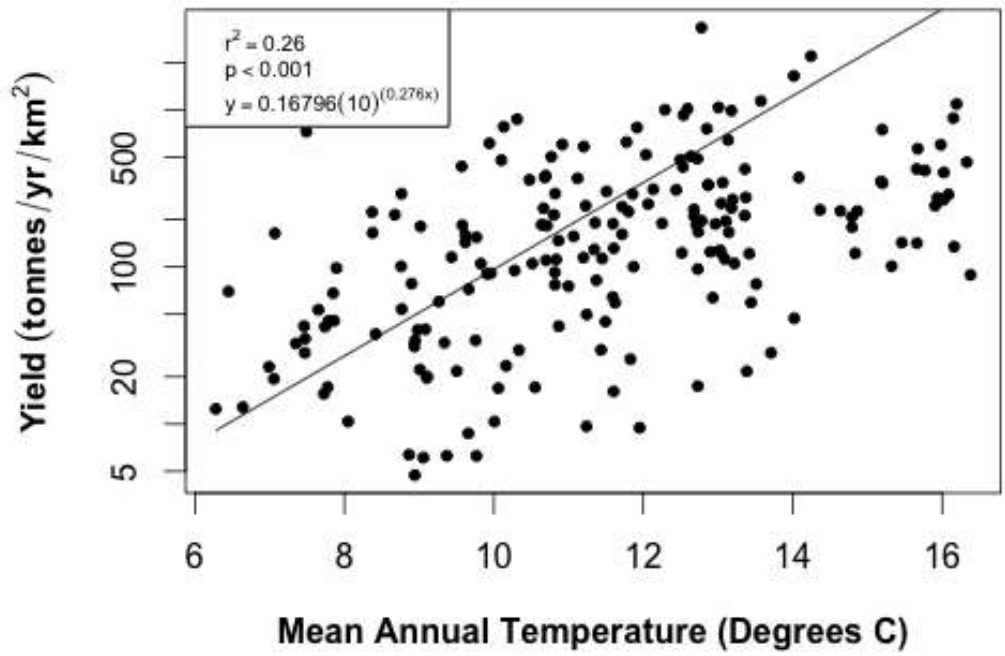


Figure 19: Log-linear scatterplot depicting  $Y$  as a function of mean annual temperature ( $MAT$ ; Degrees C; from 1961-1990). There is a positive relationship between  $MAT$  and  $Y$ .

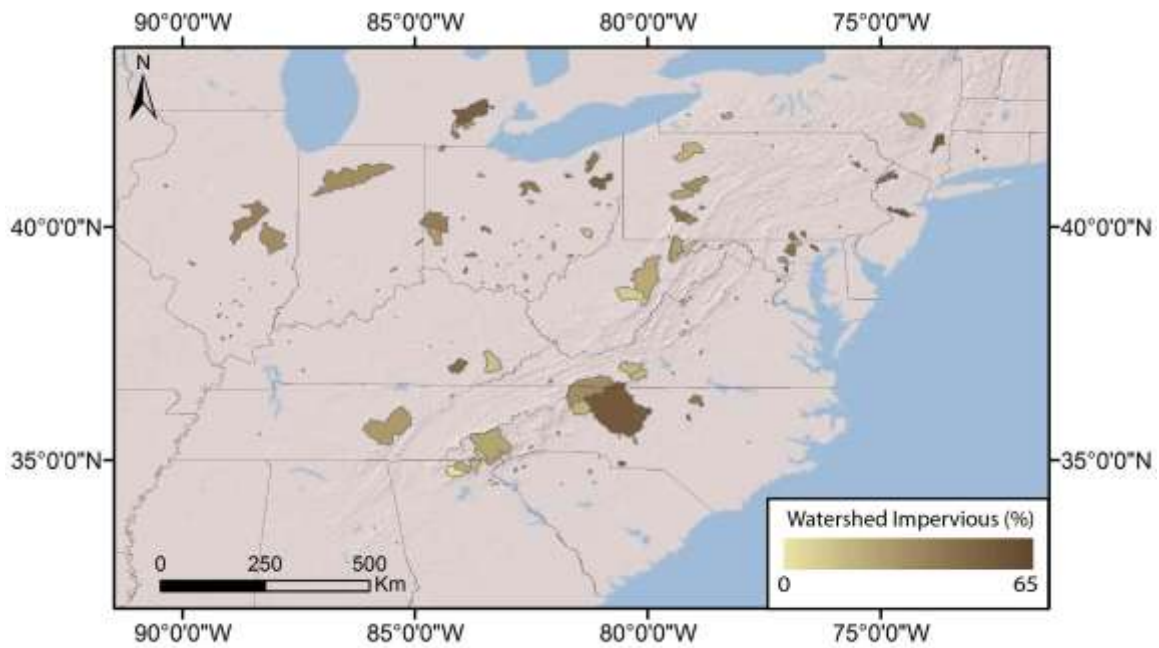


Figure 20: Map showing the spatial distribution of impervious surface percentage of ResSed watersheds ( $I$ , % of watershed) in the eastern US.

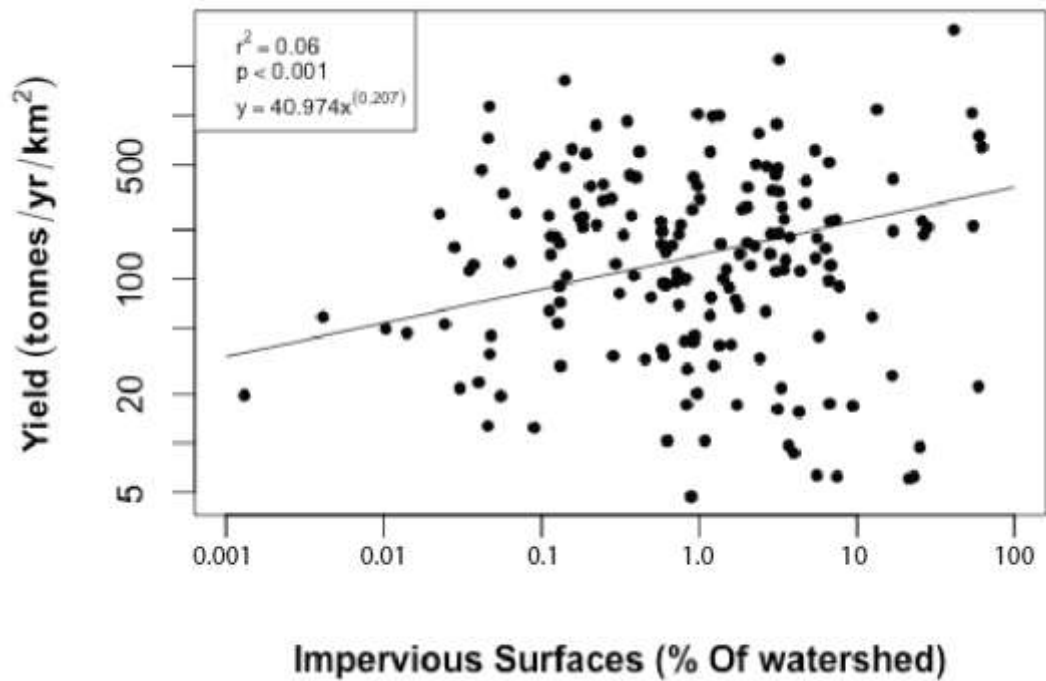


Figure 21: Logarithmic scatterplot depicting  $Y$  as a function of percent watershed impervious surface area ( $I$ ; % of watershed). There is a very weak power law relationship between  $Y$  and  $I$ .

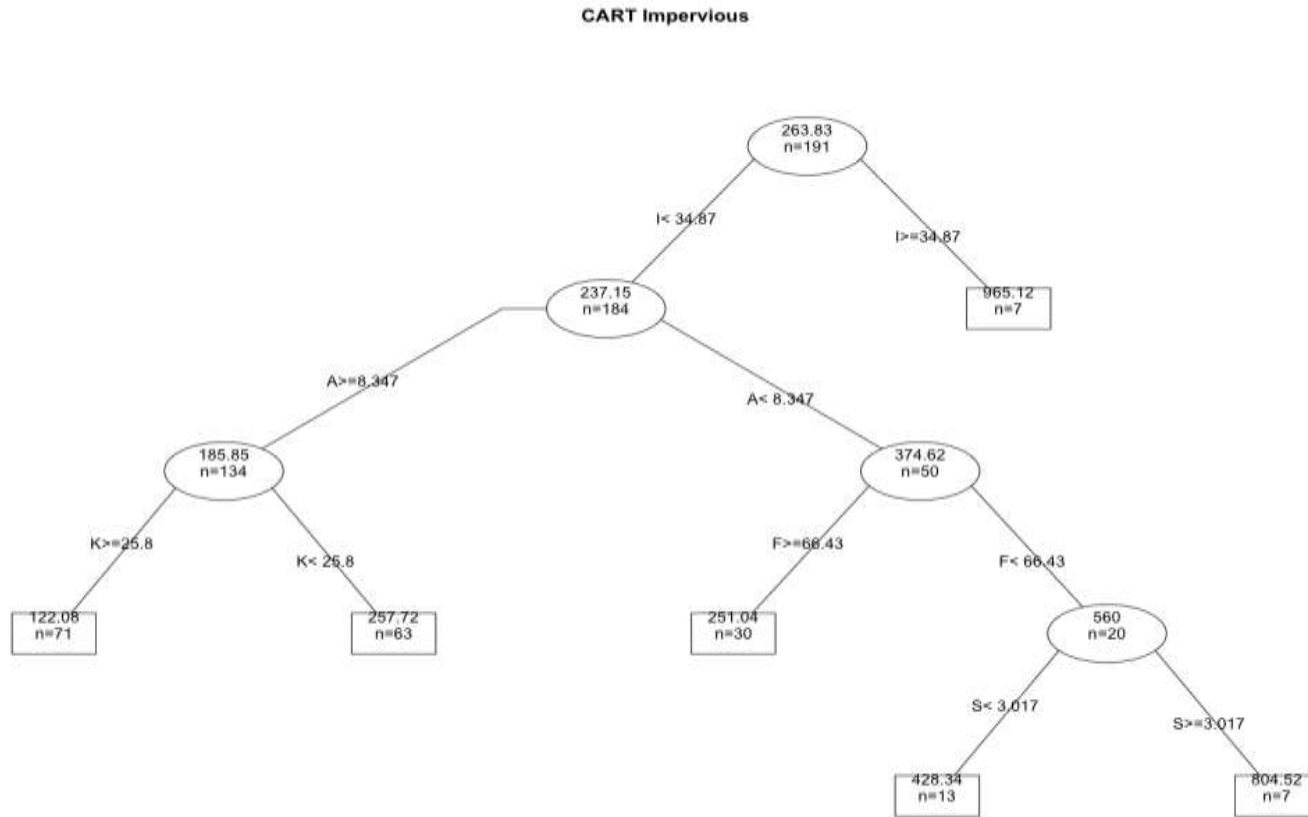


Figure 22: CART analysis showing that watersheds with greater than 34% impervious cover have higher mean  $Y$  than watersheds with less than 34% impervious cover. The numbers in circles are the mean  $Y$  values for that particular split. Threshold values are shown on the lines, or “branches” of the tree. The number of study watersheds contained within the split are shown by “ $n=xxx$ ” within circles. Squares represent a terminal node of the tree.

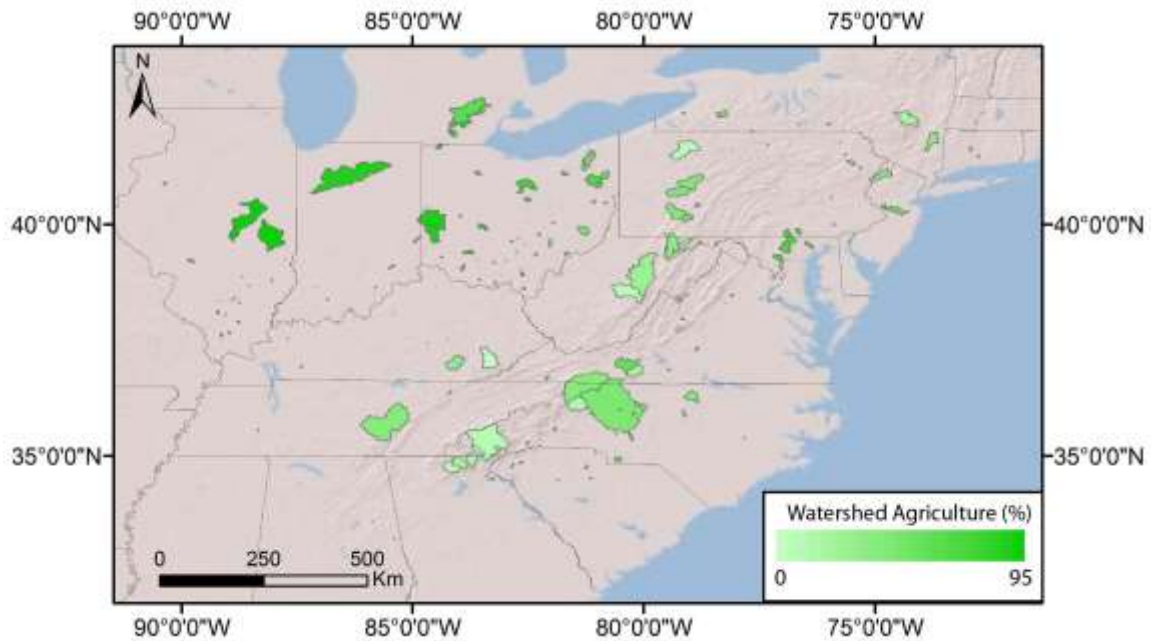


Figure 23: Map showing the spatial distribution of percent agricultural land (*Ag*, %) of ResSed watersheds of the northeastern US.

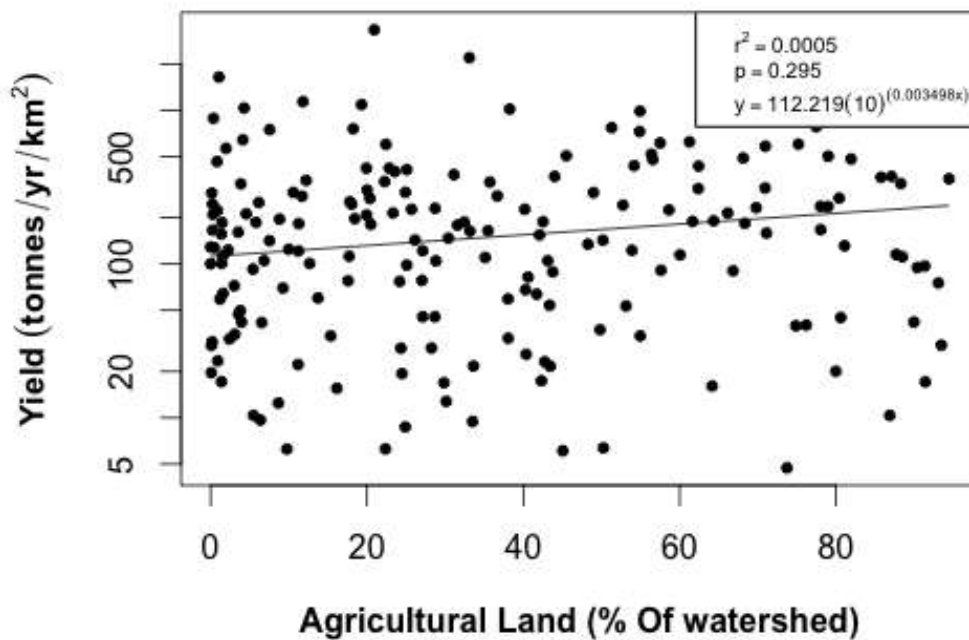


Figure 24: Log-linear scatterplot depicting *Y* as a function of mean watershed agricultural area (*Ag*; % of watershed). There is no relationship between *Y* and *Ag*.

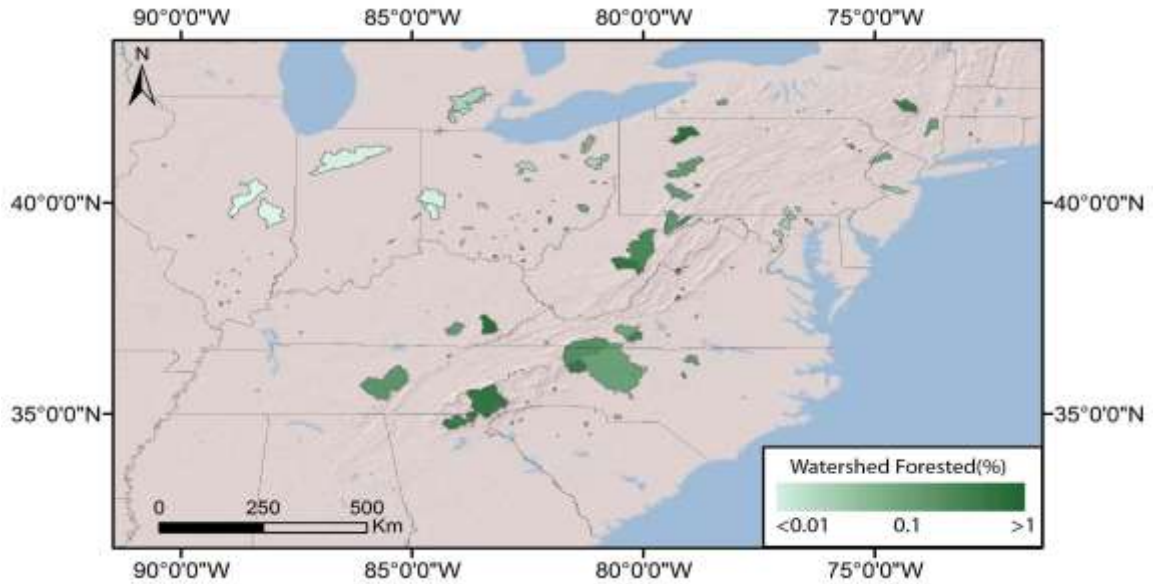


Figure 25: Map showing the spatial distribution of percent forested land by watershed ( $F$ , %) in ResSed watersheds of the northeastern US.

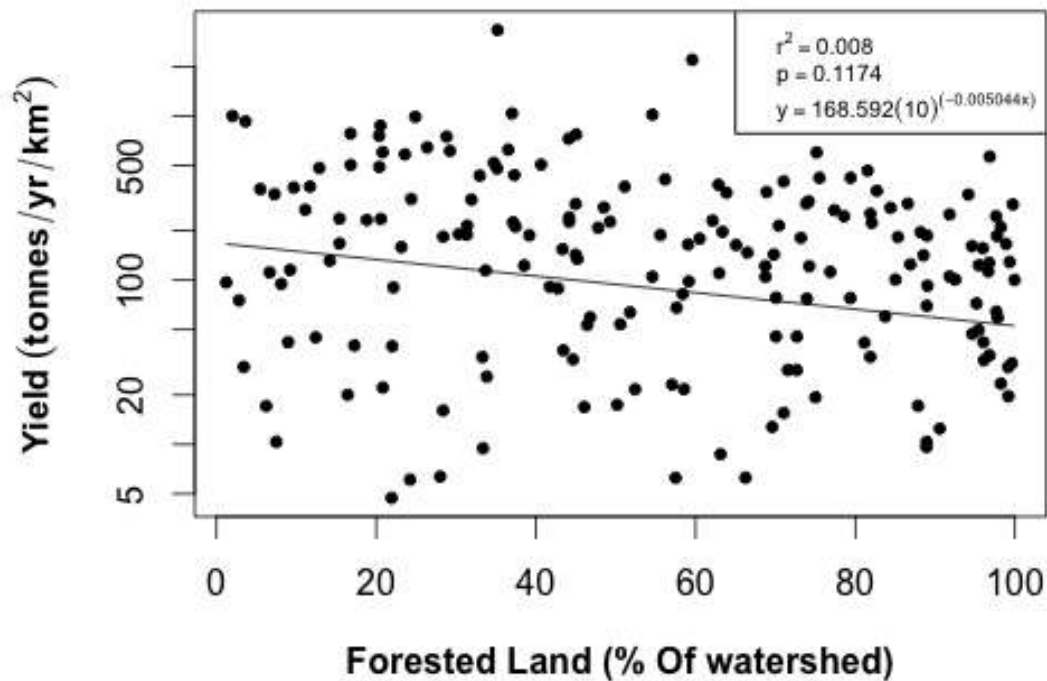


Figure 26: Log-linear plot depicting  $Y$  as a function of mean watershed forested area ( $F$ ; % of watershed). There is no relationship between  $Y$  and  $F$ , shown by the low  $R^2$  value and high  $p$  value.

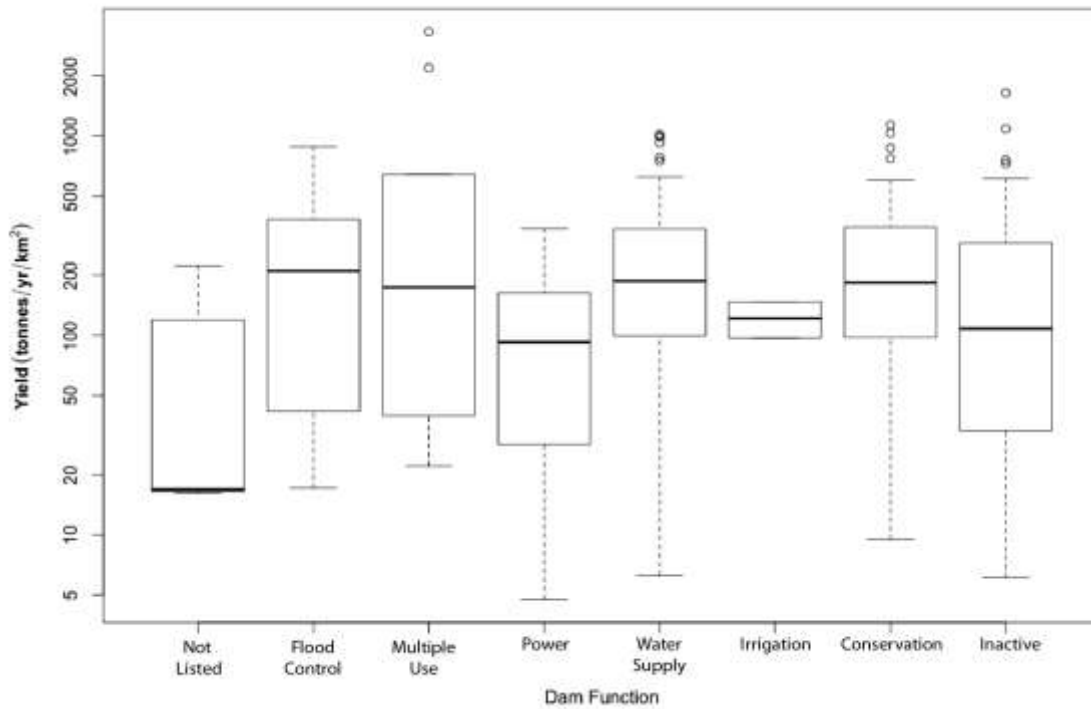


Figure 27: Boxplot depicting  $Y$  sorted by dam functions listed in ResSed. There is no significant difference in mean  $Y$  between study watersheds with different dam functions.

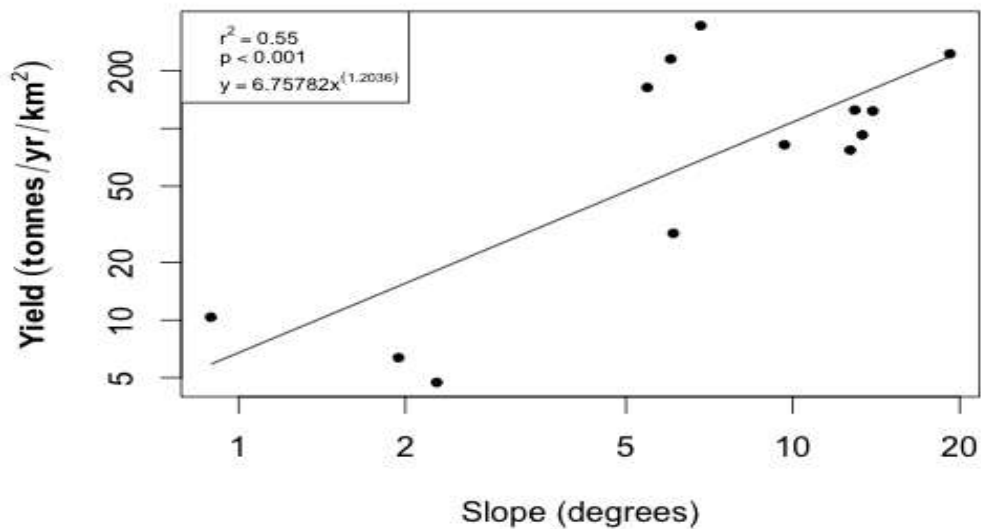


Figure 28: Logarithmic plot depicting  $Y$  as a function of  $S$  for Power dams in the ResSed database. A power-law relationship is evident.

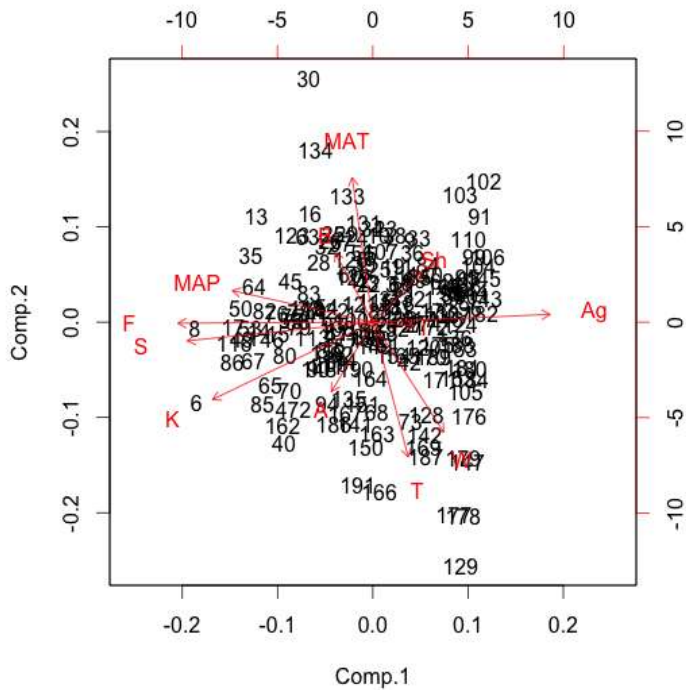


Figure 29: Principal Component Analysis (PCA) biplot showing similarities and relationships between numerical independent variables considered in this study. More data concerning PCA can be found in Appendix 2. Variable names are shown in Table 2. Watershed forested land (*F*) and mean watershed slope (*S*) are the two most closely related variables.

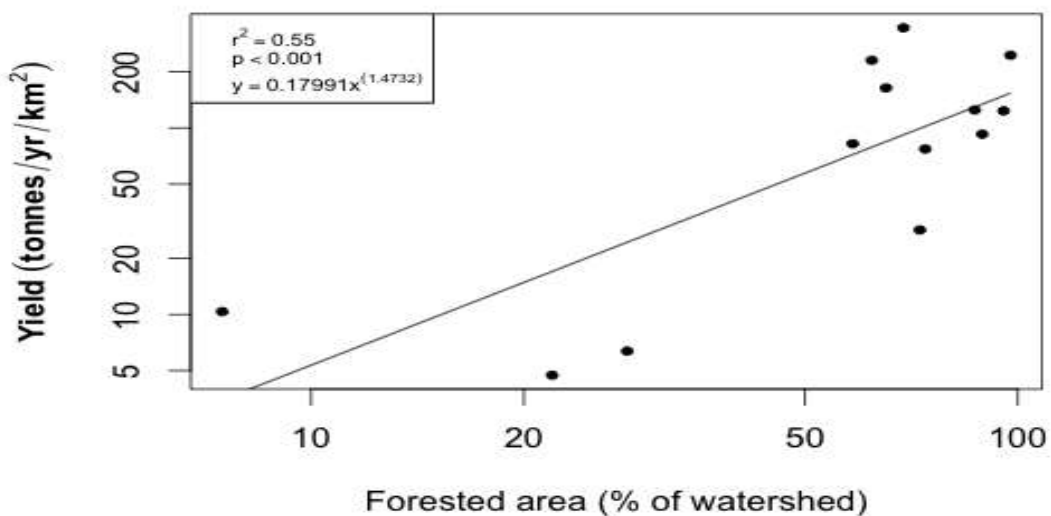


Figure 30: Logarithmic plot depicting *Y* as a function of forested land (*F*; %) for power dams (*n*=13) in the ResSed database. A power-law relationship is evident.

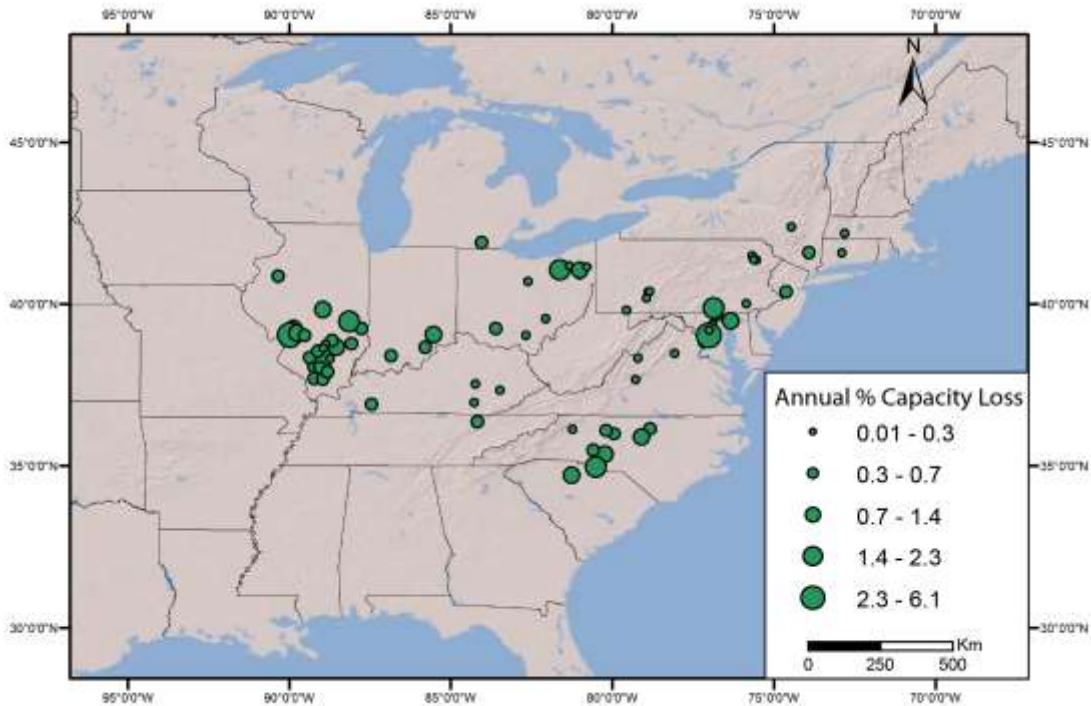


Figure 31: Map depicting annual percent capacity loss for ResSed watersheds where capacity data is available (n=76 study watersheds).

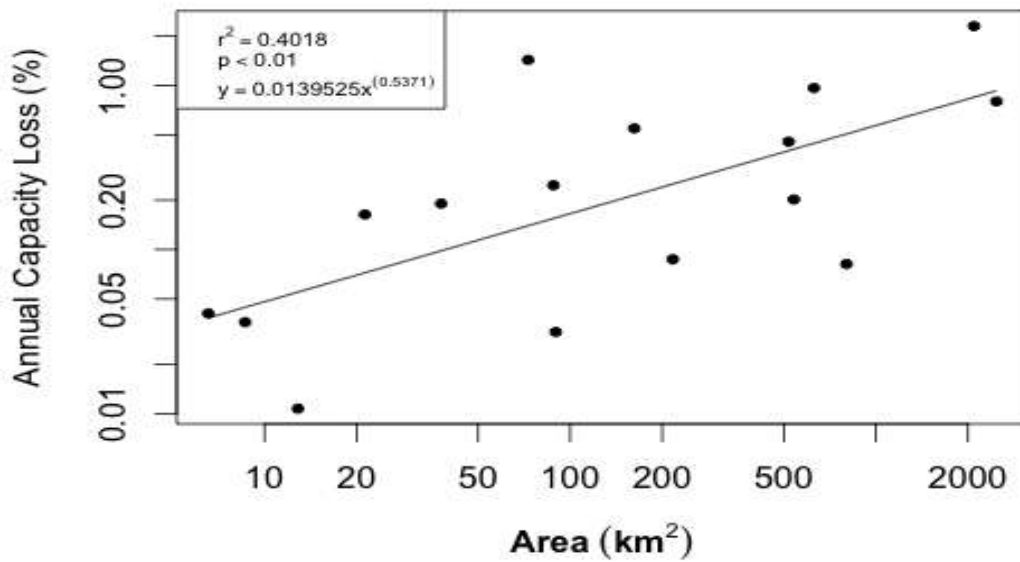


Figure 32: Logarithmic plot depicting annual percent capacity loss ( $C$ ; %) as a function of drainage area ( $A$ , km<sup>2</sup>) for formerly glaciated ResSed watersheds in the eastern US. ResSed watersheds with available capacity data. A power law relationship is evident.

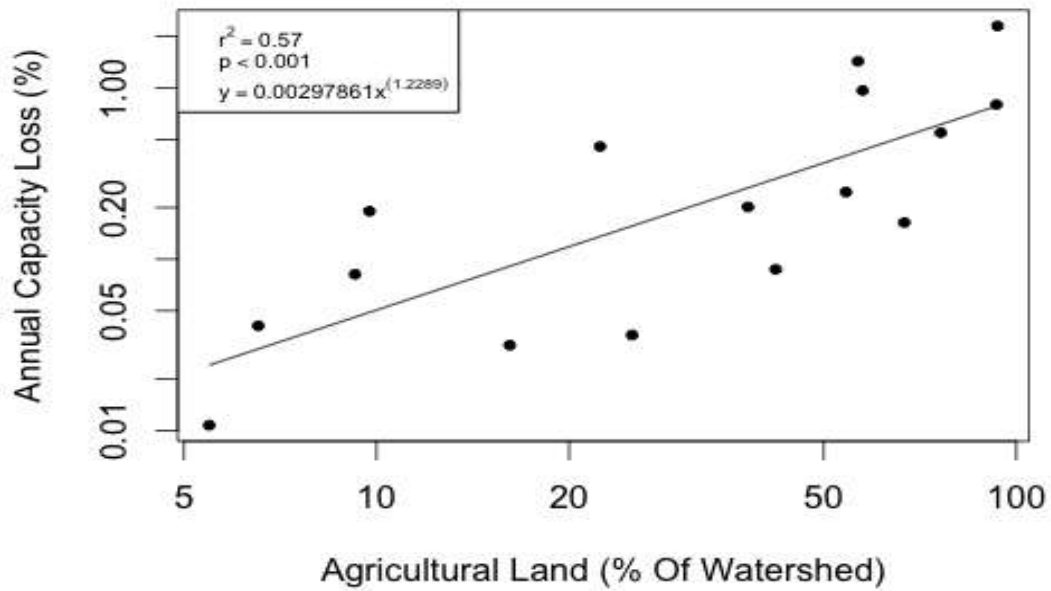


Figure 33: Logarithmic scatterplot depicting Annual percent capacity loss ( $C$ ; %) as a function of percent agricultural land ( $Ag$ , % of watershed) for formerly glaciated ResSed watersheds in the eastern US ResSed watersheds with available capacity data. A power law relationship is evident.

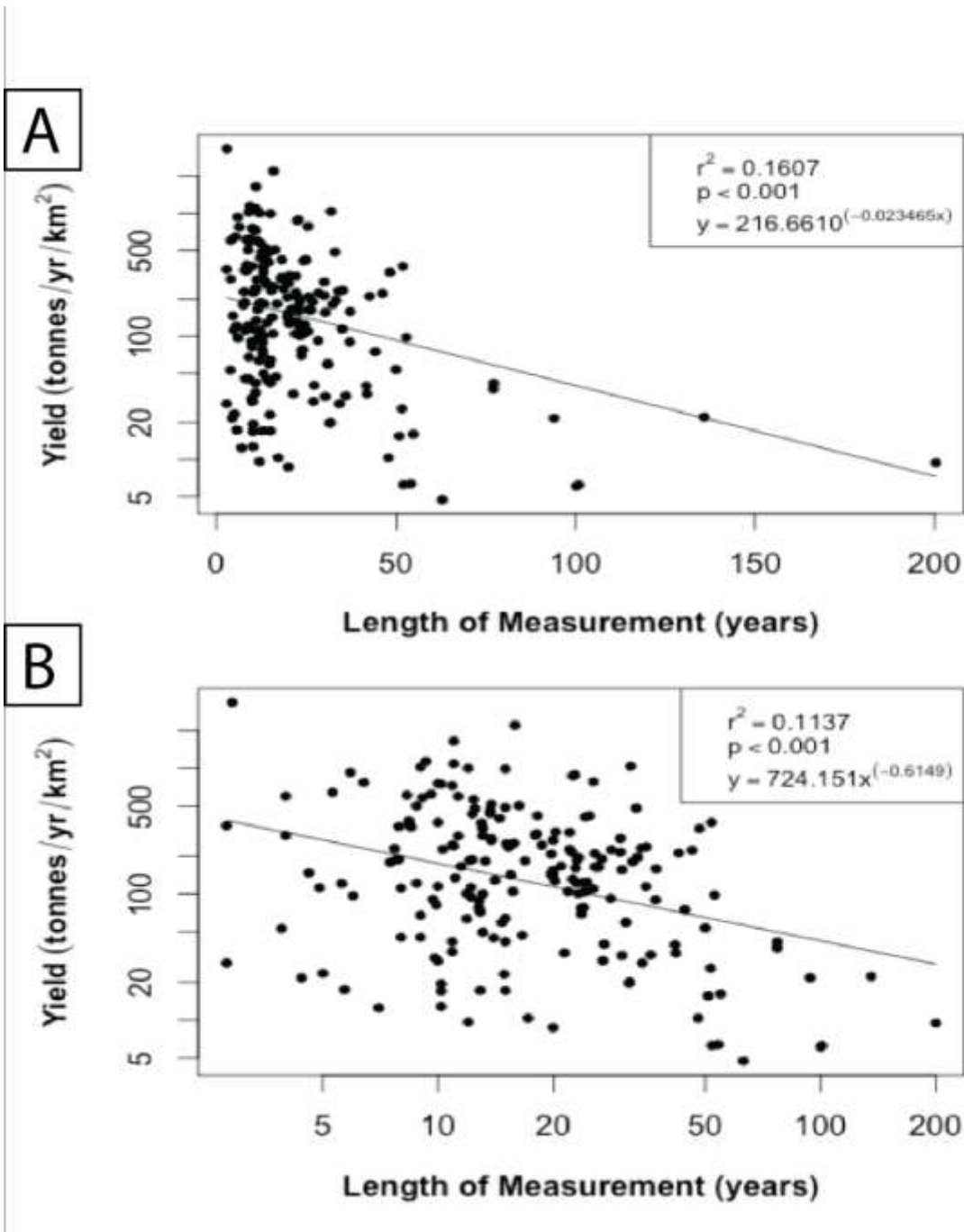


Figure 34: Scatterplots depicting the Sadler Effect within ResSed data. *Y* tends to decrease with increasing timescale of measurement. (A) Illustrates decreasing *Y* with increasing timescale of measurement on a logarithmic *x* axis. (B) Illustrates decreasing *Y* with increasing timescale of measurement on a linear *x* axis.

## 7. References

- Ackerman, K.V., D.M. Mixon, E.T. Sundquist, R.F. Stallard, G.E. Schwarz, and D.W. Stewart, 2009. RESIS-II—An updated version of the original Reservoir Sedimentation Survey Information System (RESIS) database: U.S. Geological Survey Data Series 434. <http://pubs.usgs.gov/ds/ds434>.
- Ahnert, F., 1970. Functional relationships between denudation, relief, and uplift in large, mid-latitude drainage basins. *American Journal of Science*, 268(3): 243-263.
- Anderson, R. J., Bledsoe, B. P., and W.C. Hession, 2004. Width of streams and rivers in response to vegetation, bank material, and other factors. *JAWRA Journal of the American Water Resources Association* 40(5): 1159-1172.
- Arnold, C. L., and C. J. Gibbons, 1996. Impervious surface coverage: the emergence of a key environmental indicator. *Journal of the American Planning Association* 62(2): 243-258. doi: 10.1080/01944369608975688.
- Barlow, R. J., 1989. *Statistics: a guide to the use of statistical methods in the physical sciences* (Vol. 29). John Wiley & Sons.
- Bertness, M. D., C. Crain, C. Holdredge, and N. Sala, 2008. Eutrophication and consumer control of New England salt marsh primary productivity. *Conservation Biology* 22(1): 131-139. doi: 10.1111/j.1523-1739.2007.00801.x.
- Beschta, R. L., 1978. Long-term patterns of sediment production following road construction and logging in the Oregon Coast Range. *Water Resources Research*, 14(6): 1011-1016, doi: 10.1029/WR014i006p01011.
- Bierman, P., A. Lini, P. Zehfuss, A. Church, P.T. Davis, J. Southon, and L. Baldwin, 1997. Postglacial ponds and alluvial fans: Recorders of Holocene landscape history. *GSA Today* 7(10): 1-8.
- Bierman, P., J. Howe, E. Stanley-Mann, M. Peabody, J. Hilke, and C.A. Massey, 2005. Old images record landscape change through time. *GSA Today* 15(4): 4-10, doi: 10.1130/1052-5173(2005)015<4:OIRLCT>2.0.CO;2.
- Breiman, L, J. Friedman, R. Olshen. R., and C. Stone, 1984. "Classification and Regression Trees". The WadsWorth Statistics/Probability Series. WadsWorth, Belmont, California, 19841.
- Brown, C.B., 1944. Discussion in *Sedimentation in Reservoirs*, edited by B.J. Witzig, *Translations of American Society of Civil Engineering* 109: 1047-1106.

- Burbank, D. W., Blythe, A. E., Putkonen, J., Pratt-Sitaula, B. G. A. B. E. T., Gabet, E., Oskin, M., and T.P. Ojha, 2003. Decoupling of erosion and precipitation in the Himalayas. *Nature*, 426(6967), 652-655.
- Conlon, M., 2013, September. A hindcast comparing field observation of the response of the Souhegan River to dam removal with simulations of the dam removal express assessment model-1. M.Sc Thesis. 95 p. Department of Geology and Geophysics, Boston College.
- De'ath, G., and Fabricius, K. E. (2000). Classification and regression trees: a powerful yet simple technique for ecological data analysis. *Ecology* 81(11): 3178-3192.
- Dendy, F. E., and W. A. Champion, 1978. Sediment deposition in U.S. reservoirs: Summary of data reported through 1975. US Dept. of Agriculture, Agricultural Research Service 1362: 1-68.
- Dendy, F. M., W. A., Champion, and R.B. Wilson, 1973. Reservoir sedimentation surveys in the United States. *Geophysical Monograph Series* 17: 349-357, doi:10.1029/GM017p0349.
- Dubé, S., A.P. Plamondon, and R.L. Rothwell, 1995. Watering up after clear-cutting on forested wetlands of the St. Lawrence lowland. *Water Resources Research* 31(7): 1741-1750, doi: 10.1029/95WR00427.
- FitzGerald, D. M., M.S. Fenster, B.A. Argow, and I.V. Buynevich, 2008. Coastal impacts due to sea-level rise. *Annual Review of Earth and Planetary Sciences* 36: 601-647, doi: 10.1146/annurev.earth.35.031306.140139.
- FitzGerald, D., M. Kulp, Z. Hughes, I. Georgiou, M. Miner, S. Penland, and N. Howes, 2007. Impacts of rising sea level to backbarrier wetlands, tidal inlets, and barrier islands: Barataria Coast, Louisiana. *Coastal Sediments '07*: 1179-1192, doi: 10.1061/40926(239)91.
- Flores, A. N., B.P. Bledsoe, C.O. Cuhaciyan, and E.E. Wohl, 2006. Channel-reach morphology dependence on energy, scale, and hydroclimatic processes with implications for prediction using geospatial data. *Water Resources Research*, 42(6), doi: 10.1029/2005WR004226.
- Foster, D. R., 1992. Land-use history (1730-1990) and vegetation dynamics in central New England, USA. *Journal of Ecology* 80(4): 753-771.
- Gardner, T. W., Jorgensen, D. W., Shuman, C., and C.R. Lemieux, 1987. Geomorphic and tectonic process rates: Effects of measured time interval. *Geology*, 15(3), 259-261.

Graf, W. L., E. Wohl, T. Sinha, and J.L. Sabo, 2010. Sedimentation and sustainability of western American reservoirs. *Water Resources Research* 46(12), doi: 10.1029/2009WR008836.

Gray, J., D. Stewart, E. McFaul, K. Laurent, G. Schwarz, J. Bernard, J. Stinson, M. Jonas, J. Webb, and T. Randle, 2010. Development of a national, dynamic reservoir sedimentation database. Proceedings of the 2nd Joint Federal Interagency Conference (June 27-July 1, 2010), Las Vegas, NV. 172 p.

Griffiths, P. G., R. Hereford, and R.H. Webb, 2006. Sediment yield and runoff frequency of small drainage basins in the Mojave Desert, USA. *Geomorphology* 74(1): 232-244, doi :10.1016/j.geomorph.2005.07.017.

Hicks, D. M., J. Hill, and U. Shankar, 1996. Variation of suspended sediment yields around New Zealand: the relative importance of rainfall and geology. IAHS publication, 149-156.

Hooke, R. L., 1994. On the efficacy of humans as geomorphic agents. *GSA Today*, 4(9), 217, doi : 10.1130/0091-7613(2000)28<843:OTHOHA>2.0.CO;2.

Hothorn, T, and B.S. Evritt, 2009. *A Handbook of Statistical Analyses Using R*, Second Edition. : 9781420079333: Science & Mathematics Books @ Amazon.com. CRC Press.

Jerolmack, D. J., and C. Paola, 2010. Shredding of environmental signals by sediment transport. *Geophysical Research Letters*, 37(19).

Jerolmack, D. J., and P. Sadler, P, 2007. Transience and persistence in the depositional record of continental margins. *Journal of Geophysical Research: Earth Surface* (2003–2012), 112(F3).

Joliffe, I., 2005. *Principal component analysis*. John Wiley & Sons, Ltd.

Kasprak, A., 2008, May. *Measuring Sedimentation Rates and Land-Use Change in a Dam-Influenced Lake Delta: Narraguagus River, Maine*. B.S. Thesis. 79 p. Department of Geology and Geophysics, Boston College.

Kirchner, J. W., C.R. Finkel, C.S. Riebe, D.E. Granger, J.L. Clayton, J.G. King, and W.F. Megahan, 2001. Mountain erosion over 10 yr, 10 ky, and 10 my time scales. *Geology*, 29(7): 591-594, doi: 10.1130/0091-7613(2001)029<0591:MEOYKY>2.0.CO;2

Knox, J. C., 1972. Valley Alluviation in Southwestern Wisconsin. *Annals of the Association of American Geographers* 62(3): 401-410, doi: 10.1111/j.1467-8306.1972.tb00872.x.

Koppes, M. N., and D.R. Montgomery, 2009. The relative efficacy of fluvial and glacial erosion over modern to orogenic timescales. *Nature Geoscience*, 2(9): 644-647.

Langbein, W. B., and S.A. Schumm, 1958. Yield of sediment in relation to mean annual precipitation. *Transactions, American Geophysical Union*, 39: 1076-1084.

Leeder, M. R., T. Harris, and M.J. Kirkby, 1998. Sediment supply and climate change: implications for basin stratigraphy. *Basin Research* 10(1): 7-18, doi: 10.1046/j.1365-2117.1998.00054.x.

Matson, P. A., W.J. Parton, A.G. Power, and M.J. Swift, 1997. Agricultural intensification and ecosystem properties. *Science*, 277(5325): 504-509, doi: 10.1126/science.277.5325.504

Meade, R. H., 1982. Sources, sinks, and storage of river sediment in the Atlantic drainage of the United States. *The Journal of Geology* 90(3): 235-252, doi: 0022-1376829003-002\$1.00.

Merritts, D., R. Walter, M. Rahnis, J. Hartranft, S. Cox, A. Gellis, N. Potter, W. Hilgartner, M. Langland, L. Manion, C. Lippincott, S. Siddiqui, Z. Rehman, C. Scheid, L. Kratz, A. Shilling, M. Jenschke, K. Datin, E. Cranmer, A. Reed, D. Matuszewski, M. Voli, E. Ohlson, A. Neugebauer, A. Ahamed, C. Neal, A. Winter, and S. Becker, 2011. Anthropocene streams and base-level controls from historic dams in the unglaciated mid-Atlantic region, USA. *Philosophical Transactions of the Royal Society A: Mathematical, Physical and Engineering Sciences* 369(1938): 976-1009, doi: 10.1098/rsta.2010.0335.

Milliman, J. D., and J.P. Syvitski, 1992. Geomorphic/tectonic control of sediment discharge to the ocean: the importance of small mountainous rivers. *The Journal of Geology* 100(5): 525-544, doi: 0022-1376/92/10005-00\$1.00.

Milliman, J. D., and R.H. Meade, 1983. World-wide delivery of river sediment to the oceans. *The Journal of Geology* 91(1): 1-21, doi: 0022-13768379101-002\$1.00.

Milliman, J. D., Y.S. Gin, M.E. Ren, and Y. Saito, 1987. Man's influence on the erosion and transport of sediment by Asian rivers: The Yellow River (Huanghe) example. *Journal of Geology* 95(6), 751-762, doi: 0022-1376/87/9506-0004\$1.00.

Minear, J. T., and G.M. Kondolf, 2009. Estimating reservoir sedimentation rates at large spatial and temporal scales: A case study of California. *Water Resources Research* 45(12), doi: 10.1029/2007WR006703.

Molnar, P., 2004. Late Cenozoic increase in accumulation rates of terrestrial sediment: how might climate change have affected erosion rates?. *Annu. Rev. Earth Planet. Sci.*, 32, 67-89.

Montgomery, D. R., and M.T. Brandon, 2002. Topographic controls on erosion rates in tectonically active mountain ranges. *Earth and Planetary Science Letters* 201(3): 481-489, doi: 10.1016/S0012-821X(02)00725-2.

Montgomery, D. R., 2007. Soil erosion and agricultural sustainability. *Proceedings of the National Academy of Sciences* 104(33): 13268-13272. doi: 10.1073/pnas.0611508104.s

Morris, G.L., and J Fan, 1998. *Reservoir Sedimentation Handbook: Design and Management of Dams, Reservoirs and Watersheds for Sustainable Use*. McGraw-Hill. 848 pp.

National Research Council (NRC), Committee on Atlantic Salmon in Maine. 2004. *Atlantic salmon in Maine*, 304 pages, PDF version available from National Academic Press at <http://www.nap.edu/catalog/10892.html>.

Noel, D. S., C.S. Martin, and C.A. Federer, 1986. Effects of forest clearcutting in New England on stream macroinvertebrates and periphyton. *Environmental Management* 10(5), 661-670, doi: 10.1016/j.geomorph.2006.03.024.

Pearce, F., 1991. A dammed fine mess. *New Scientist* 130(1767): 36-39.

Pearson, A. J., N.P. Snyder, and M.J. Collins, 2011. Rates and processes of channel response to dam removal with a sand-filled impoundment. *Water Resources Research* 47(8), doi: 10.1029/2010WR009733.

Pimentel, D., C. Harvey, P. Resosudarmo, K Sinclair, D. Kurz, M. McNair, and R. Blair, 1995. Environmental and economic costs of soil erosion and conservation benefits. *SCIENCE-NEW YORK THEN WASHINGTON-*, 1117-1117.

Pinet, P., and M. Souriau, 1988. Continental erosion and large- scale relief. *Tectonics*, 7(3): 563-582. Doi: 0278-7407/88/007T-0908510. 00

Poff, N. L., J.D. Allan, M.B. Bain, J.R. Karr, K.L. Prestegard, B.D. Richter, and J.C. Stromberg, 1997. The natural flow regime. *BioScience*, 47(11): 769-784.

Raymo, M. E., and W.F. Ruddiman, 1992. Tectonic forcing of late Cenozoic climate. *Nature* 359(6391): 117-122.

Reiners, P. W., 2005. "Past, Present, and Future of Thermochronology". *Reviews in Mineralogy and Geochemistry* 58(1). doi:10.2138/rmg.2005.58.1.

Renard, K. G., Foster, G. R., Weesies, G. A., McCool, D. K., and D.C. Yoder, 1997. Predicting soil erosion by water: a guide to conservation planning with the revised universal soil loss equation (RUSLE). *Agriculture Handbook* (Washington), (703).

- Renwick, W. H., S.V. Smith, J.D. Bartley, and R.W. Buddemeier, 2005. The role of impoundments in the sediment budget of the conterminous United States. *Geomorphology* 71(1): 99-111, doi: 10.1016/j.geomorph.2004.01.010.
- Sanborn, S. C., and B.P. Bledsoe, 2006. Predicting streamflow regime metrics for ungauged streams in Colorado, Washington, and Oregon. *Journal of Hydrology*, 325(1), 241-261, doi: 10.1016/j.jhydrol.2005.10.018
- Saunders, I., and A. Young, 1983. Rates of surface processes on slopes, slope retreat, and denudation. *Earth Surface Processes and Landforms* 8(5): 473-501, doi: 10.1002/esp.3290080508.
- Schaller, M., F. Von Blanckenburg, N. Hovius, and P.W. Kubik, 2001. Large-scale erosion rates from in situ-produced cosmogenic nuclides in European river sediments. *Earth and Planetary Science Letters*, 188(3): 441-458. DOI: 10.1016/S0012-821X(01)00320-X
- Schumer, R., Jerolmack, D., and B. McElroy, 2011. The stratigraphic filter and bias in measurement of geologic rates. *Geophysical Research Letters* 38(11).
- Schumm, S. A., 1979. Geomorphic thresholds: the concept and its applications. *Transactions of the Institute of British Geographers*, 485-515.
- Smith, S. V., W.H. Renwick, J.D. Bartley, and R.W. Buddemeier, 2002. Distribution and significance of small, artificial water bodies across the United States landscape. *Science of the Total Environment* 299(1): 21-36, doi: S0048-9697(02)00222-X.
- Snyder, N.P., M.R. Castele, and J.R. Wright, 2008. Bedload Entrainment in Low-Gradient Paraglacial Coastal Rivers of Maine, U.S.A.: Implication for Habitat Restoration. *Geomorphology* 103:430-446, doi: 10.1016/j.geomorph.2008.07.013.
- Snyder, Noah P et al, 2013. Predicting grain size in gravel-bedded rivers using digital elevation models: 2 application to three Maine watersheds. *GSA Bulletin* 125(1-2), 148-163, doi: 10.1130/B30694.1.
- Southworth, M., and Ben-Joseph, E., 1995. Street Standards and the Shaping of Suburbia. *Journal of the American Planning Association* 61(1): 65-81, doi: 10.1080/01944369508975620.
- Stevaert, L. T and G.R. Knox, 2008. Reconstructed historical land cover and biophysical parameters for studies of land- atmosphere interactions within the eastern United States. *Journal of Geophysical Research: Atmospheres* (1984–2012): 113(D2), doi: 10.1029/2006JD008277

- Summerfield, M. A., and J.N. Hulton, 1994. Natural controls of fluvial denudation rates in major world drainage basins. *Journal of Geophysical Research: Solid Earth* (1978–2012), 99(B7): 13871-13883. doi: 10.1029/94JB00715
- Syvitski, J. P., A.J. Kettner, I. Overeem, E.W. Hutton, M.T. Hannon, G.R. Brakenridge, and R.J. Nicholls, 2009. Sinking deltas due to human activities. *Nature Geoscience*, 2(10), 681-686, doi: 10.1038/ngeo629.
- Therneau, T. M., and E.J. Atkinson, 1997. An introduction to recursive partitioning using the RPART routines. Technical Report 61, Section of Biostatistics, Rochester, Mayo Clinic.
- Turner, R. E., and N.N. Rabalais, 1994. Coastal eutrophication near the Mississippi river delta. *Nature* 368: 619 – 621, doi:10.1038/368619a0.
- USACE, United States Army Corps of Engineers, 2000. National inventory of dams. CD-ROM Federal Emergency Management Agency. <http://crunch.tec.army.mil/nid/webpages/nid.cfm>.
- USEPA, United States Environmental Protection Agency, 1991. Guidance for water quality–based decisions in the TMDL process. EPA 440/4–91–001. Washington, D.C.: U.S. EPA, Office of Water. [www.epa.gov/OWOW/tmdl/decisions](http://www.epa.gov/OWOW/tmdl/decisions).
- USEPA, United States Environmental Protection Agency, 2004. National water quality inventory: 2004 report to United States Congress. EPA 841-R-08-001. Washington, D.C.: U.S. EPA.
- USFWS, United States Fish and Wildlife Service, 1999. Biological report on the status of Atlantic salmon in Maine. <http://library.fws.gov/salmon/index.html>.
- Vörösmarty, C. J., M. Meybeck, B. Fekete, K. Sharma, P. Green, and J.P. Syvitski, 2003. Anthropogenic sediment retention: major global impact from registered river impoundments. *Global and Planetary Change*, 39(1), 169-190, doi: 10.1016/S0921-8181(03)00023-7.
- Walling, D. E., 1977. Assessing the accuracy of suspended sediment rating curves for a small basin. *Water Resources Research*, 13(3): 531-538.
- Walter, R.C. and D.J. Merritts, 2008. Natural Streams and the Legacy of Water-Powered Mills. *Science* 319:299-304, doi: 10.1126/science.1151716.
- Waythomas, C. F., and G.P. Williams, 1988. Sediment yield and spurious correlation—toward a better portrayal of the annual suspended-sediment load of rivers. *Geomorphology* 1(4): 309-316, doi: 10.1016/0169-555X(88)90003-7.

Wilkins, B. C., and N.P. Snyder, 2011. Geomorphic comparison of two Atlantic coastal rivers: toward an understanding of physical controls on Atlantic salmon habitat. *River Research and Applications* 27(2): 135-156, doi: 10.1002/rra.1343.

Willenbring, J. K., and F. von Blanckenburg, 2010. Long-term stability of global erosion rates and weathering during late-Cenozoic cooling. *Nature*, 465(7295), 211-214.

## 8. Appendices

### 8.1 Appendix 1: Master Data Table

Please see the following google document for a copy of the data table.

<https://docs.google.com/a/bc.edu/spreadsheets/d/11D869JAFd11aqnETsVuq4FHS tW4h8EqUbG8v3uAzD2Y/edit?usp=sharing>

### 8.2 Appendix 2: PCA and CART analyses

Performing PCA on the data was of limited usefulness. Principal components 1 and 2 (Figure 29) only accounted for 43 percent of the variance in the data, indicating that the dataset is not highly correlated.

Importance of components:

	Comp.1	Comp.2	Comp.3	Comp.4	Comp.5	Comp.6	Comp.7	Comp.8	Comp.9	Comp.10	Comp.11	Comp.12
Standard deviation	1.914965	1.2603874	1.2312979	1.0779825	1.00727329	0.95429248	0.89587599	0.72753361	0.59977833	0.52253826	0.4179320	0.03963180
Proportion of Variance	0.305591	0.1323814	0.1263412	0.0968372	0.08454996	0.07588951	0.06688282	0.04410876	0.02997784	0.02275385	0.0145556	0.00013089
Cumulative Proportion	0.305591	0.4379724	0.5643136	0.6611508	0.74570073	0.82159024	0.88847306	0.93258182	0.96255966	0.98531351	0.9998691	1.00000000

Figure A2.1: Loadings showing how much proportion of the variance can be explained by each principal component (PCA biplot shown in Figure 30).

fit

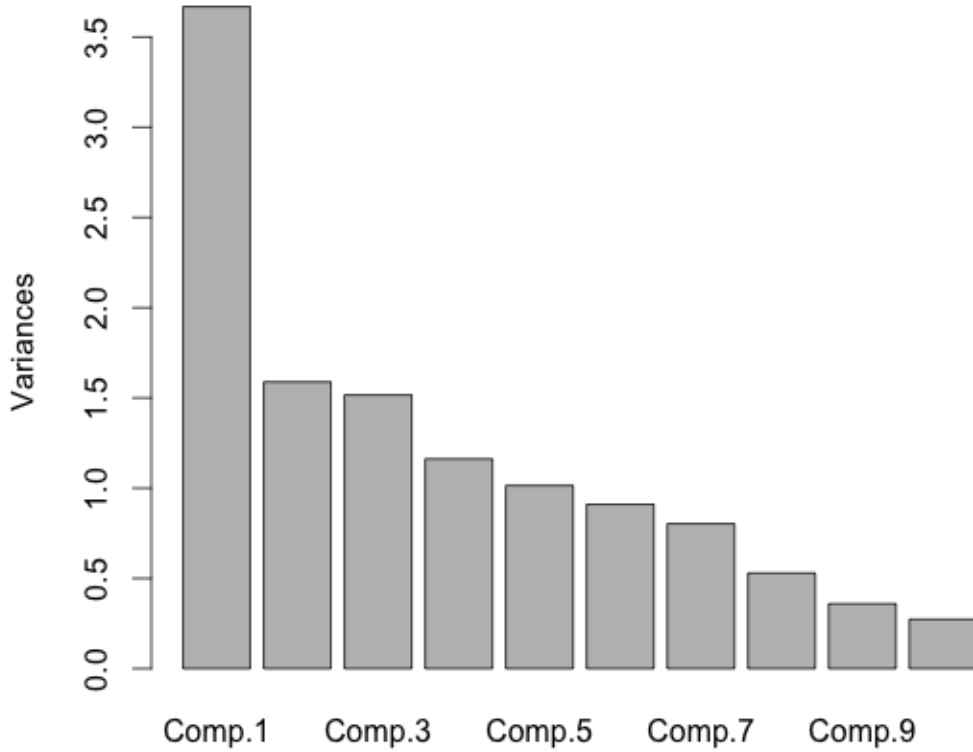


Figure A2.2: Scree plot showing that Principal component 1 accounted for most of the variability in the dataset. This indicates that the dataset is not highly correlated. This is a graphical representation of Figure A2.1.

	A	T	S	K	MAT	MAP	I	B	F	Sh	Ag	W
A	1.000000e+00	-1.897291e-05	0.09930153	0.49256114	-0.006373699	0.08173281	-0.09627564	-0.01643613	0.01818193	-0.02906650	0.01959001	0.002927131
T	-1.897291e-05	1.000000e+00	-0.13354425	-0.01882687	-0.218538138	-0.02766773	0.25358400	-0.02424456	-0.11393853	-0.03188324	-0.02401411	0.433758888
S	0.09930153	-0.13354425	1.00000000	0.67213712	-0.060546133	0.45471995	-0.22240999	0.01077175	0.78773996	-0.15524445	-0.68420824	-0.333504163
K	0.49256114	-0.01882687	0.67213712	1.00000000	-0.136370095	0.41694436	-0.15587691	0.02639229	0.56516184	-0.19486848	-0.49590457	-0.154890190
MAT	-0.006373699	-0.218538138	-0.060546133	-0.136370095	1.000000000	0.34604098	0.16775017	0.23558142	0.03385339	0.07866126	-0.10292555	-0.135307350
MAP	0.08173281	-0.02766773	0.45471995	0.41694436	0.346040979	1.00000000	-0.11508441	0.10893704	-0.53673732	-0.05681690	-0.58292795	-0.095969234
I	-0.09627564	0.25358400	-0.22240999	-0.15587691	0.167750168	-0.11508441	1.00000000	0.03789008	-0.23884917	-0.04758912	-0.16235934	0.072351623
B	-0.01643613	-0.02424456	0.01077175	0.02639229	0.235581417	0.10893704	0.03789008	1.00000000	0.15646514	-0.05179392	-0.21887593	-0.051807343
F	0.01818193	-0.11393853	0.78773996	0.56516184	0.033853390	0.53673732	-0.23884917	0.15646514	1.00000000	-0.17348731	-0.91164207	-0.230956197
Sh	-0.02906650	-0.03188324	-0.15524445	-0.19486848	0.078661261	-0.05681690	0.04758912	-0.05179392	-0.17348731	1.00000000	0.16575066	0.021813100
Ag	0.01959001	-0.02401411	-0.68420824	-0.49590457	-0.102925548	-0.58292795	-0.16235934	-0.21887593	-0.91164207	0.16575066	1.00000000	0.112314434
W	0.002927131	0.433758888	-0.33350416	-0.15489019	-0.135307350	-0.09596923	0.07235162	-0.05180734	-0.23095620	0.02181310	0.11231443	1.000000000

Table A2.3: Covariance matrix showing relationships between independent variables used in this study.

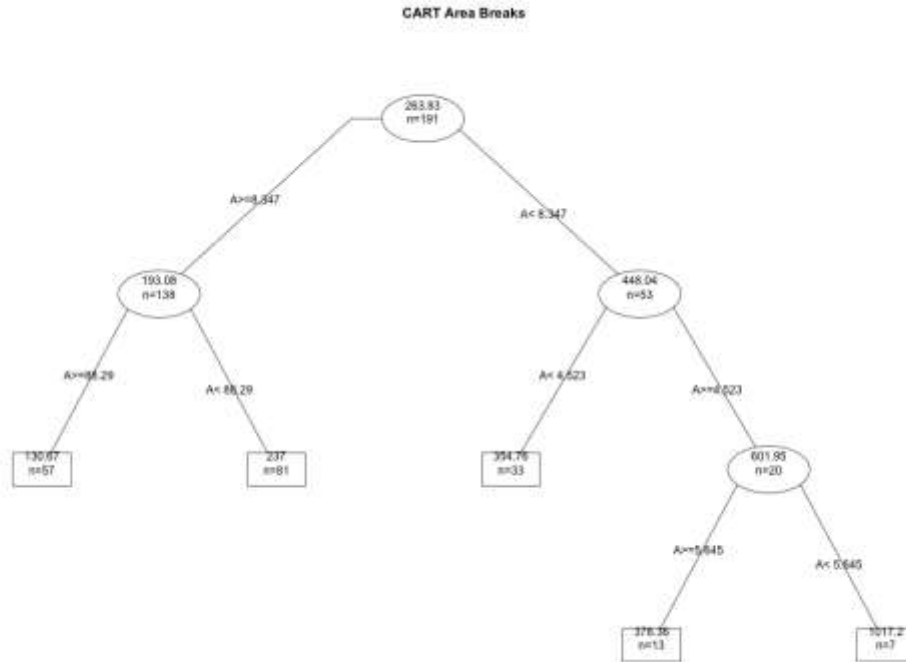


Figure A2.4: CART Analysis showing breaks in watershed area ( $A$ ) in the data. Watersheds were classified as either small ( $0-8.3 \text{ km}^2$ ), medium ( $8.3 - 88.3 \text{ km}^2$ ) or large ( $> 88.3 \text{ km}^2$ ) to aid in analysis. Numbers in circles are the mean  $Y$  values for that particular split. Threshold values are shown on the lines, or “branches” of the tree. The number of study watersheds contained within the split are shown by “ $n=xxx$ ” within circles. Squares represent a terminal node of the tree.

8.3 Appendix 3: Figures and Tables Not Included in Thesis

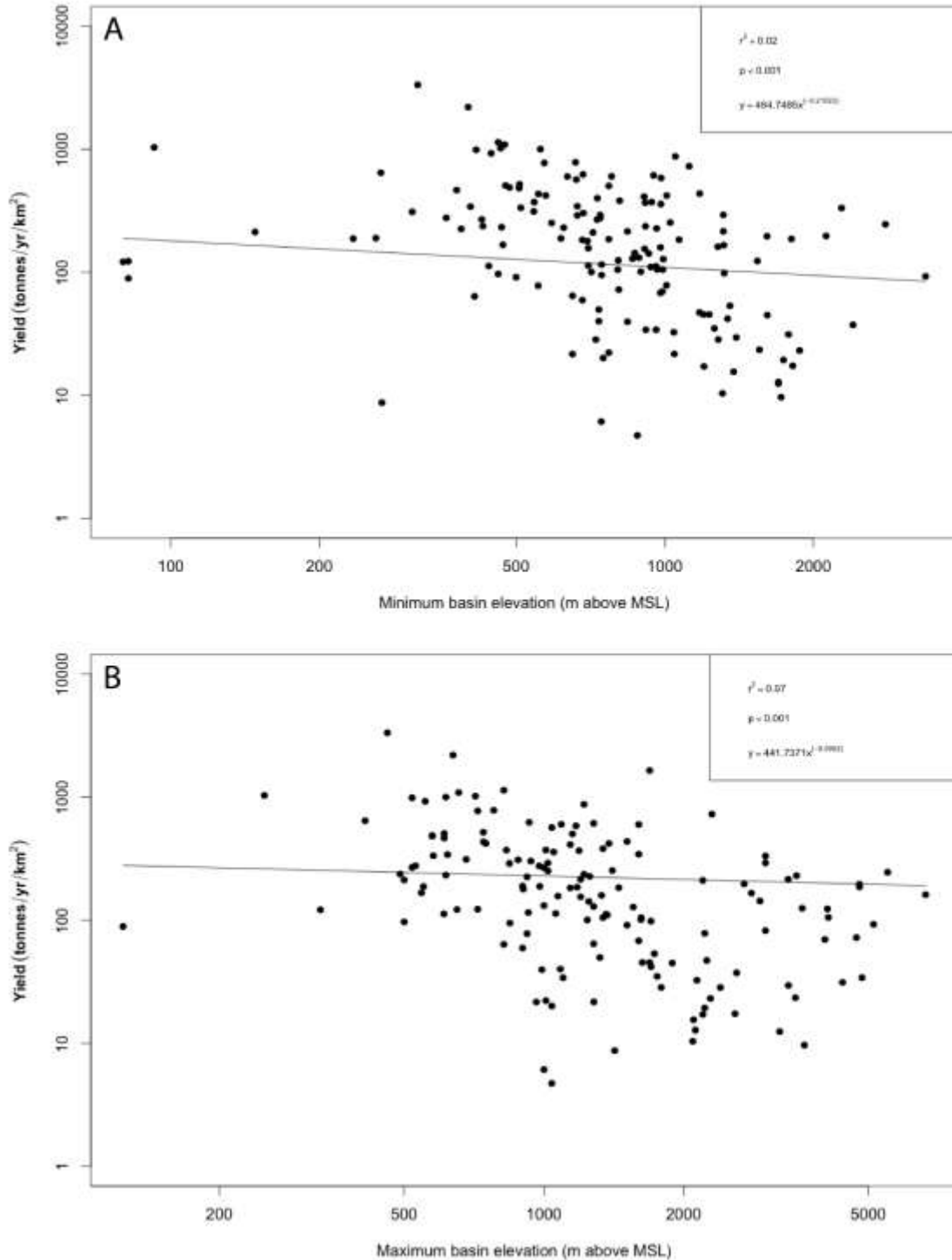


Figure A3.1: Logarithmic scatterplots depicting (A)  $Y$  as a function of minimum basin elevation ( $MinEl$ ; meters above mean sea level). (B)  $Y$  as a function of maximum basin elevation ( $MaxEl$ ; meters above mean sea level). These plots were excluded from the thesis because the residuals of these regressions were not normally distributed.

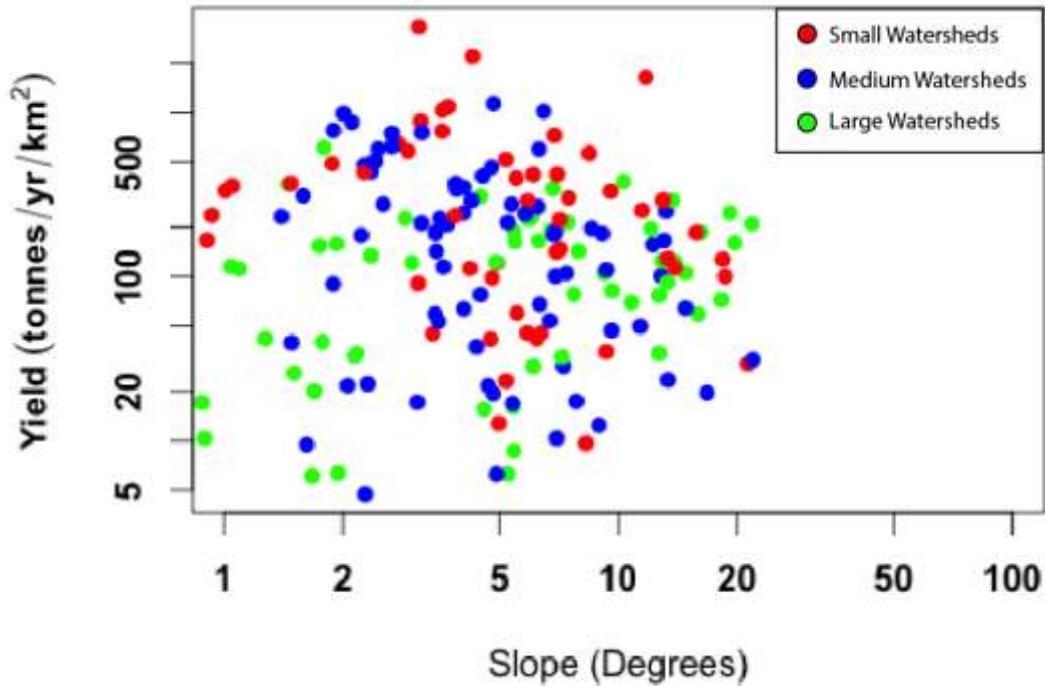


Figure A3.2: Logarithmic scatterplot displaying  $Y$  as a function of mean watershed slope ( $S$ , degrees) for study watersheds in the eastern US categorized by watershed size.

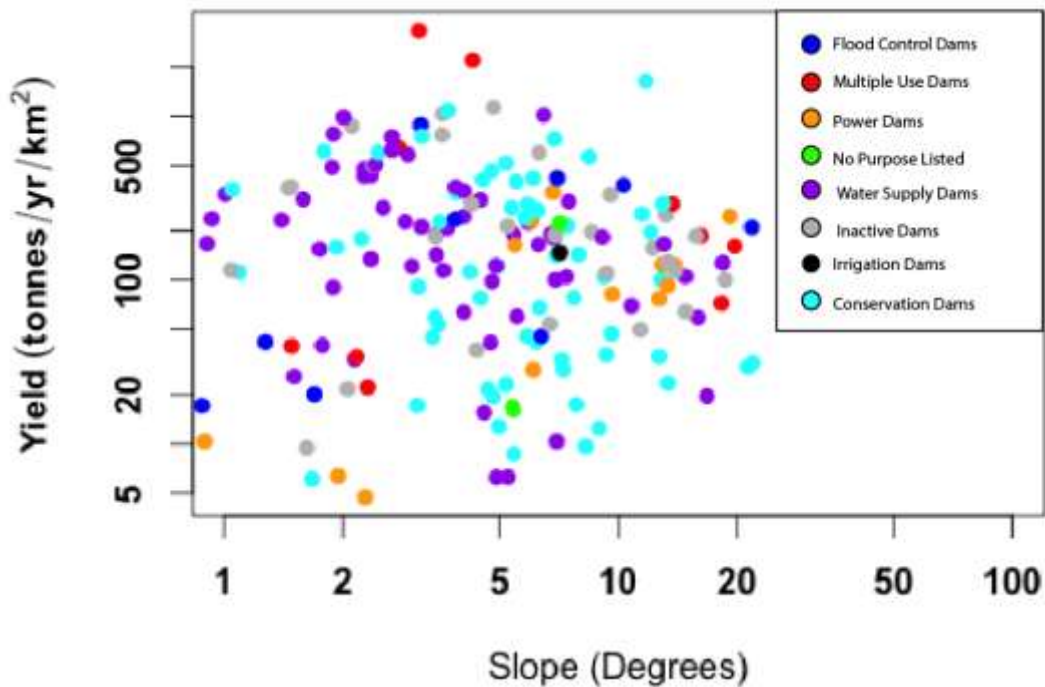


Figure A3.3: Logarithmic scatterplot displaying  $Y$  as a function of mean watershed slope ( $S$ , degrees) for study watersheds in the eastern US categorized by dam function.

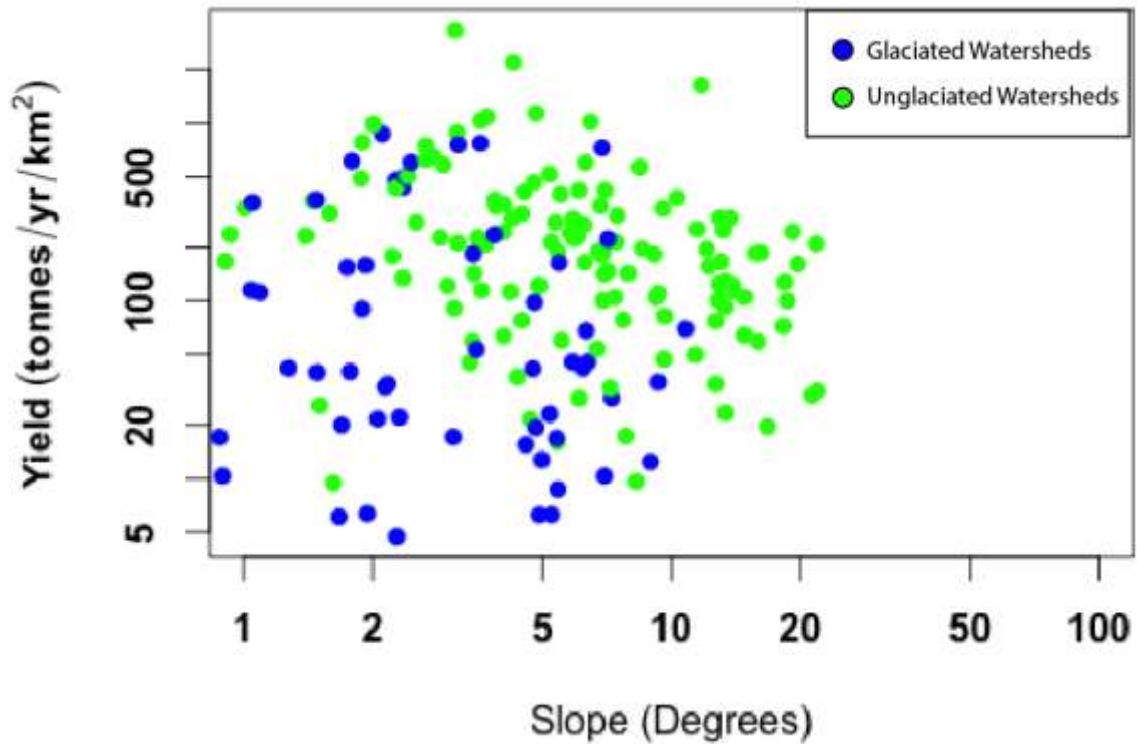


Figure A3.4: Logarithmic scatterplot displaying  $Y$  as a function of mean watershed slope ( $S$ , degrees) for study watersheds in the eastern US categorized by glacial history

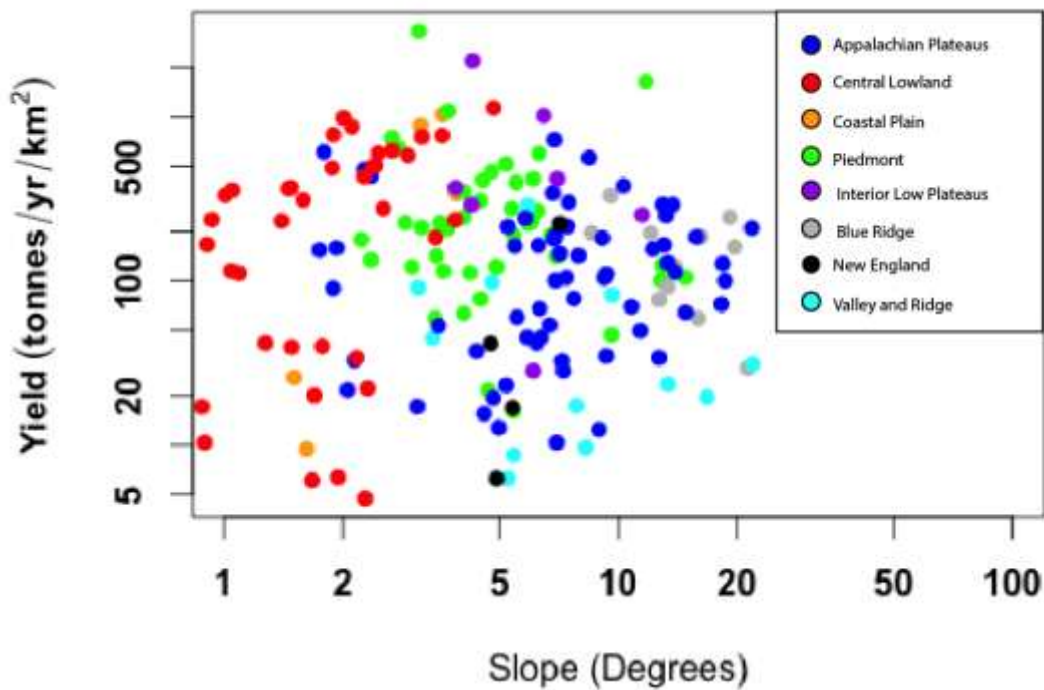


Figure A3.5: Logarithmic scatterplot displaying  $Y$  as a function of mean watershed slope ( $S$ , degrees) for study watersheds in the eastern US categorized by physiographic province.

Table A3.1: R<sup>2</sup> Values for a simple linear regression, with Y as the dependent variable, for individual categories. Variable names are those listed in Table 2.

<b>Dam Type</b>	<b>S</b>	<b>A</b>	<b>K</b>	<b>MAP</b>	<b>MAT</b>	<b>I</b>	<b>Ag</b>	<b>F</b>
Flood Control (n=9)	0.29	0.16	-0.24	0.37	0.47	-0.13	0.29	0.49
Multiple Use (n=10)	0.12	0.12	-0.1	-0.009	0.59	-0.05	-0.12	-0.08
Power (n=13)	0.55	0.09	0.48	0.35	0.11	-0.03	0.24	0.55
Water Supply (n=63)	0.09	0.16	0.35	0.05	0.24	-0.01	0.13	0.13
Irrigation (n=2)	NA	NA	NA	NA	NA	NA	NA	NA
Conservation (n=31)	0.03	0.02	-0.03	-0.03	0.2	-0.03	-0.03	-0.03
Inactive (n=60)	0.001	0.13	0.14	0.05	0.31	0.01	-0.008	0.01
Not Listed (n=3)	0.99	0.6	NA	-0.95	0.64	0.11	0.95	0.61
<b>Area Class</b>								
Small (n=56)	0.05	NA	0.17	0.007	0.32	0.09	0.02	0.05
Medium (n=78)	0.04	NA	0.16	-0.01	0.3	-0.01	0.04	0.04
Large (n=57)	0.1	NA	-0.02	0.07	0.09	0.02	0.01	0.04
<b>Glacial History</b>								
Unglaciaded (n=134)	0.07	0.07	0.2	-0.007	0.15	0.03	0.02	0.04
Glaciaded (n=57)	-0.004	0.04	-0.004	0.0009	0.13	-0.02	0.08	0.03
<b>Physiographic Province</b>								
Coastal Plain (n=6)	0.26	0.4	0.27	-0.15	0.17	-0.23	0.36	0.28
Piedmont (n= 43)	-0.009	0.06	0.07	0.03	0.06	0.13	0.04	-0.02
Blue Ridge (n=11)	0.12	-0.1	-0.11	0.39	0.44	-0.07	0.05	-0.08
Valley and Ridge (n=12)	-0.05	0.2	0.18	0.1	0.04	0.09	-0.08	-0.09
Appalachian Plateaus (n=61)	-0.007	0.01	-0.01	0.03	0.36	-0.001	-0.001	0.04
New England (n=5)	0.43	0.96	NA	0.9	0.19	0.67	0.52	0.29
Interior Low Plateaus (n=7)	-0.14	0.54	0.68	0.38	-0.19	-0.1	-0.09	-0.07
Central Lowland (n=46)	0.02	0.4	0.01	0.48	0.47	-0.004	-0.01	-0.008

Table A3.2: P Values for categorical linear regressions. Variable names are those listed in Table 2.

<b>Dam Type</b>	<b>Slope</b>	<b>Area</b>	<b>Relief</b>	<b>MAP</b>	<b>MAT</b>	<b>I</b>	<b>Ag</b>	<b>F</b>
Flood Control (n=9)	0.07	0.15	0.9	0.05	0.025	0.8	0.08	0.02
Multiple Use (n=10)	0.8	0.18	0.67	0.37	0.005	0.36	0.87	0.57
Power (n=13)	0.002	0.98	0.02	0.02	0.14	0.43	0.05	0.002
Water Supply (n=63)	0.008	0.0006	0.000003	0.04	0.00002	0.65	0.0002	0.002
Irrigation (n=2)	NA	NA	NA	NA	NA	NA	NA	NA
Conservation (n=31)	0.88	0.53	0.67	0.89	0.007	0.69	0.78	0.87
Inactive (n=60)	0.3	0.18	0.003	0.05	0.000003	0.2	0.45	0.2
Not Listed (n=3)	0.02	0.29	NA	0.89	0.28	0.46	0.1	0.29
<b>Area Class</b>								
Small (n=56)	0.05	NA	0.001	0.24	0.000002	0.01	0.17	0.06
Medium (n=78)	0.05	NA	0.0009	0.81	0.0000001	0.74	0.05	0.04
Large (n=57)	0.01	NA	0.53	0.02	0.01	0.15	0.21	0.08
<b>Glacial History</b>								
Unglaciaded (n=134)	0.0008	0.0008	0.000004	0.92	0.000002	0.02	0.08	0.009
Glaciaded (n=57)	0.38	0.08	0.38	0.31	0.004	0.87	0.02	0.12
<b>Physiographic Province</b>								
Coastal Plain (n=6)	0.18	0.1	0.41	0.58	0.23	0.86	0.12	0.16
Piedmont (n= 43)	0.43	0.06	0.07	0.15	0.06	0.01	0.09	0.85
Blue Ridge (n=11)	0.16	0.8	0.67	0.02	0.02	0.56	0.25	0.62
Valley and Ridge (n=12)	0.49	0.08	0.12	0.17	0.26	0.18	0.69	0.73
Appalachian Plateaus (n=61)	0.47	0.2	0.64	0.1	0.0000002	0.35	0.35	0.06
New England (n=5)	0.21	0.1	NA	0.03	0.32	0.12	0.18	0.27
Interior Low Plateaus (n=7)	0.61	0.04	0.06	0.08	0.92	0.55	0.5	0.48
Central Lowland (n=46)	0.18	0.0000001	0.2	0.00000004	0.000000009	0.37	0.69	0.42

